NANO · MICRO small
www.small-journal.com

Fiber Surface/Interfacial Engineering on Wearable Electronics

Ruimin Xiao, Guiqin Yu, Ben Bin Xu, Nan Wang, and Xuqing Liu**

Surface/interfacial engineering is an essential technique to explore the fiber materials properties and fulfil new functionalities. An extensive scope of current physical and chemical treating methods is reviewed here together with a variety of real-world applications. Moreover, a new surface/interface engineering approach is also introduced: self-assembly via π–π stacking, which has great potential for the surface modification of fiber materials due to its nondestructive working principle. A new fiber family member, metal-oxide framework (MOF) fiber shows promising candidacy for fiber based wearable electronics. The understanding of surface/interfacial engineering techniques on fiber materials is advanced here and it is expected to guide the rational design of future fiber based wearable electronics.

1. Introduction

Fiber, a natural or man-made substance with a high aspect ratio (its length is normally longer than its width), is often present in the preparation of other materials. For instance, two of the strongest engineering materials, carbon fiber (CF) and ultra-high-molecular-weight polyethylene (UHMWPE) incorporate fibers.[1] They have been used to fabricate light-weight and high modulus products for both military and civil applications such as aerospace,[2] car seat,[3] concrete,[4] and textiles.[5] Fibers can be sorted into two categories, depending on their origin: natural fibers and synthetic fibers.

With increasing technological advances, clothes made of natural and synthetic fibers have also become a platform for wearable electronics that are in close contact with skin to monitor human activities, as well as providing warmth and changing aesthetic appearance.[7] In theory, the perfect wearable electronic device is entirely self-contained within the textile,[8] which can function as a sensor to detect human motion and physiological signals.[9] Therefore the fiber-based wearable electronics—or so called smart textiles—are able to interact with the environment or user by being embedded within the final products such as natural/synthetic fibers based on their woven, knitted, or nonwoven structure.[10]

Natural fibers collected and produced from plants, animals, and geological processes are essential in modern industries.[1] The raw materials for producing natural fibers are cheap, abundant, and easy for collection. Varieties of natural fibers are shown in **Figure 1**.

Synthetic fibers, on the other hand, are significantly modified in their chemical composition, structure, etc., during the production process. Several typical synthetic fibers are shown in **Figure 2**. One of the recent popular choices is cellulose fiber, which is the most abundant biopolymer on earth and comes from green, low-cost, easy-collecting, renewable, and biodegradable natural resources.[11]

The final products of natural fibers are normally biodegradable, nontoxic, and lightweight, with high specific strength and fatigue resistance. However, the limitations of natural fibers are also obvious, in particular their high moisture absorption, nonregular mechanical properties, poor chemical/fire resistance, and poor interfacial interactions with a polymeric matrix.[12] Synthetic fibers have a wider variety of applications than natural fibers but also suffer from a decrease in comfort during wear, in exchange for higher mechanical strength, conductivity, water repellency, etc. These drawbacks significantly decrease the performance of current textile-based wearable electronics. Therefore, it is pertinent to achieve better-performing materials through fiber modification to improve the original drawbacks of both kinds of fibers since fibers are the key component of textile-based wearable electronics.

Smart textiles can sense and respond to changes under certain external conditions, so have attracted widespread interest and investment (**Figure 3**).[14] Smart textiles can be catalogued as either passive or active. Passive smart textiles can change their properties in response to external environmental variation: typical examples include shape memory materials[15] and hydrophobic/hydrophilic[16] textiles. The collected data can

R. Xiao, X. Liu
Department of Materials
Faculty of Science and Engineering
University of Manchester
Oxford Rd., Manchester M13 9PL, UK
E-mail: xuqing.liu@postgrad.manchester.ac.uk
G. Yu
College of Chemistry and Chemical Engineering
Lanzhou University
222 Tianshui Southern Road, Lanzhou, Gansu 730000, China
B. B. Xu
Mechanical and Construction Engineering
Faculty of Engineering and Environment
Northumbria University
Newcastle upon Tyne NE1 8ST, UK
E-mail: BEN.XU@NORTHUMBRIA.AC.UK
N. Wang
The Nanoscience Centre
University of Cambridge
Cambridge CB3 0FF, UK

The ORCID identification number(s) for the author(s) of this article can be found under https://doi.org/10.1002/smll.202102903.

DOI: 10.1002/smll.202102903

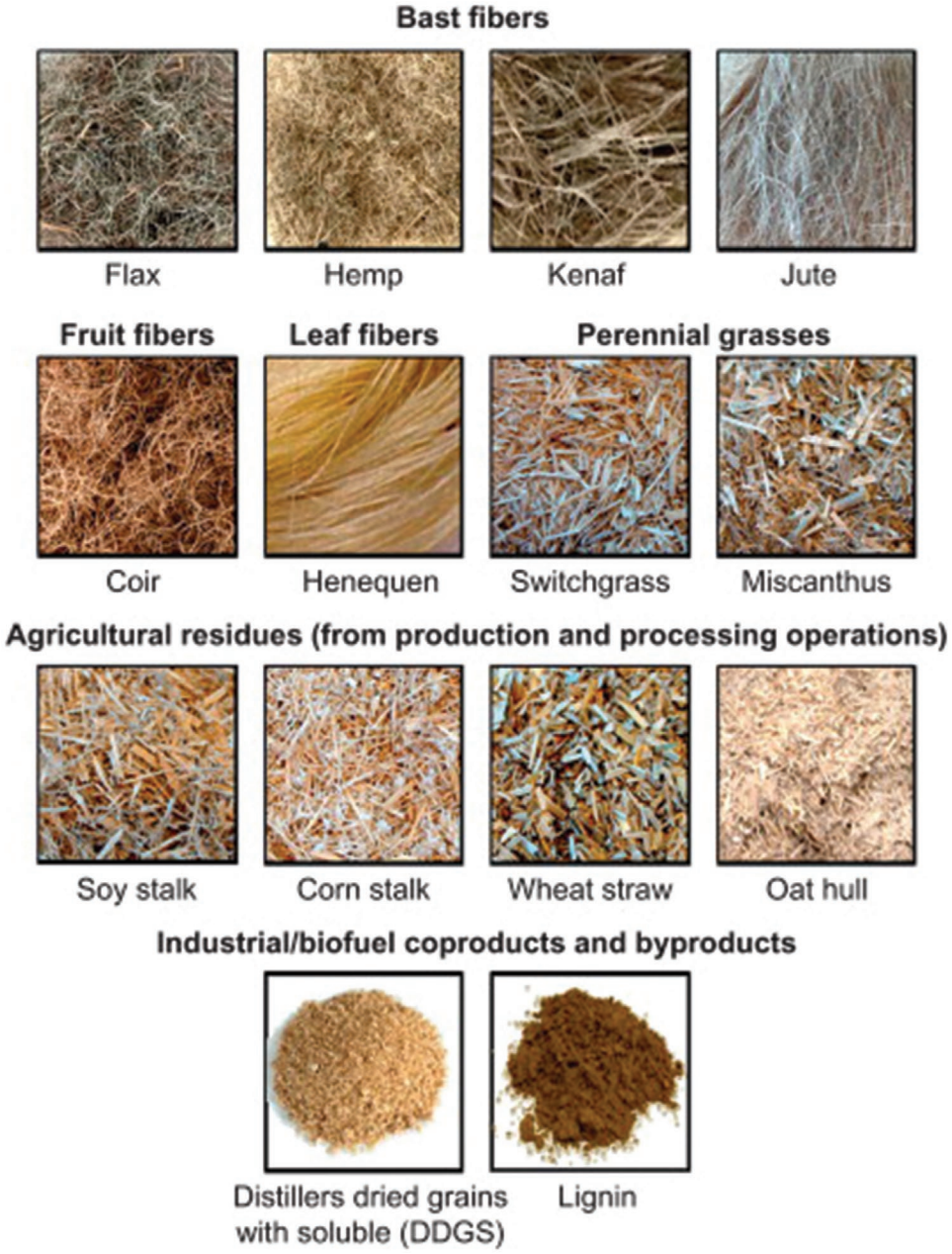

Figure 1. General classification of naturally existed fibers. Reproduced with permission.[6] Copyright 2015, Elsevier.

include, but is not limited to, temperature, light intensity, pressure, humidity, and pollution.[17–19] By contrast, active smart materials can directly change their surrounding environment, for example, various textile-based actuators, including textile displays, microvibrating devices, and light-emitting diode (LED), organic light-emitting diode (OLED). More examples of these smart materials are shown in **Figure 4**. Furthermore, smart textiles which are embedded with electronic circuits used for power generation, communication, etc., can be fully self-operational or controlled remotely via wireless connection to clouds containing data bases or artificial intelligence.[20]

Since smart materials created solely from either natural fibers or synthetic fibers each have their own drawbacks, it is highly desirable to improve the performance of fiber-based wearable electronics through modification of the fiber properties via techniques including chemical addition, coating, and surface modification. In this review, we will focus on the surface modification of fibers, and how these modifications can improve fiber-polymer bonding in an attempt to gain insight into how best to improve smart textiles for future developments.

During surface modification, the interaction forces upon the fiber surface include, but are not limited to, van der Waals forces, covalent bonding and π–π stacking. This technique is mainly used to reduce the water absorption of fibers and enable them to combine with polymeric matrices with an increased interfacial adhesion.[13]

In general, there are three main approaches for the surface treatment of fibers: physical, chemical, and biological. Since

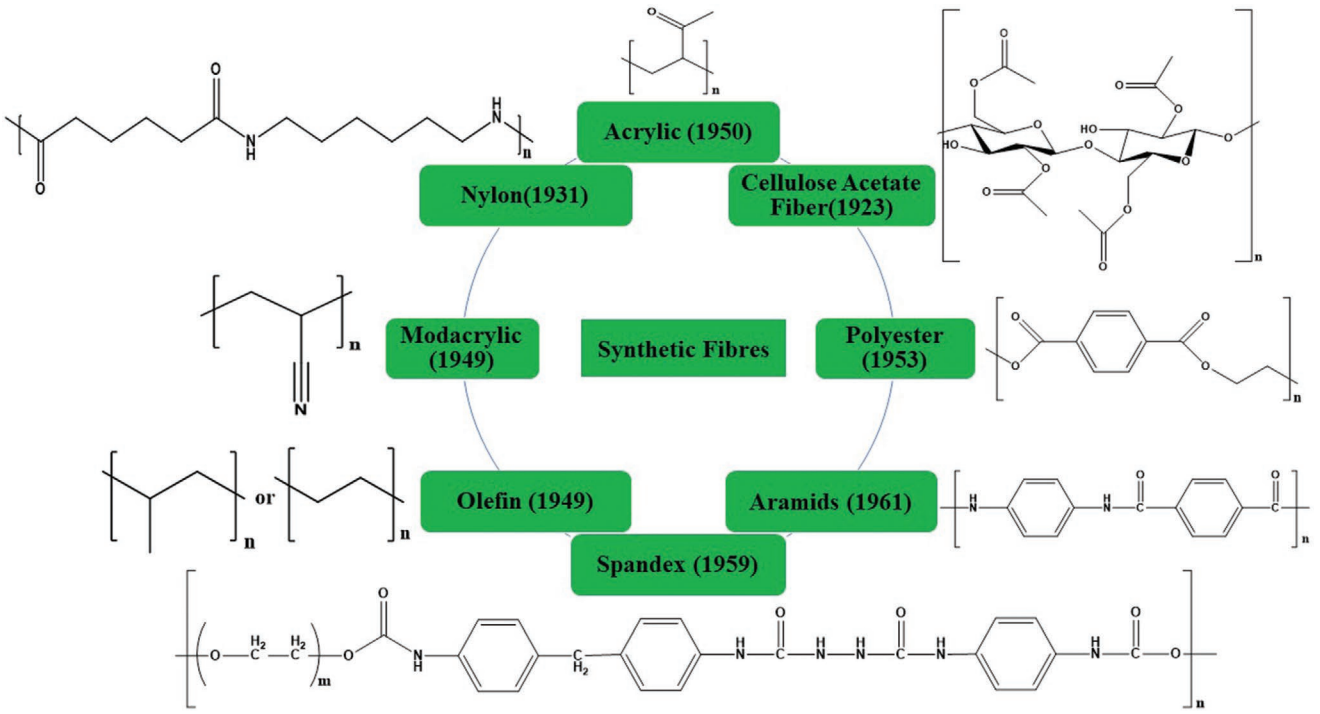

Figure 2. Typical synthetic fibers with their birthdays and chemical schemes.

biological treatments typically require very different techniques and are often used in unique environments, only physical and chemical treatments are discussed in detail here due to their wider relevance.

2. Physical Treatment

The fibers can be reinforced by two main types of treatment, one of which is physical treatment. Methods of physical treatment

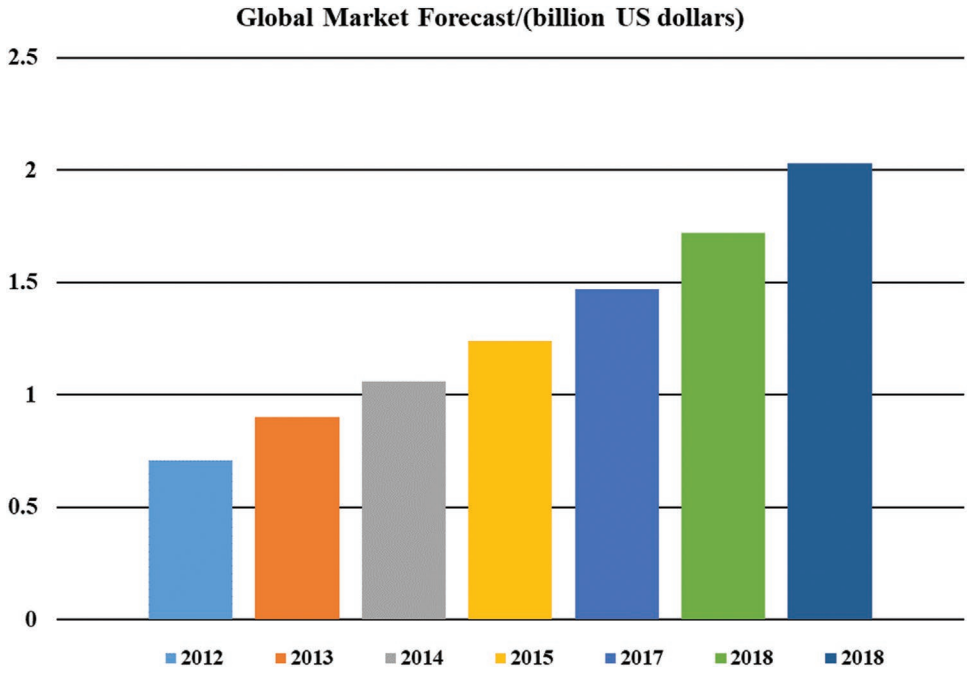

Figure 3. The global market forecast (billion US dollars) of smart/intelligent/digital/interactive fabrics or textiles between 2012 and 2018. Reproduced with permission.[14] Copyright 2016, Elsevier Science.

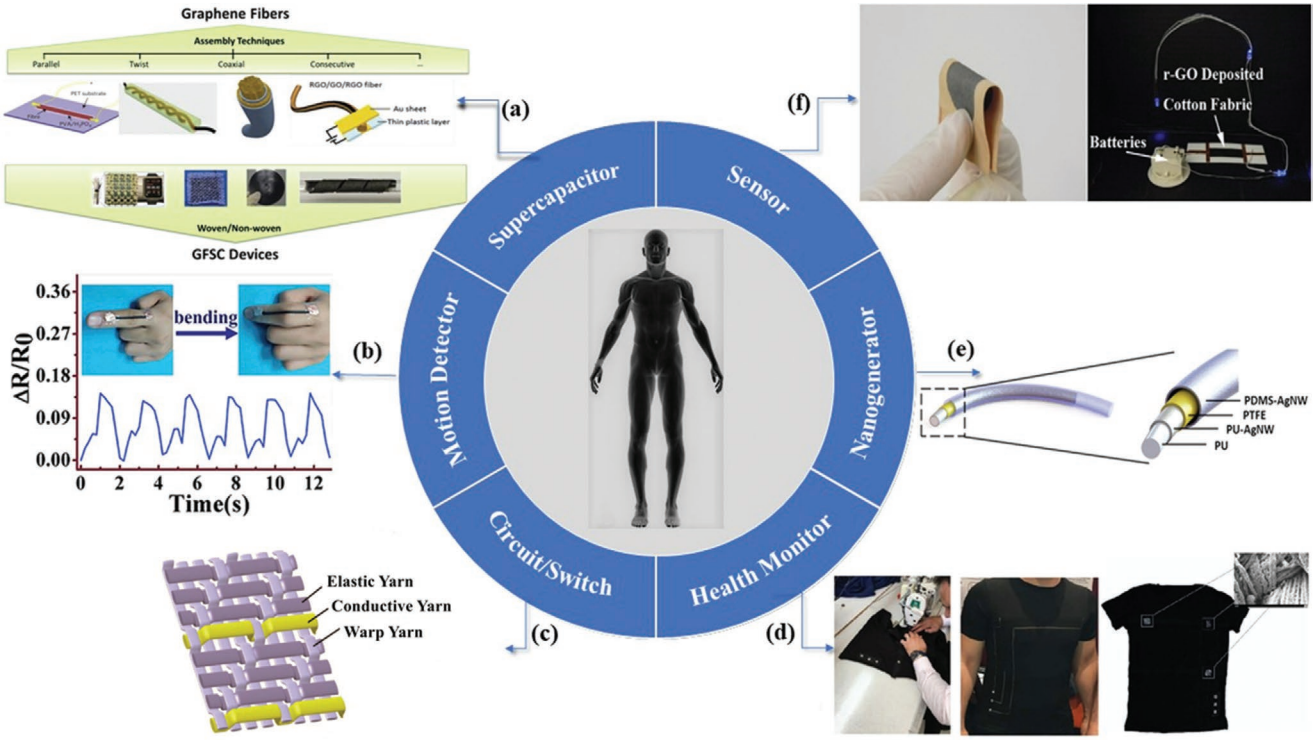

Figure 4. Common applications of smart textiles for human body. a) Assembly techniques for GFSC devices. Reproduced with permission.[27] Copyright 2018, Elsevier. b) CNT/thermoplastic polyurethane fiber motion sensor. Reproduced with permission.[30] Copyright 2018, Elsevier. c) Stretchable woven fabric circuit board. Reproduced with permission.[32] Copyright 2019, MDPI. d) A fiber heartbeat monitor. Reproduced with permission.[34] Copyright 2017, KSU. e) A stretchable nanogenerator based on PU fiber and AgNW. Reproduced with permission.[36] Copyright 2017, Elsevier. f) The strain sensor of rGO/cotton fabric. Reproduced with permission.[37] Copyright 2016, Elsevier.

include using plasma, irradiation, annealing, surface covering, and nanocrystal generation (**Figure 5**). The mechanical bonding of polymers to the fibers is affected after physical treatments due to the change of structure and surface of the fiber. However, the chemical composition of the fibers is left unchanged. Thus, the physical techniques generally enhance the interface through the increased mechanical bonding between the fiber and the matrix.

2.1. Plasma Activation

Plasma is one of the four fundamental states of matter, and was first mentioned by chemist Irving Langmuir in 1920s.[43] Plasma has two categories, thermal and nonthermal plasma, which are classified depending on the temperature.[44,45] Thermal (hot) plasma is generated via sources of direct/alternating current or radio frequency/microwave at high pressure(>10 kPa) and high temperatures (≈2000–20 000 K).[46,47] Nonthermal (nonequilibrium) plasmas have low pressure status and are produced through high electron temperatures, low ion, and neutral temperatures.[47–50] Plasma contains four main different components, as shown in **Table 1**.[51]

These components are able to carry a large amount of internal energy, enabling facile fiber surface modification using plasma.[52] The ionized gaseous substance of plasma is highly electrically conductive so that long-range electric and magnetic fields decide the behavior of the matter. Plasma activation, also known as plasma functionalization, is a method of surface modification to employ plasma processing, which can improve surface adhesion properties of many materials, including metals, glass, ceramics, a broad range of polymers, and textiles.[39] Even natural fibers like wood and seeds can be treated. **Figure 6** presents a theoretical model to explain how ions interact with the material surface and result in surface modification. The example here features a modified carbon fiber.

Plasma treatment is used widely during industrial production to treat surfaces for bonding, gluing, coating, and painting. The treatments work through a combination of reduction of metal oxides, ultrafine surface cleaning from organic contaminants, modification of the surface topography, and deposition of functional chemical groups. More importantly, the plasma activation can be performed at atmospheric pressure using air or typical industrial gases like hydrogen, nitrogen, and oxygen. Therefore, expensive vacuum equipment or wet chemistry is not needed for plasma surface modification. This significantly reduces the process costs and environmental impact and increases the safety of the process. A fast processing speed also leads to more potential industrial applications. This method uses the characteristic of plasma to directly hit the surface of fiber. The electrons within the fiber molecules are activated, and interact with electrons of plasma and transfer energy. The substances within the plasma then form strong bonds or are embedded within the surface of the original fiber to form a new material. Specific textile properties can be improved after such treatment. For example, in a graft-polymerization procedure induced by Ar-plasma, two kinds of modified cotton fabric were

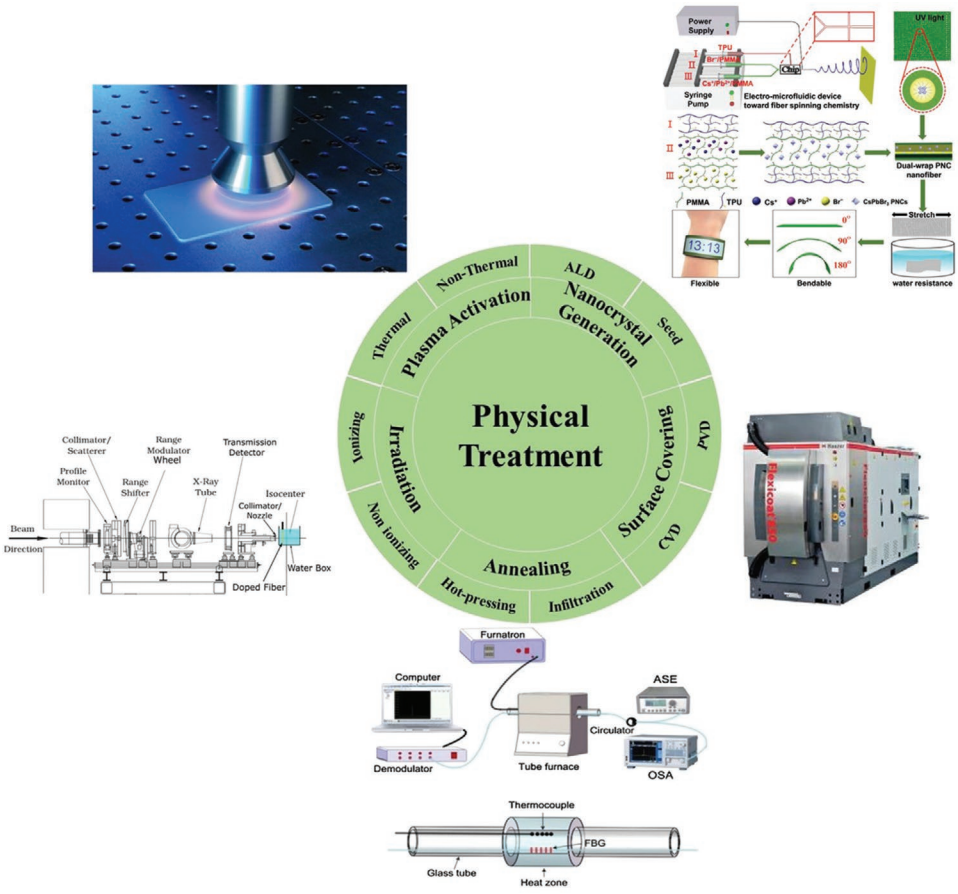

Figure 5. Different methods and common approaches for physical treatment. a) Plasma activation. Reproduced with permission.[38] Copyright 2019, Wiley-VCH. b) Irradiation. Reproduced with permission.[39] Copyright 2017, Elsevier. c) Annealing. Reproduced with permission.[40] Copyright 2018, Elsevier. d) Surface covering. Reproduced with permission.[41] Copyright 2016, Elsevier. e) Nanocrystal generation. Reproduced with permission.[42] Copyright 2019, Wiley-VCH.

fabricated by the cold plasma technique to attach polyDEAEPN and polyAC8 on the fiber surface for improving the textile's fire- and water-resistance properties.[54]

The sodium battery remains a popular topic across the world for energy storage research, with many groups exploring more efficient new materials to replace the traditional lithium-ion battery. As part of this research, a facile and rapid carbon-plasma strategy to generate hierarchical graphene (hG) bundled onto tin sulfide networks was proposed in **Figure 7**a.[55] Compared with the previous works, this hG/SnS battery could maintain 93% capacity after 1600 cycles of high-rate long-term cycling, while pure SnS only 19%/250 cycles and rGO/SnS 68%/650 cycles. Therefore, this work is a very successful example for physical fiber surface modification. Ion plasma beams were also used for fluorocarbon coatings on polyethylene terephthalate (PET) fabrics with good hydrophobicity[56], which were good for waterproof breathable fiber materials. Additionally, plasma treatment can establish various functional groups on the natural fiber surface, which are able to form strong covalent bonds with a polymer matrix. The strong fiber/matrix interface will improve the performance of fiber. It was reported that plasma method could graft amine functional groups on cellulose acetate (CA) fibers.[57] The NH_3/He or mixture of N_2/H_2 gases were used to graft amine functional groups on the surface of CA fibers as shown in Figure 7b.[57] The density of grafted amines was proved as stable after a period of 60 days.

Meanwhile, the plasma method has also been performed during smart textile manufacture. A wearable graphene-coated fiber sensor[58] was fabricated to monitor the key motions of human body during sports activities like basketball and soccer using this process. The wound polyester (PE) fibers around a polyurethane (PU) core fiber were etched via air plasma treatment, which generated oxygen-containing polar functional groups on the fiber surface, meaning that the hydrophilicity of fiber was significantly increased. This facilitated the combining of fibers with graphene oxide (GO), resulting in an easier and lower cost fabrication process. The final product plasma

Table 1. Plasma components.

Component	Wavelength [nm]	Energy [eV]
Electrons	–	0–10
Ions	–	10–30
UV	$200 < \lambda < 400$	3–40
Vacuum UV	$\lambda < 200$	

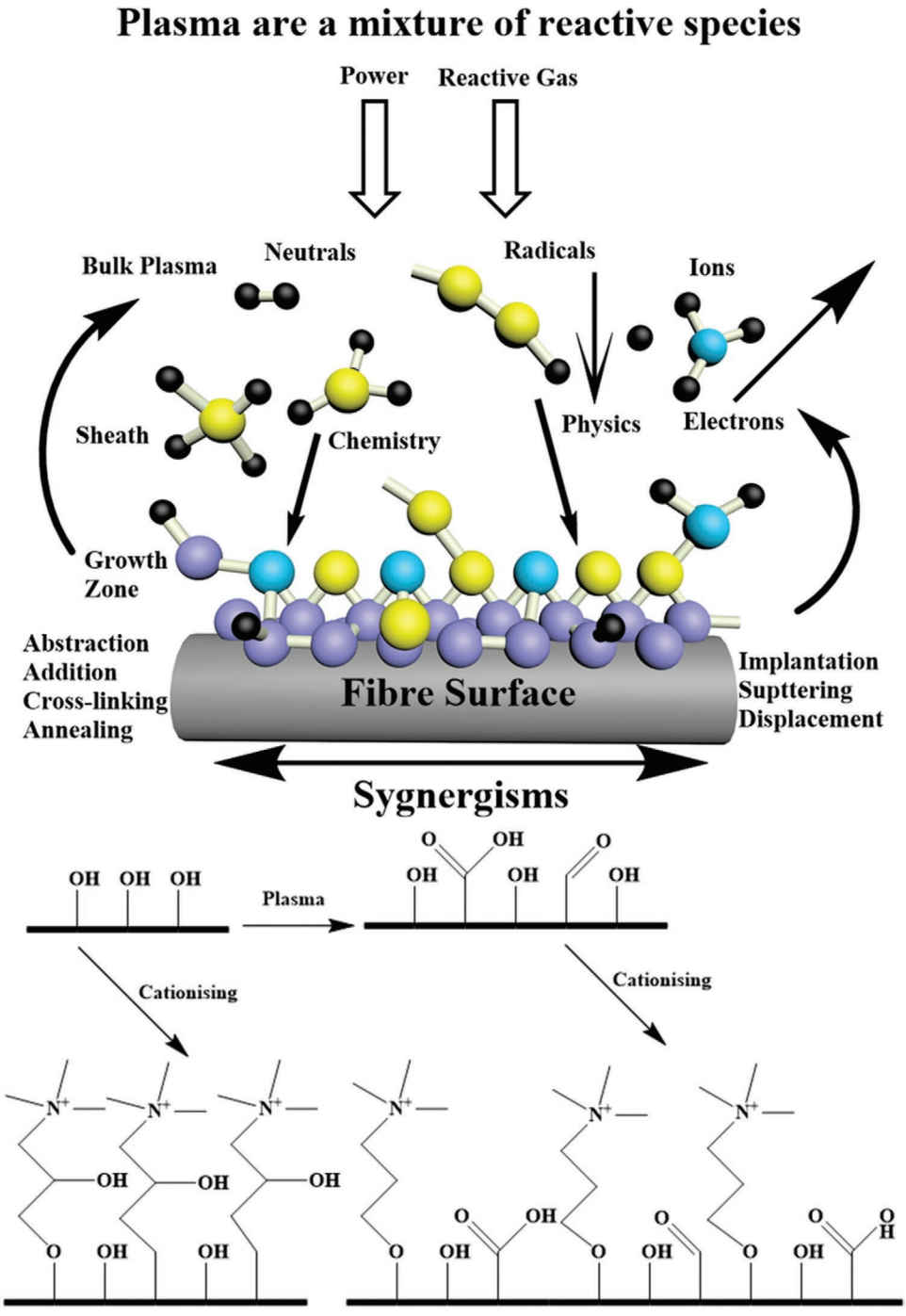

Figure 6. The theory model of plasma effects on modified fiber with different kinds of species from plasma. Reproduced with permission.[43] Copyright 2019, Henniker Plasma (top). The details of plasma effects on modified carbon fiber to improve the dyeability of fabric. Reproduced with permission.[53] Copyright 2013, IntechOpen (bottom).

double-covered yarn–reduced graphene oxide (RGO) fiber was light (at only 0.28 g m^{-1}) enough to be worn on any position of human body. During stretching tests, the resistance of fiber increased proportionally with the change in strain up to 50%. Relatively good linearity was observed and gave the sensor great sensitivity. Regardless of the strain, the fiber maintained stable and accurate performance. The results of motion monitoring were also ideal, with a rapid response time of up to 1–2 s and maintenance of a high sensitivity over many cycles. The fibers showed great potential for sports motion monitoring.

Wu's research group used PE textiles/silver nanowires (AgNWs)/GO to fabricate wearable electricity generators and wearable solar textiles (Figure 7c,d).[59,60] The PE fibers were treated by plasma surface treatment under an oxygen atmosphere to generate

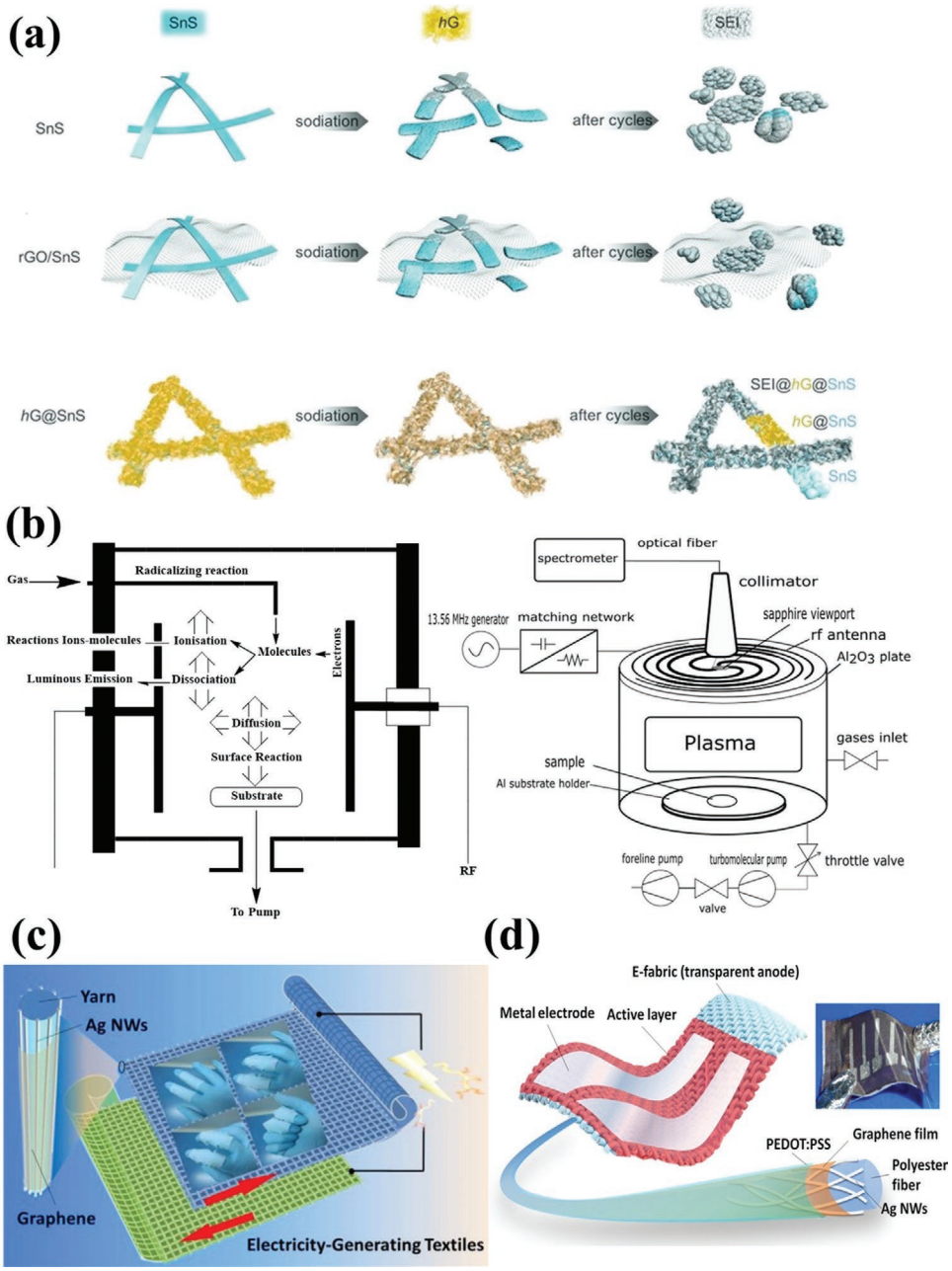

Figure 7. a) Schematic illustration of three types of electrode configurations and their structural evolutions of pure SnS, rGO/SnS, and hG@SnS. Reproduced with permission.[55] Copyright 2018, Wiley-VCH. b) Low pressure plasma 13.56 MHz radiofrequency discharge and low pressure inductively coupled RF reactor with optical emission analyzer. Reproduced with permission.[57] Copyright 2019, Elsevier. c) The structure and mechanism of wearable triboelectric generators made of polyester/AgNWs/ graphene. Reproduced with permission.[59] Copyright 2016, American Chemistry Society. d) Schematic diagram of the PST using a transparent e-fabric with a polyester/AgNW film/graphene core-shell structure as a transparent anode. Reproduced with permission.[60] Copyright 2017, Elsevier.

oxygen-containing polar functional groups. The surface of fibers could then form a better connection with the PE/AgNWs/graphene, which made the product more stable and lead to excellent performance. During these applications, plasma treatment is normally used to produce a uniform coating or etching. The generation of specific functional groups improved the stability of the bond between the fibers and other layers, and improved the quality of final product.

2.2. Irradiation

Irradiation is the process in which an object is exposed to radiation. Usually, there are two types of radiations: ionizing radiation[61] and nonionizing radiation.[62] Ionizing radiation carries enough energy to detach electrons from atoms or molecules and ionize them. Ionizing radiation includes gamma rays, X-rays, and the higher-energy ultraviolet part of the electromagnetic

(EM) spectrum. Conversely, all of the EM spectrum below UV, along with the lower ultraviolet part, is a nonionizing radiation. This includes visible light, laser, infrared, microwaves, and radio waves. Obviously, as its name described, nonionizing radiation lacks the energy to ionize molecules or atoms.[63] An example of UV irradiation is its use on polymer optical fibers (POFs) made of polymethyl methacrylate (PMMA)/gold as shown in **Figure 8**h.[64] The functional groups on the surface of PMMA fiber were modified after irradiation treatment.

By using the characteristics of radiation, surface modification of fiber at different radiation frequencies can be used to combine or detach specific functional groups, depending on the properties of fibers. With irradiation, the structure of fiber surface will change, as evidenced from the surface modification of polyacrylonitrile (PAN) carbon fibers.[65] A 10–30 keV Ar+ high fluence ion irradiation was performed at normal and oblique incidence with PAN-fibers between room temperature and 400 °C. Radiation exposure significantly changed the structure of graphite-like materials up to full amorphization. Recrystallization and crimping of the material shifted the peaks of fiber further from typical graphite-like materials as observed in the material's Raman spectrum.

By selectively reducing GO fiber through laser irradiation, a high-performance graphene fiber power generator (GF-Pg) was produced as in Figure 8a–f.[66] The highly oriented GO sheets assembled within the fiber could provide ideal channels for efficient ion transport to harvest energy from the moisture. A single GF-pg(less than 1 mm, diameter = 80 µm) was produced (355 mV output) due to the humidity variation. This voltage was increased to 1.3 V by adding more device units. Another moisture-activated application[67] was made of GF, which was half reduced via direct laser reduction. The laser writing reduction process has been used for the manufacture of GF or GO/rGO fiber and relevant smart textiles applications for a long time. Like the novel bamboo-like series of in-fiber graphene supercapacitors,[68] GO/rGO fiber was fabricated through the laser reduction and checked by energy-dispersive X-ray spectroscopy. The high energy of the laser can transfer enough energy to break the bond of functional groups, enabling the GO to be reduced to rGO. The degree of reduction was controlled through

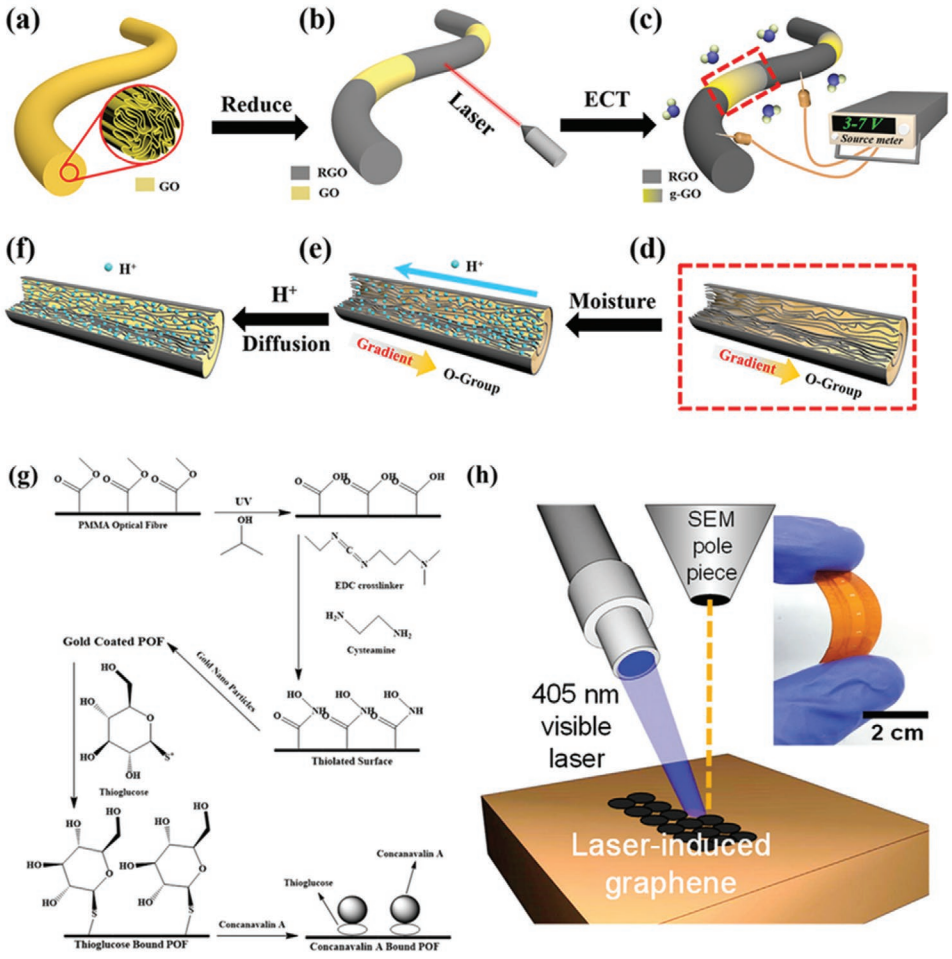

Figure 8. a–f) Schematic illustration of the fabrication of a GF-Pg. H^+ was ionized from the oxygen-related groups and directly transported from the oxidized end to the reduced end derived by the concentration gradients while GO part absorbed moisture. Reproduced with permission.[66] Copyright 2017, Elsevier. g) Reaction designs for POF surface modification and binding tests, PMMA fiber was treated with UV radiation to attach EDC, then could be coated with gold. Reproduced with permission.[64] Copyright 2019, UNSW Australia. h) Laser-induced graphene for wearable humidity sensor. Reproduced with permission.[70] Copyright 2020, Journal of the American Chemical Society.

the laser energy level, effect time, and position. The high capacitance was formed due to the stacking layers of rGO, which prevented penetration and transport of electrolyte. A similar supercapacitor was made of hollow GO fiber, which was treated with high intensity laser for reduction.[69] It also had high specific capacitance of 76.1 F g^{-1}. The similar laser method was used to prepare flexible and wearable humidity sensor made of graphene as shown in Figure 8h,[70] which had high sensitivity of only 250 ms response time to detect human breath.

Cellulose nanofibers (CNFs) can be provided with new features after polymer grafting. However, the process requires large amount of organic solvent which presents a threat to the environment. Instead, UV was used to irradiate an aqueous suspension of CNFs, which generated radicals on the surfaces of the CNFs to further initiate polymer grafting without the use of solvents.[71] The aggregation of CNF-g-PMMA in water facilitated the dewatering process. The resulting dry product had better compatibility with polymers and was easier for storage and supply of CNF materials.

2.3. Annealing

Annealing is a heat treatment to change the physical and sometimes chemical properties of materials, which raises the ductility and reduces the hardness, making materials more workable.[72] The annealing process involves heating a material above its recrystallization temperature, maintaining this temperature for a certain time, and then cooling and recrystallizing. During annealing, atoms migrate in the crystal lattice and the number of dislocations decreases, leading to a change in both ductility and hardness. For fiber surface modification, annealing treatments are usually done by hot pressing or infiltration. Hot pressing is a simple method which directly uses high pressure and high temperature to melt target compounds (typically polymers) on the surface of fibers, which then form strong interface connections through simple adhesion.[73] For some porous fibers, the target compounds are melted and immersed inside fibers. After cooling, the infiltration is finished and new material is produced.[74] Annealing treatments can improve poor bonding at the interface of composites and increase the efficiency of load transfer from matrix to fiber, resulting in better mechanical properties and environmental attack resistance.

The crystallinity of fiber will change after annealing, alongside the structure and functional groups on fiber surface (although this is dependent on annealing temperature). A typical example of natural fiber is Kraft lignin. The glass transition temperature of Kraft lignin is at 142 °C;[76] this increases if the proportion of moisture inside the fibers is decreased using a heat treatment. Degradation of the lignin occurs at ≈214 °C, so some softening is expected to be observed at 200 °C.[77] During this heat treatment, depolymerization of the lignin and some hemi-cellulose occurs, producing lower molecule aldehyde and phenolic-functionalities so that only cellulosic microfibrils are left after annealing.[78] When fibers undergo thermal treatment close to the glass transition temperature of lignin, it is assumed that lignin will be released from the fiber bundles and the remaining fiber constituents are free to produce new single fibers. In this case, the single fibers have greater strength and stiffness than the fiber bundles, which is proven by a study of unidirectional long Kraft fiber reinforced polylactic acid through hot pressing process.[73]

POFs are important in the sensors research field. POF Bragg grating (POFBG) sensors have high sensitivity in pressure, stress, and acoustic-wave detection.[75] The phase-mask technique is the most reliable and simplest method of creating these sensors. However, for specific POFs, the wavelength is unique and a new phase mask must be created, which brings a heavy cost. Since 2011, annealing has become a new method for production like in **Figure 9**a. POF was exposed above its glass-transition temperature. Then the polymer molecules become mobilized, the fiber shrinks in length and the Bragg grating period becomes shorter. The fiber shrinkage possibly occurs due to the removal of residual internal stress, which can be produced during the POF drawing stage. The conditions of annealing here determine the fiber stretching, which is a key factor for the direction and degree of Bragg wavelength shifting and which determines the final properties of POFBG sensors.

Shape memory polymers (SMPs) are able to deform and recover their shapes under certain environmental conditions. They have attracted large interest across the world. Due to the requirements of low-cost processing, low-density, excellent shape memory ability, and flexibility, PU becomes the most suitable material for SMPs. Figure 9b demonstrates Xu's work, which featured PU and clay, the latter of which was first heated at 850 °C for 2 h and held for 12 h under 100 °C.[79] The clay and PU were then treated at 200 °C under mechanical mixing and formed a SMP through a hot-pressing method. The clay content significantly improved the strength of the SMPs and reached peak performance with 30 wt%. After two test cycles, the shape recovery reached 97%, meaning almost full recovery. The annealing treatment was used as a simple method to achieve such a material by improving the connection of the clay and PU. The high temperature melted the surface and made them interact with each other to form stronger bonding.

Annealing is also an ideal treatment method for improving layer-to-layer connections within a smart textile. For wearable electronics power supply, body heat can be effectively transferred into electrical energy using a thermoelectric (TE) power generator. Bi_2Te_3 (n-type) and Sb_2Te_3 (p-type) were two precursors.[80] Both TE films were processing annealing at 530 °C/500 °C under N_2 atmosphere for crystallization and densification of the film. Because of the high thermal tolerance of the glass fiber (600 °C), the fiber remained undamaged and combined better with the precursors. Due to the high temperature, the liquid-like paste of precursors easily infiltrated the glass-fabric meshes through the force of capillary action to form films of several hundreds of microns in thickness. The final product was thin (about 500 μm), light (about 0.13 g cm^{-2}), flexible, and with a remarkable output (28 mW g^{-1} at a Δ = 50 K). The design also significantly reduced the thermal transfer loss.

Similarly, new anode materials of lithium-ion batteries were produced by annealing treatment as shown in Figure 9c.[81] The $ZnCo_2O_4$/C@CF was obtained by annealing the as-synthesized sample at 400 °C for 3 h under N_2 flow. This sample exhibited outstanding cycling stability with capacity of 463 mAh g^{-1} at 50 mA g^{-1} after 100 cycles (201% higher than pristine CF). The hydrophobic coatings of CNFs were made by hot-press with

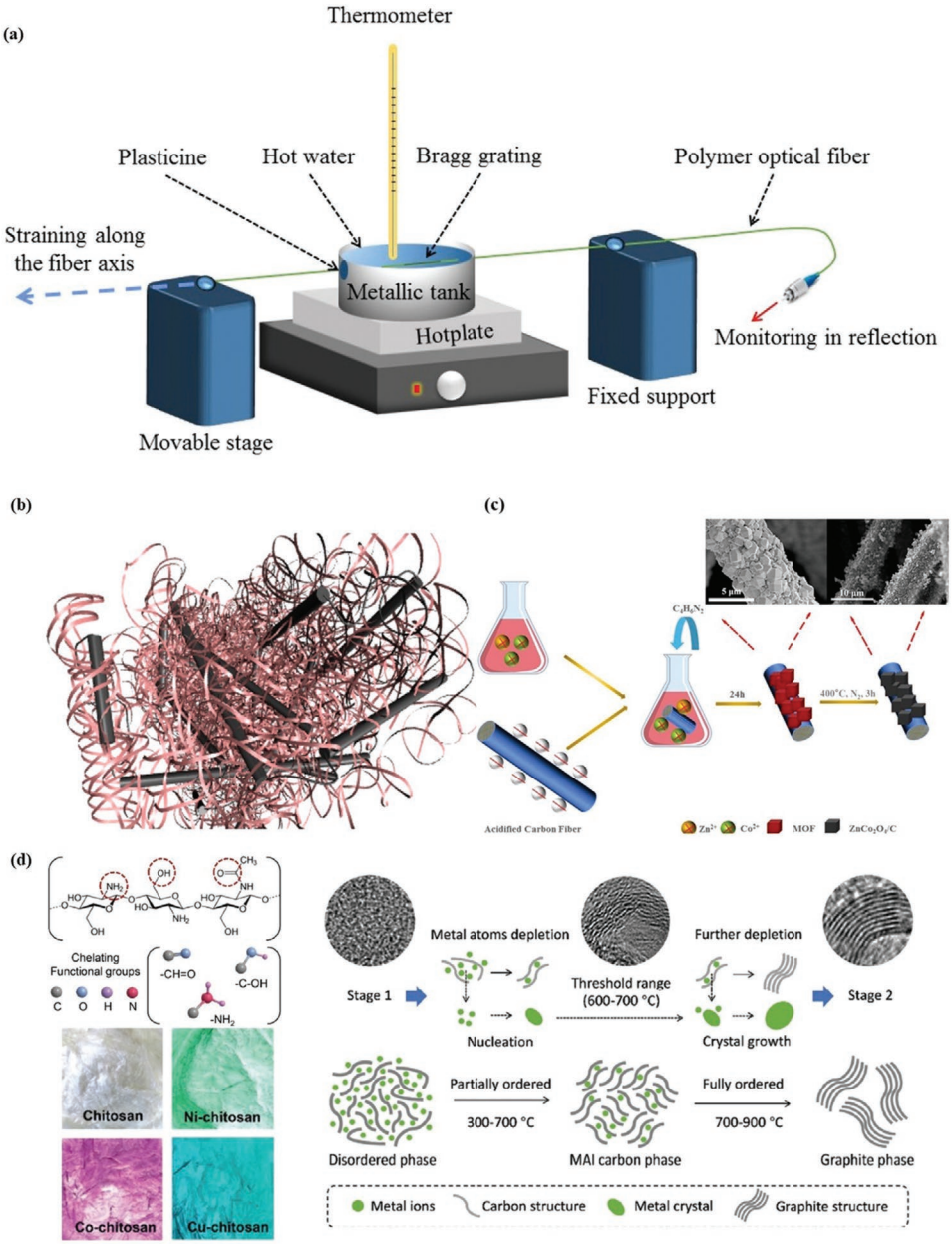

Figure 9. a) Experimental setup to strain and anneal the POFBG: The POFBG was kept in the water at room temperature (25 ± 2 °C). After 40 min, the Bragg wavelength had stopped shifting due to water absorption, then the annealing began. Reproduced with permission.[75] Copyright 2018, The Optical Society. b) Nanoclay embedded inside the PU matrix. Reproduced with permission.[79] Copyright 2010, MDPI. c) The process of MOF-derived $ZnCo_2O_4$/C anchored on carbon fiber via a facile and subsequent annealing treatment. Reproduced with permission.[81] Copyright 2019, Chinese Chemical Society. d) The chelating functional groups in chitosan and frozen samples, alongside the illustration of annealing process. Reproduced with permission.[84] Copyright 2020, Wiley-VCH.

a pressure of 1800 kg cm^{-2} at 100 °C for 2 h.[82] The nitrogen-doped mesoporous carbon (NMC) was modified by 2D transition metal selenides to form catalysts.[83] NMC was first annealed at 900 °C for 1 h using a ramp rate of 5 °C min^{-1} in Ar atmosphere, then nanosheets (CoSe, FeSe, or $FeCoSe_2$) were added in liquid under stirring and 150 °C annealing for 10 h to facilitate strong bonding. CoSe@NMC possessed 1.52 V potential for OER and 0.90 V half-wave potential for ORR even after 5000 ADT cycles, further presenting annealing as a promising, simple technique for high performance electrochemical applications.

Lastly, the correlation between the crystallization–precipitation graphitization period process and the spatial graphitization of a carbon network was determined by the annealing treatment of different temperature from 300 to 900 °C with Ni/Co/Cu metal atoms as shown in Figure 9d.[84] The structure and properties of the formed carbon networks were influenced through different crystallization mechanisms of transition-metal catalysts, which showed great potential for customizing carbon networks to meet different requirements of the applications of energy storage/conversion systems.

2.4. Surface Covering

The surface covering technique is also known as surface coating. This method involves coating a particular material onto another material for a specific purpose, such as improving hardness, acid and alkali resistance, chemical shield, light penetration, etc.[85] The purpose of applying the coating may be decorative, functional, or both. Functional coatings may be applied to change the surface properties of the substrate, such as adhesion, wettability, corrosion resistance, or wear resistance. Surface coating of textiles can be defined as physical or chemical depending on whether the coating forms crosslinks with fibers. If the chemical reaction occurs away from the fiber, the final product is simply coated on the fiber surface—this is a kind of physical method. If chemical reactions occur at the fiber surface, it is a chemical method. The typical physical methods are physical vapor deposition (PVD) and chemical vapor deposition (CVD). When coating natural and synthetic fibers, wetting and adhesion of the surface, along with the coating thickness, are key factors for high product quality. For improved adhesion, the fiber and matrix should maintain a constant intermolecular distance.

In **Figure 10**, a typical CVD process is described, which begins with reactants in different tanks, including an initiator (red) and one or more monomers (purple and blue). These are the building blocks of the desired polymer coating. Through heating or reducing the pressure, the reactants are vaporized. After that, they are introduced into a vacuum chamber containing the material to be coated (the substrate material). The function of the initiator is to increase the speed of process by increasing the rate of monomer linkage. Finally, polymers form on the surface of the substrate material.

Boron nitride (BN) is a potential interface material for preparing continuous fiber reinforced ceramic matrix composites (CFCCs or CMCs). However, the coating of BN on ceramic fibers remains uncontrollable. Recently, a low temperature CVD method was used to produce controllable coating BN on alumina fibers by using BH_3NH_3 as single source precursor under atmospheric pressure.[88] The results from X-ray photoelectron spectroscopy (XPS) and Fourier-transform infrared spectroscopy (FTIR) have confirmed the high purity of coatings obtained at the deposition temperature of 700 °C. A variation of deposition temperature and duration can control the thickness and structure of the BN coatings. The tensile strength retention reached up to 94.9%, which proved the great potential for this method to fabricate high performance CFCCs or CMCs. Figure 10 describes a typical PVD process. The usual three steps involve[88]

1) Using a high temperature vacuum or hitting a solid source of the coating material with gaseous plasma to vaporize it.
2) Transfer the vapor to the substrate surface under full/partial vacuum situation.
3) Produce thin films by condensation on the substrate surface.

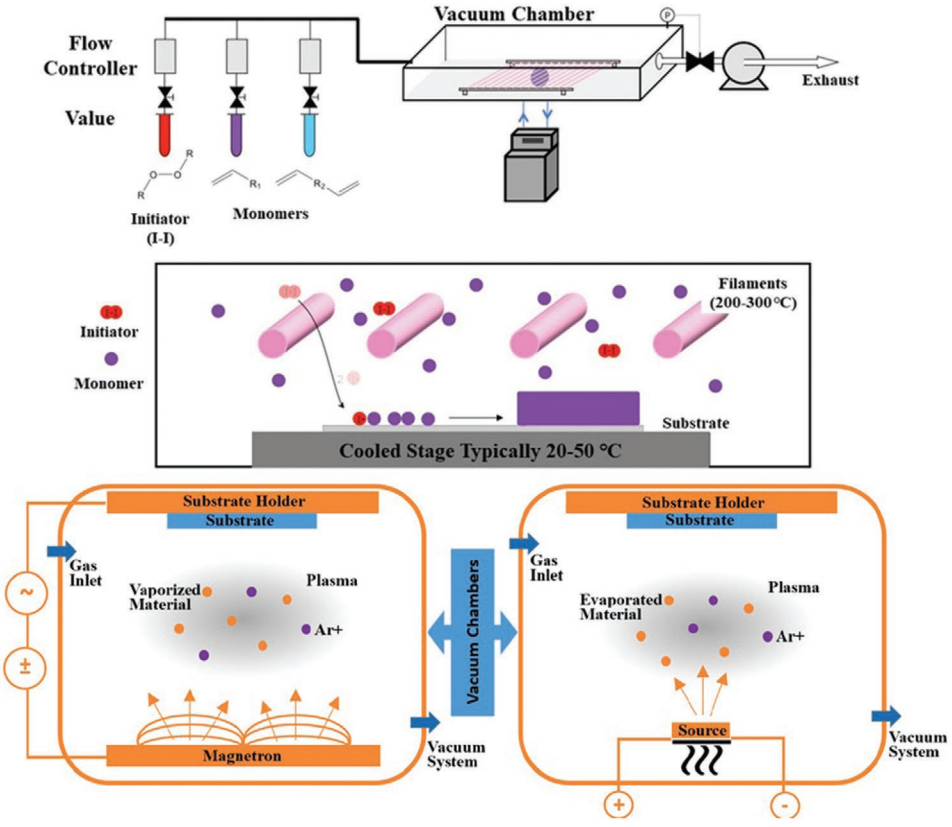

Figure 10. The theory model of CVD process. Reproduced with permission.[86] Copyright 2015, Massachusetts Institute of Technology (top). The illustration of PVD process. Reproduced with permission.[87] Copyright 2018, MDPI (bottom).

The two most common PVD processes are thermal evaporation and sputtering. Thermal evaporation relies on heating the material through appropriate methods in vacuum to generate vapor. Sputtering generates a vapor by hitting the source with accelerated gaseous ions (typically Argon). Then, the coating is achieved after proper cooling setting.

The PVD method is a successful method for creating protective coatings. Carbon fiber reinforced polymers (CFRP) have poor wear resistance and can cause severe problems while the material is subjected to solid particle erosion. Coatings of Ti, Al, Cr and Ti/TiN were coated on CFRP by PVD.[89] The results showed that Ti/TiN hybrid coating had the best performance to prevent erosion.

Surface covering was also used to forge anti-UV radiation smart textiles as well.[90] Unlike the current fabrication process, this technique did not require complicated equipment, complex procedures, and hazardous chemicals (**Figure 11**a). Instead, the raw materials were simply mixed for 10 min and the O-In functional groups inside the metal-oxide framework (MOF) interacted with hydroxyl groups on the cotton surface and amide groups on the aramid/polyester surface, resulting in the final product being stable enough to be used for many cycles.

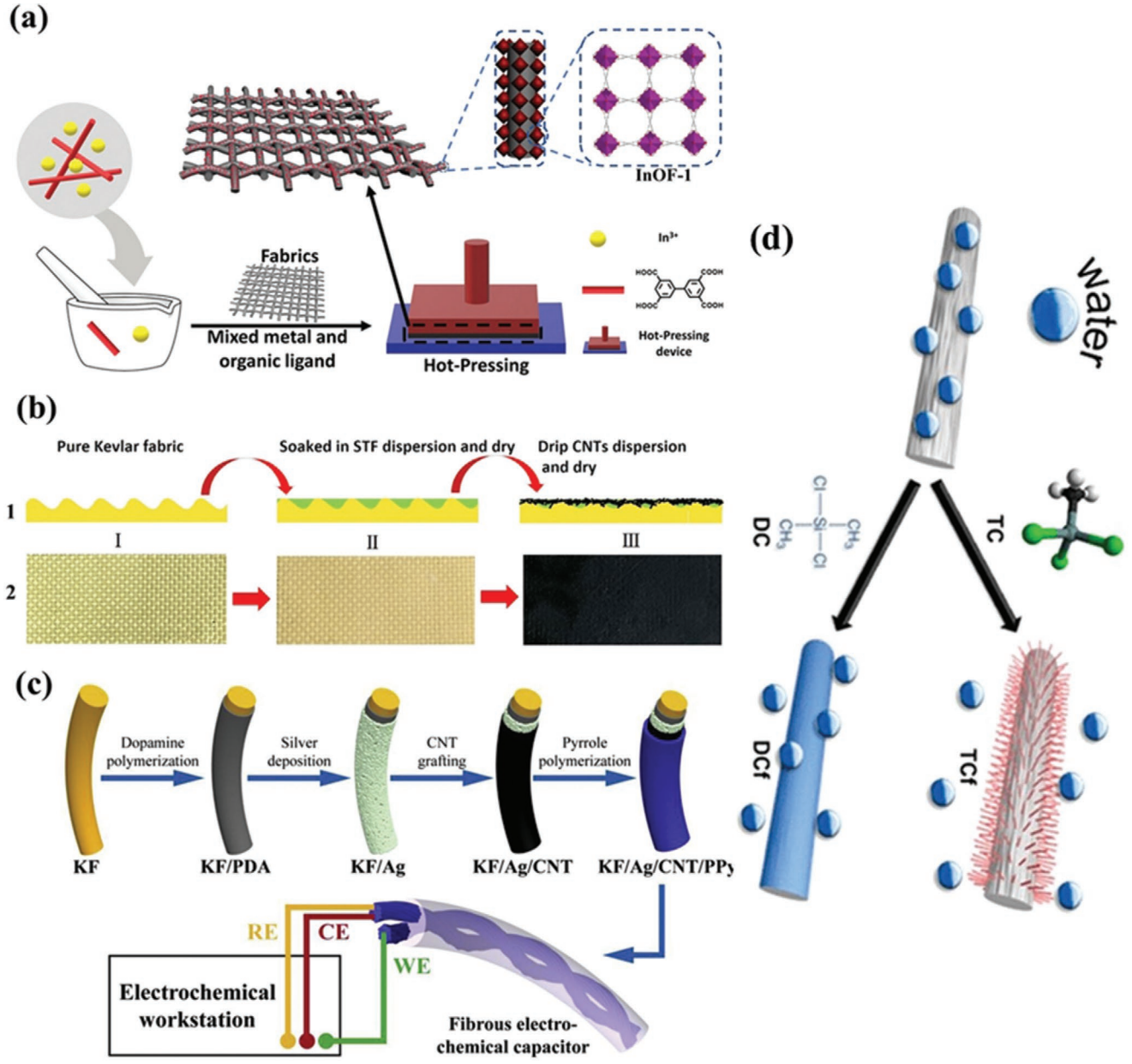

Figure 11. a) The glass fiber and two different precursors. Reproduced with permission.[90] Copyright 2019, Wiley-VCH. b) Formation process of the CNT/shear thickening fluid (STF)/Kevlar composite in series 1, Pristine Kevlar in series 2, along with (I), STF/Kevlar(II), CNT/STF/Kevlar(III). Reproduced with permission.[91] Copyright 2019, Elsevier. c) Schematic preparation of KFs/AgNPs/CNTs/PPy. Reproduced with permission.[92] Copyright 2019, Elsevier. d) The chemical modification of a CNF filament with TC and DC. Reproduced with permission.[93] Copyright 2018, American Chemical Society.

The modified cotton and polyester textile samples reached ultraviolet protection factor >>50, which displays excellent anti-UV properties for use as wearables. The test results also indicated that the water vapor permeability remained almost unchanged, which is optimal for human comfort. Separately, a new smart textile with excellent protective and sensing performance was designed by Kevlar.[91] Their final composite achieved the maximum resistance force of 1232 N in dynamic impact resistance test through the single-layer structure, ≈ 65.15% higher than pristine Kevlar (746 N). The results were notable since the composite was fabricated through a simple dip-dry process repeated several times, as shown in Figure 11b.

Sometimes, nanocrystal generation also occurs during the fabrication of smart textiles by alkaline treatment, such as in Figure 11c, with nanocrystals of aramid fibres (KFs)/silver nanoparticles (AgNPs)/carbon nanotubes (CNTs)/PPy.[92] This smart textile exhibited excellent cyclability and wearability while the capacitance retained 94.0% after 1000 cycles and 93.2% after bending 500 times. Cellulose fibers possess a high moisture sorption capacity,[94–96] which is beneficial in wearable textiles. Many methods have been performed for obtaining textile filaments from CNFs through spinning.[97–110] A simple CVD method using trichloromethylsilane and dimethyldichlorosilane could cover the hydrophobic CNFs with a smooth and soft coating like polydimethylsiloxane (PDMS) as shown in Figure 11d.[93] The results indicated that water contact angles up to 116° could be achieved with lower surface energy requirements, which was caused by the unique fiber surface of continuous, homogeneous coating layers or 3D hair-like assemblies. The wet strength of the samples was increased by almost 200% than pristine CNFs. Equivalently, polymethylsilsesquioxane (PMSQ) nanofilaments were coated on cotton, wool, 2,5-acetate, and polyethylene glycol (PEG) fibers via simple one-step approach under gas phase for creating superhydrophobic textiles.[111] The property of hydrophobicity was further promoted for functional textiles. These methods have continued potential applications on many different fiber-based materials.

2.5. Nanocrystal Generation

This method is used to create a nanocrystal seed layer on the surface of fiber through a specific approach like dip-coating. The layer can then grow in an environment of precursor chemical solutions as shown in **Figure 12**.

The most common approaches for this employ the dip-coating method for ZnO seed generation on fiber surfaces and the hydrothermal method for nanowire growth. The CF/ZnO–ZnSe[112] was a typical flexible nanogenerator (NG) device with high-output current ≈333 μA (66% increase) when the device was subjected to a –0.55% tensile strain via simple two-step hydrothermal method. The ZnO nanoarray acted as the anchor for ZnSe nanocrystals and formed a strong connection as shown in Figure 12a. Ehlert and co-worker's work used this method to coat the ZnO nanowires interphase on carbon fibers.[113] The results showed that the growth of ZnO does not affect fiber strength. Meanwhile, the interfacial shear strength can be increased by 113%, plus 37.8% and 38.8% increase on the laminar shear strength and modulus. Due to piezoelectric and semiconductive properties of ZnO, embedded functionality was also enabled at the interface. Another new ZnO reinforced CF was fabricated with varying nanowire dimensions.[114] The interfacial shear strength was significantly increased by up to 228%. More importantly, the tensile strength of the ZnO nanowire coated fibers was unaffected during all growth procedures. For wearable electronics, a new triboelectric nanogenerator (TENG)-cloth was produced through ZnO seed nanocrystal generation at 95 °C during 3 h in Figure 12b.[115] The results indicated that output voltage and current were as high as 120 V and 65 μA on a nanopatterned PDMS/Ag/textile/ZnO fabric, while nonnanopatterned fabrics only achieved 30 V and 20 μA, indicating a significant improvement when using nanocrystal functionality. Additionally, cotton fabric was dip-coated with chitosan/pentasodium tripolyphosphate for antibacterial purposes,[116] with an easy and low cost method for large scale of production. Even the hydrophilic cotton fabric could be changed to superhydrophobic through dip-coating to produce a ZnO nanorod array.[117] The ZnO nanorod/PVDF nanofibers were produced by dip-coating in zinc acetate three times and converting the mechanical movements effectively, especially human motions into electricity.[118] Multiple applications may be produced via this treatment method.

However, it is difficult to control the size and shape of ZnO seeds by the dip-coating method. The alignment and properties of hybrid fibers with ZnO nanoarrays will also be decreased by a low seeding quality. To overcome this, atomic layer deposition (ALD) was used to produce ZnO nanoarrays on hybrid structural fibers in Wang's work.[119] ALD has been well accepted as a micromanufacturing technology to grow thin films. It is able to meet the requirements for sequential and self-limiting surface reactions to control atomic layer and conformal deposition. ALD can be performed at low temperatures, which benefits sensitive materials and substrates. The results indicated that regardless of changes to the reagent concentrations and hydrothermal process time, the crystal structure remained the same. ALD has been further promoted to deposit ZnO, Al_2O_3, and TiO_2 on the surface of polypropylene for coupling volatile organic compound oxidation catalysts in Figure 12c.[120] The thin films combined MnO_2 crystals with the largest fraction of available surface oxygen groups, resulting in 99.5% reduction of formaldehyde after 60 min, which was a huge improvement. This offered a good solution to fabricate light-weight structural composites with enhanced interfacial properties.

Cellulose fibers also offered a benefit from dip-coating. The relevant networks with two unique layers of paraffin wax and poly(dimethylsiloxane)-*b*-poly(ethylene oxide) (PDMS-*b*-PEO) diblock copolymer on the surface showed oil separation efficiency up to 99% via a two-step dip-coating in Figure 12d.[121] The sample presented superhydrophilicity and underwater superoleophobicity. Compared with the chemical treatment through methyltrimethoxysilane, dip-coating method was easier and had 11.1% higher oil separation efficiency.[122]

3. Chemical Treatment

Chemical treatment, as evidenced by the name, is a method to treat fibers with a variety of chemicals for surface modification.

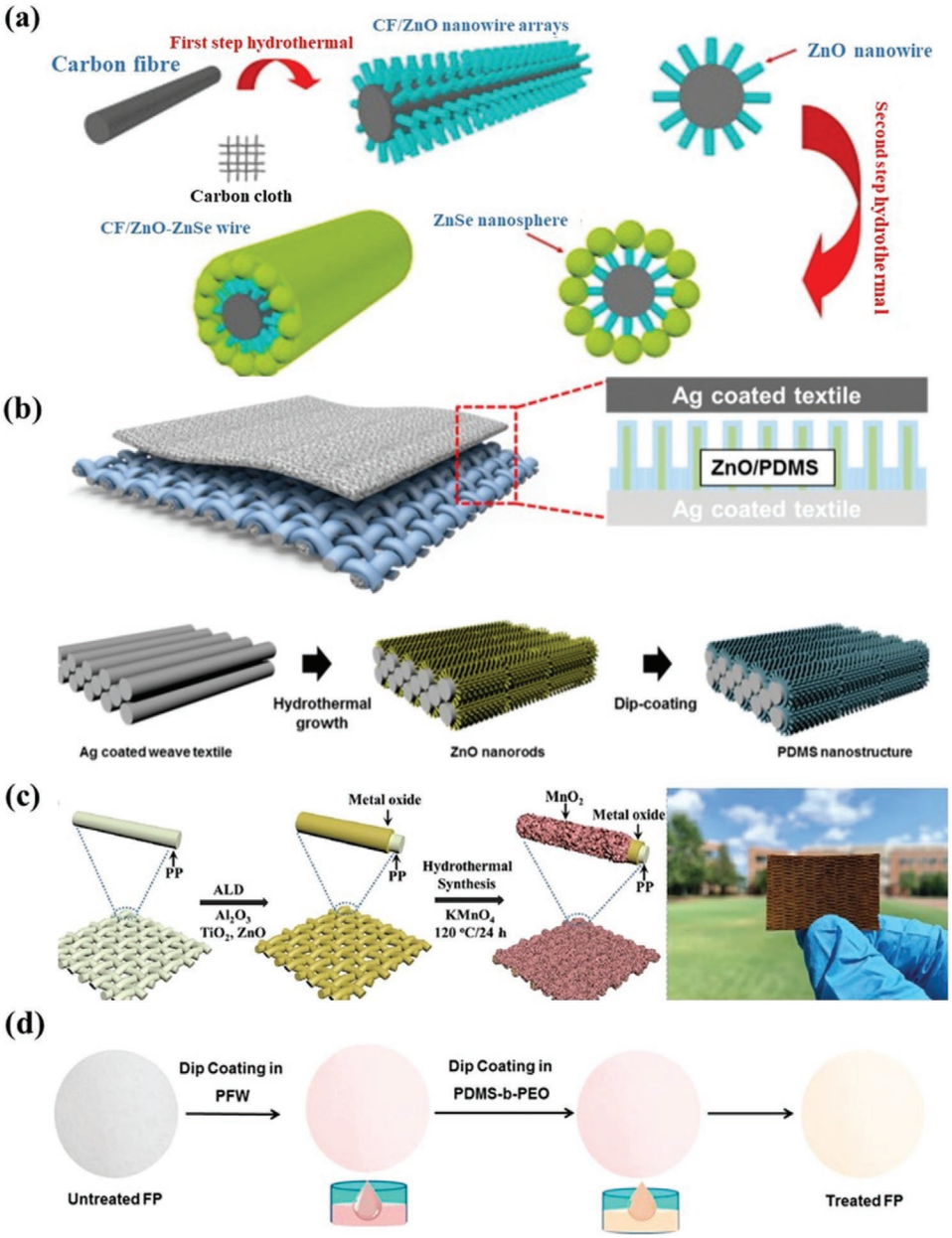

Figure 12. a) The hydrothermal process of ZnO/CF fabric. Reproduced with permission.[112] Copyright 2014, Elsevier. b) The hydrothermal process of the formation of the PDMS/Ag/textile/ZnO fabric. Reproduced with permission.[115] Copyright 2015, American Chemical Society. c) The fabrication of MnO_2@MO@PP fibrous filter. The original white PP mat becomes uniformly yellowish after ALD, then becomes uniformly dark after MnO_2 growth. Reproduced with permission.[120] Copyright 2020, Wiley-VCH. d) The fabrication step of PFW/PDMS-*b*-PEO-treated fiber paper. Reproduced with permission.[121] Copyright 2016, MDPI.

The chemicals include alkalis, silane, water repelling agents, peroxides, permanganates, etc.[13] It has been reported that the mechanical properties of natural fibers can be improved using this method by modifying their crystalline structure along with removing weak components like hemicelluloses and lignin from original structure. In addition, moisture absorption and subsequent swelling of natural fibers, as previously mentioned, can be reduced through selective chemical treatments (like water repelling agents). Moreover, the fiber and matrix interfacial interactions can be strengthened with the formation of strong chemical bonding after specific chemical treatments (such as silane coupling agents), which result in considerable improvement in terms of mechanical performance. The relevant methods are introduced as listed in **Figure 13**.

3.1. Alkaline and Acid Treatment

Alkaline treatment, also known as mercerization, is a method to increase interfacial bonding strength between ligno-cellulosic

Figure 13. Typical methods of chemical treatment for fiber surface modification.

fibers and thermoset resins. It is one of the most widespread chemical treatments of natural fibers, particularly for reinforcement of thermoplastics and thermosets. After alkaline treatment, the fiber diameter is reduced,[92] and lignin, hemicellulose, wax, and oils covering the surface of the fiber are removed. Alkaline treatment disrupts the hydrogen bonding in the network structure, which increases surface roughness: the development of a rough surface topography leads to better fiber–matrix interface adhesion. The proportion of cellulose exposed on fiber surface is increased so that the degree of bonding between fiber surface and polymer increases as well. Therefore, fibers are often treated with NaOH alkaline solution to improve their physical and mechanical properties like in Equation (1)

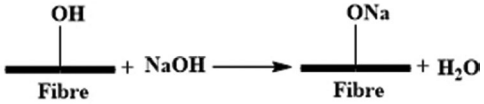

(1)

In this case. the cellulose fibril, the degree of polymerization, and the extraction of lignin and hemi cellulosic compounds are directly affected by alkaline processing.[123] In nature, banana fibers are directly gathered from the stems of banana trees, which are cheap and abundant. However, due to the drawbacks of natural fiber, banana fibers are highly unlikely to be used as a single-component strong material. However, the used agricultural waste of banana fibers was used for matrix composite reinforcements after alkaline treatment,[124] with 5 wt% of sodium hydroxide used to treat the fibers. Various fiber loadings of composites were prepared and tested ranging from 5 to 20 wt% in **Figure 14**a. The alkaline treatment of the banana fibers caused better adhesion of the epoxy and created surface roughness, which enhanced the bonding between fiber and matrix and led to better tensile and yield strength. Another successful example of alkaline treatment reinforced a resin matrix through the inclusion of kenaf fibers pretreated in a 6 wt% NaOH solution at room temperature for 48 and 144 h.[125] The alkaline treatment increased the mechanical properties of the composites because of improved fiber–matrix compatibility. The composites with randomly oriented fibers with length of 40 mm increased the tensile strength and modulus by 36% and 12%, respectively, compared to the composites with untreated fibers; it was an obvious enhancement. A similar method was

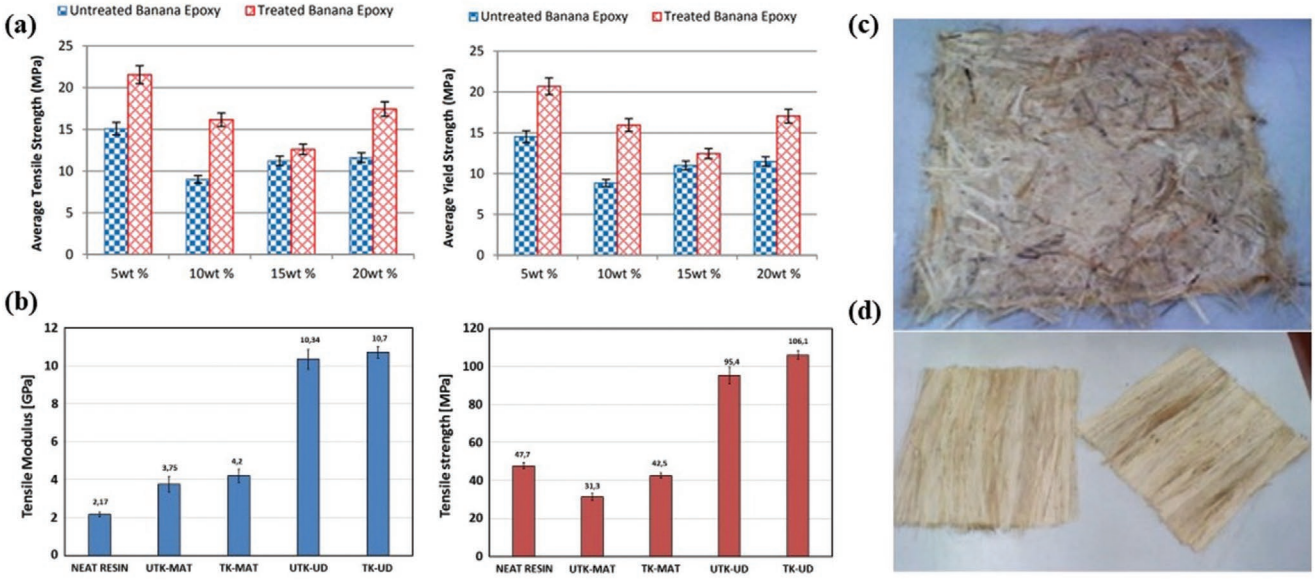

Figure 14. a) The effects of banana fiber loading on tensile strength and yield strength. Reproduced with permission.[125] Copyright 2017, Elsevier. b) Tensile modulus and strength between pristine composites and after alkaline treatment. Kenaf layers samples of c) used MAT and d) UD. Reproduced with permission.[127] Copyright 2014, Elsevier.

used to obtain thin and uniform cellulose nanofibers with 6 wt% KOH.[126] First, hemicelluloses were formed into a solution by mixing 12–16 nm width nanofibers and then easily separating them by a simple mechanical treatment to isolate the 15 nm width samples, as the strong hydrogen bonding between the bundles post removal of the matrix was broken.

With the alkaline treatment, selected parts of the fiber surface can be removed to change specific properties. The laminated hybrid composite materials based on Rafia fibers and glass fibers in a sandwich structure successfully demonstrated this idea, as shown in Figure 14b–d.[127] The removal from the fiber surface of a certain amount of wax, hemicellulose, pectin, and lignin was confirmed by FTIR. Compared with untreated samples, the flexural modulus increased by 3.4–3.6 GPa after alkaline treatment along with a sharp increase of 38% in shear stress and a decrease in the thermal conductivity.

Alkaline treatment was also used to produce smart textiles. A fibrous electrochemical capacitor (FEC) of KFs/AgNPs/CNTs/capacitive polypyrene (PPy) was fabricated through alkaline treatment.[91] Sodium/ammonium hydroxide was used to treat the surface of KF fiber to produce functional groups and form a stable connection with polydopamine (PDA), which was then exchanged for Ag. The capacitance retention was 94.0% after 1000 cycles and 93.2% after bending for 500 times, which were excellent performances as a wearable FEC.

Surface functionalization with acid is the most widely used carboxyl functionalization method, especially for carbon fiber.[128] Due to the smooth surface and lack of oxygen-containing functional groups, the interfacial adhesion of carbon-fiber-reinforced materials is poor. HNO_3 was used to generate oxygen-containing functional groups on the surface and a greater polymer content was added to the composite (5%–30%), resulting in an increase in tensile strength and tensile modulus.[129] A coupling agent *N*-(4-amino-phenyl)-2-methyl-acrylamide was used to facilitate the covalent bonding between carbon fibers and vinyl ester resin (VE) by the treatment of H_2SO_4/HNO_3, which exhibited 19.4% and 90.5% increase of flexural strength and interface shear strength than pristine CFs/VE composites.[130] CFs/VE could also be enhanced by grafting acrylamide with epoxy sizing agent on CFs surface as shown in **Figure 15**a[131] with similar acid treatment. The surface functional groups such as carboxyl and hydroxyl increase the activity of the carbon electrodes due to an enhanced electron transfer.[132] In this case, acid treatment is also effective for the carbon electrode materials.

However, HNO_3 is such strong oxidant that it can cause overoxidation: $H_3PO_4/H_2SO_4/HNO_3$(v:v:v = 1:9:3) were used together to prevent this.[133] The carboxyl groups and other acidic functionalization groups were generated by H_2SO_4 and HNO_3. Through the formation of a cyclic structure with carbon—carbon bonds and prevention of bonds breakage, H_3PO_4 hindered the formation of defects on the turbostratic structure of carbon fibers so that the tensile strength of carbon fibers was preserved and a better electrochemical performance was achieved. This method may be generally applicable to other graphene-containing materials, including CNTs and highly

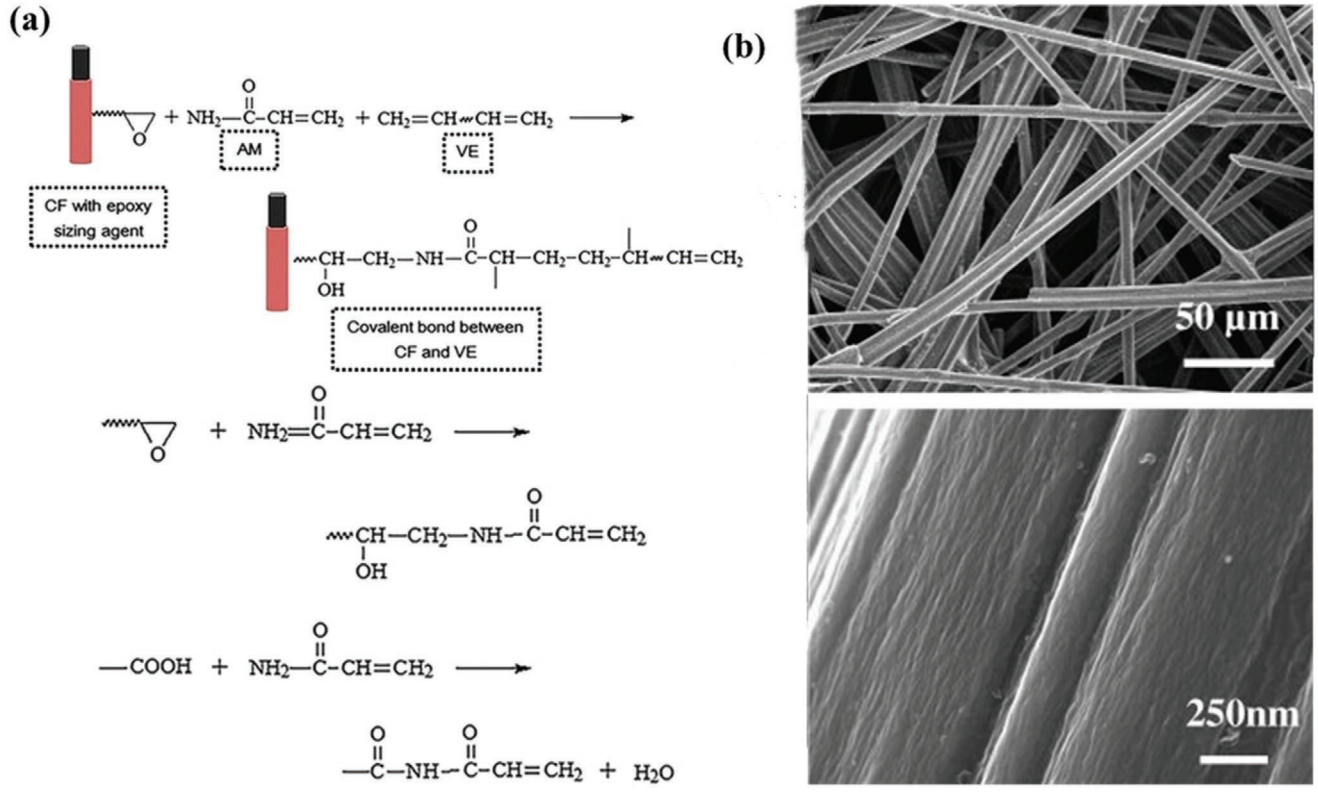

Figure 15. a) The combination process of CFs/VE. Reproduced with permission.[131] Copyright 2017, Springer. b) Surface morphology of carbon fiber after 4 h acid treatment. Reproduced with permission.[134] Copyright 2008, Elsevier.

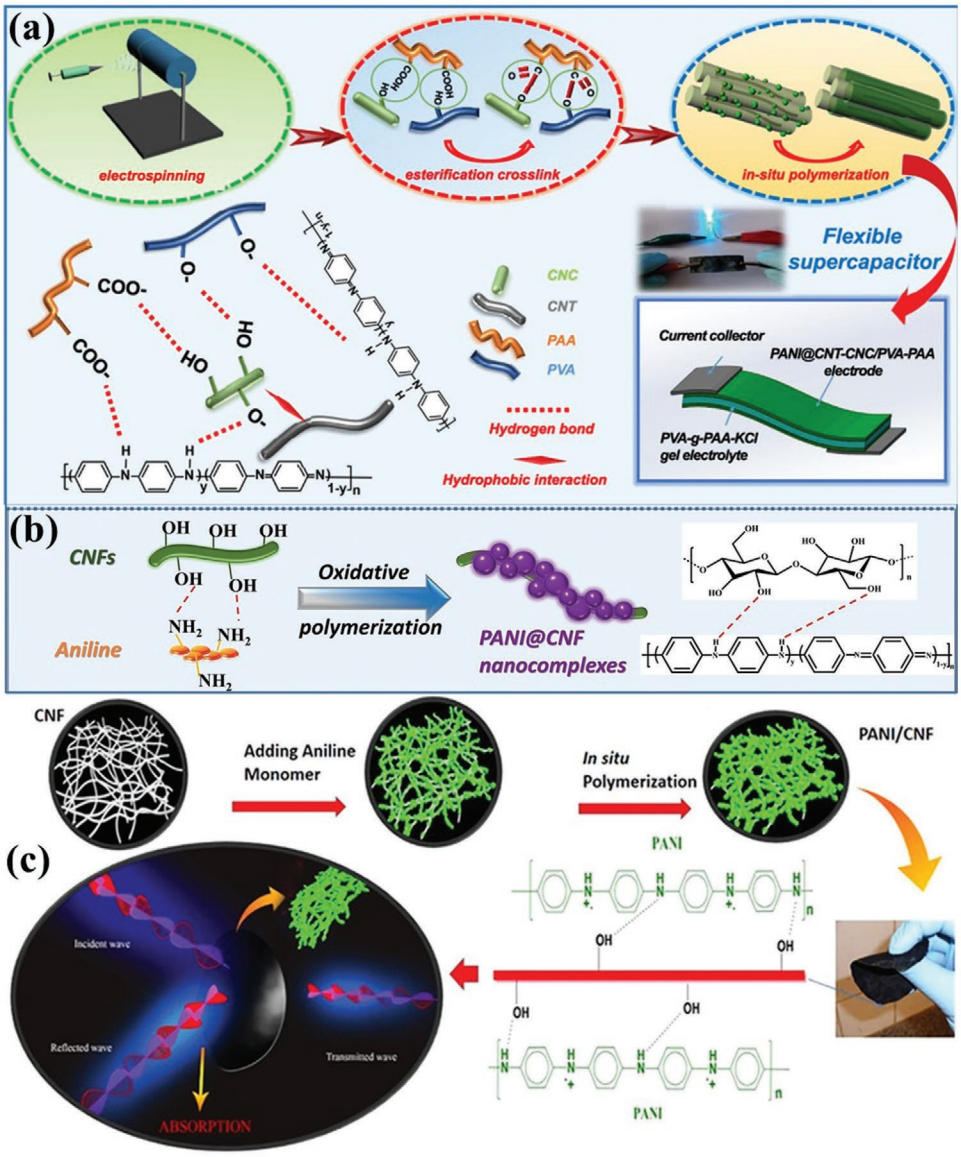

Figure 16. a) The coating process of ANI or Py on the surface of CNF. Reproduced with permission.[135] Copyright 2019, American Chemical Society. b) The mechanism of PANI/CNF or PPy/CNF combination. Reproduced with permission.[136] Copyright 2019, Elsevier. c) The images of polymerization of aniline monomers onto cellulose nanofibers. Reproduced with permission.[137] Copyright 2018, American Chemistry Society.

oriented pyrolytic graphite, by using similar H_2SO_4/HNO_3 ratios, as shown in Figure 15b.[134]

To preserve the tensile strength, increase the capacity, display a positive effect on electrochemical kinetics, decrease the charge–transfer impedance, and ensure the stability and reversibility of the capacity, an acid treatment is a good choice, as it can enhance the bonding between carbon fibers and other suitable materials such as polymers. In addition, the acid treatment is necessary for the oxidative polymerization of nanofibrous membranes (typically polyaniline (PANI) attached on the surface of CNF), such as PANI@CNT–CNC/PVA–PAA,[135] PANI@CNF–PVA,[136] PANI/CNF nanopapers[137] as shown in **Figure 16**.[138] The HCl was applied on pretreatment of CNF to form CNF–COOH as initial regents with sufficient functional groups as in **Figure 17**.[139] To further decrease the energy requirements, dilute oxalic acid was used to pretreat a kraft bleached eucalyptus pulp (BEP) fibers.[140] The mechanical fibrillation process was facilitated by pretreatment, and the natural chain length of fibers was not decreased by the acid hydrolysis and milling in general. Meanwhile, the mechanical strength was retained.[141]

3.2. Silane Treatment

Silane treatment is the most effective method to reduce moisture uptake of fibers under humid environments. Extended use of natural fibers is limited due to their hydrophilic properties, which influences their adhesion with a hydrophobic matrix and decreases the mechanical properties of the final

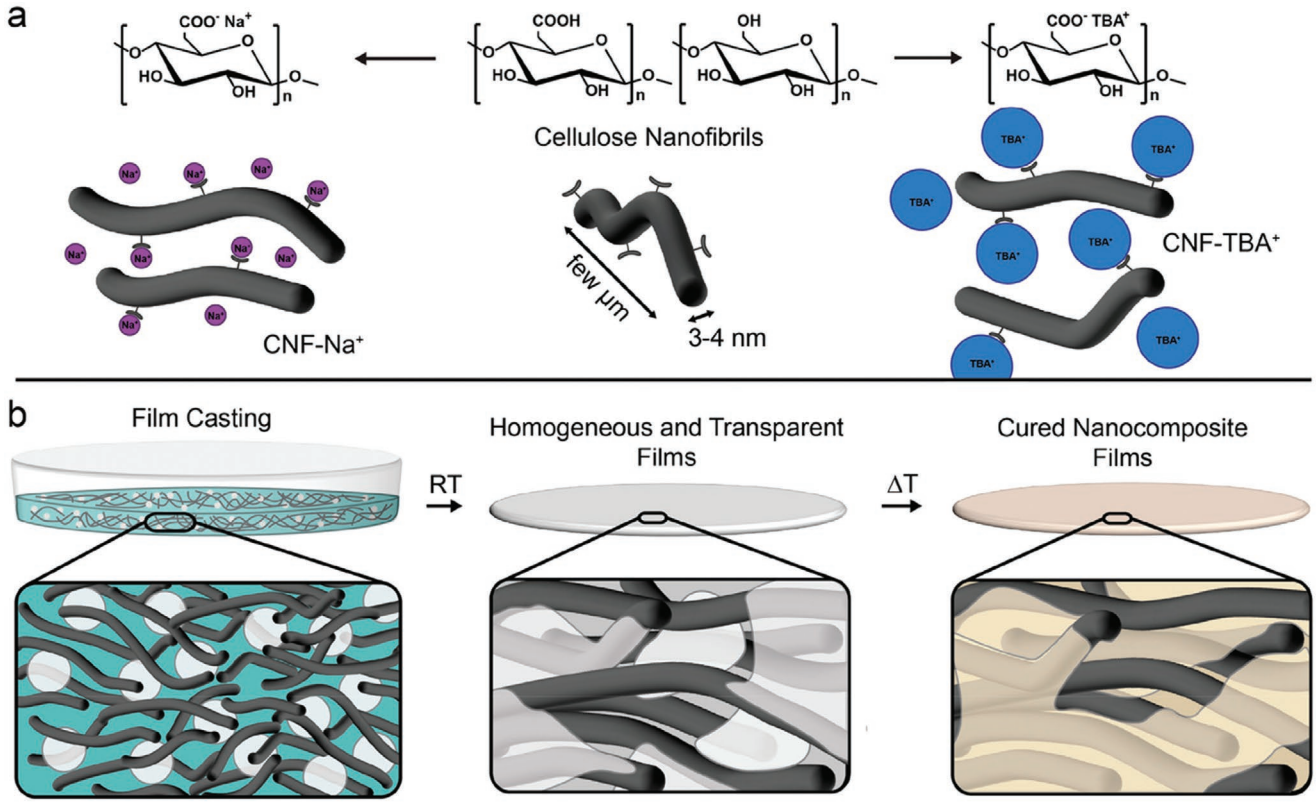

Figure 17. a) Counterion-exchanged with alkali metal (Na^+)/quaternized ammonium (TBA^+) for CNF–COOH suspensions at neutral pH. b) The CNF network was infiltrated by the Pu resin during water evaporation and formed PU/CNFs via cross-linking interaction. Reproduced with permission.[139] Copyright 2019, American Chemistry Society.

composite material. Thus, the chemical coupling method has proved an important surface modification method to improve the interfacial adhesion. The fiber surface is treated with a compound that can form bridging chemical bonds between the fiber and the matrix. Silane coupling agents are hydrophilic compounds in which a silicon atom can be bonded with various functional groups and act as a bridge: one end interacts with matrix, and the other one is connected with hydrophilic fiber as shown in Equations (2) and (3)[142]

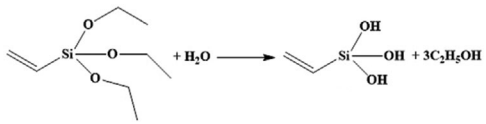

(2)

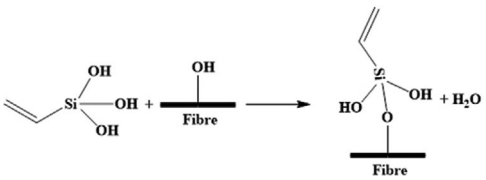

(3)

SiH_4 is the chemical formula of silane. Silane coupling agents can reduce the number of cellulose hydroxyl groups in the fiber/matrix interface: hydrolysable alkoxy groups attached to the silane lead to the formation of silanols when in humid environments. The silanol will react with the hydroxyl group of the fiber and form stable covalent bonds to the cellulosic cell walls of the fiber; these are attached onto the fiber surface chemically.[143,144] The details of this process are shown in **Figure 18**a–d.

As mentioned above, the water absorption of the fiber can be reduced after silane treatment. For this reason, Liu et al.'s[145] work examined silane-treated corn stalk fiber (CSF) reinforced polymer composites that exhibited a promising property of low density. Additionally, the apparent porosity of the polymer system was effectively decreased after silane treatment. In this case, the formation of superhydrophobic fiber surfaces was highly possible. Gao et al. created fabric samples by using silica sol nanoparticles and nonfluorinated alkylsilane, which greatly increased the roughness of fiber surface as shown in Figure 18f,g.[146] The treated cotton and polyester samples were resistant to hydrolysis after 30 washing cycles while demonstrating a <10% reduction in the fabric tensile strength and negligible changes in fabric whiteness and air permeability. Another superhydrophobic modified cotton fabric was fabricated through SiO_2 nanoparticles, ZnO nanorod arrays, and subsequent *n*-dodecyltrimethoxysilane(DTMS), to produce a static water contact angle of >150 for a 5 mL water droplet.[147] For the epoxy-functionalized cotton textiles with a coating of amino- and epoxy-functionalized silica nanoparticles, the hydrophobic samples reached 170° for a 5 μL droplet.[148] The 102° water contact angle CNF was surface silylated with hexamethyldisiloxane by roll-to-roll plasma deposition.[149]

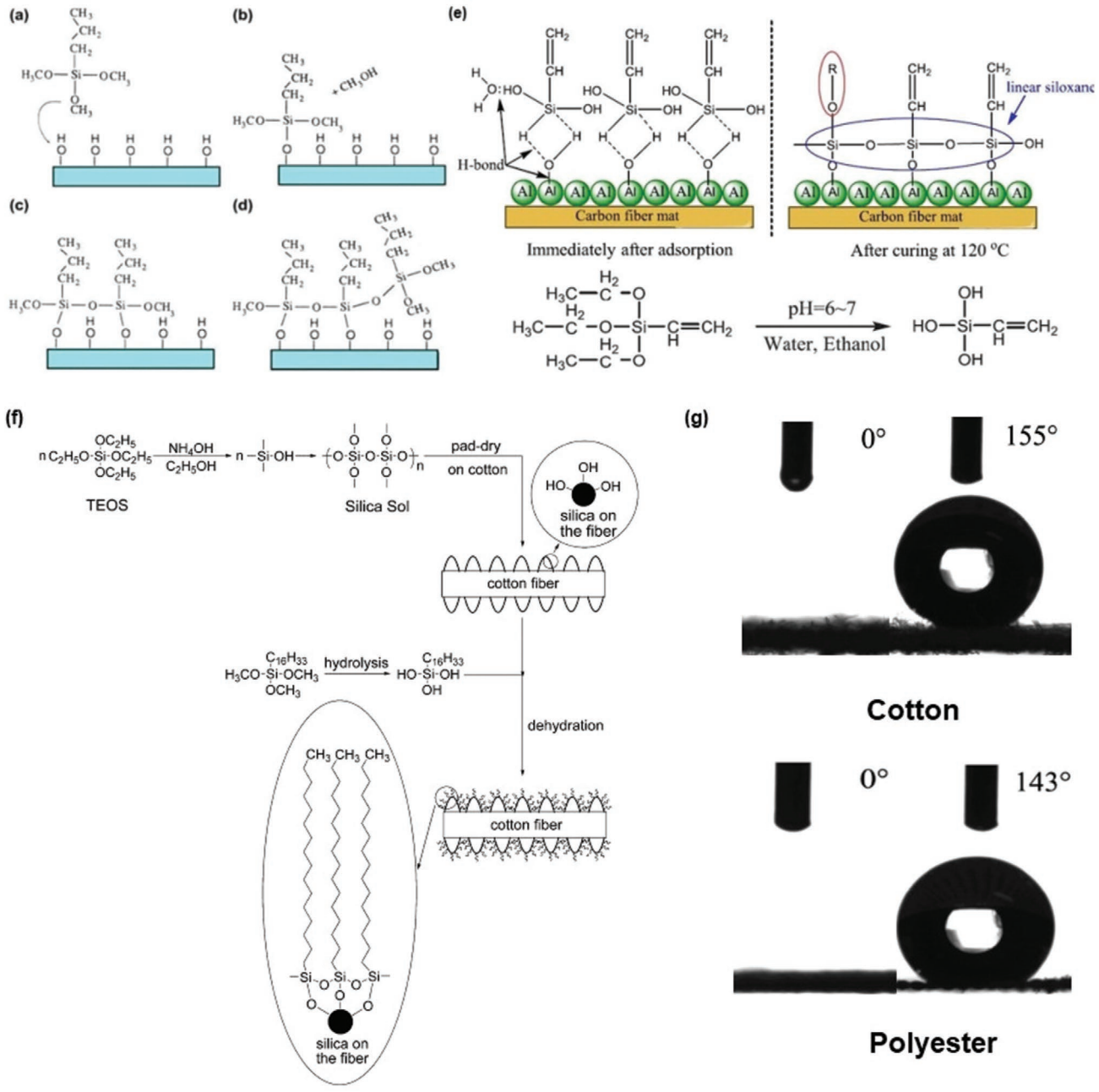

Figure 18. a–d) The Mechanism of Silane Treatment. Reproduced with permission.[143] Copyright 2017, Elsevier. e) The Formation Process of Siloxane Modified Al Layer, which was treated under 120°C for 20 min to modify the Al surface by siloxane groups. Reproduced with permission.[151] Copyright 2019, Elsevier. f) Formation of a superhydrophobic surface of cotton based on Silica Sol and HDTMS and g) water angle test for cotton/polyester samples before and after treatment. Reproduced with permission.[146] Copyright 2009, American Chemical Society.

Correspondingly, Guo et al.[150] developed a silane coated KH560 and carbon fiber reinforced PA6 composite with 30% mass fiber (Cf/PA6) and AA6061-T4 (a common aluminum alloy). Silane pretreatment improved the static strengths of the adhesive-bonded Cf/PA6-Cf/PA6 and Cf/PA6-AA6061 by 23% and 21%, respectively, which corresponded to the formation of Si—O—Si and Si—N covalent bonds on the surface of Cf/PA6 and enhancement of the bond adhesion between the silane coating, adhesive, and adherends. SMPs will deform their shape under specific environmental conditions and recover after the change is reversed. Another new high efficiency method for the SMP based on electrically resistive heating is shown in Figure 18e.[151] The recovery time was only 30 s with 6.0 V applied, but it increased to 150 s when the voltage dropped to 4.0 V. This could be used as the control method of recovery behavior for SMP nanocomposite due to Joule's law. The silane treatment of Al nanoparticles significantly enhanced the electrothermal

efficiency and improved the shape recovery performance of SMP nanocomposites. Silane surface treatment also plays an important role on cellulose microfibrils,[152] which became readily dispersible in low polarity solvents like tetrahydrofuran. The final suspensions were stable and appeared birefringent without flocculation.[153]

3.3. Acetylation of Natural Fibers

Acetylation is a reaction that introduces an acetyl functional group into an organic compound. Acetylation is used widely for plasticization of cellulosic fibers. The reaction generates acetic acid as a side product, which must be removed from the lignocellulosic material before the fiber is used. The fiber surface modification is then performed using acetic anhydride to replace the polymer hydroxyl groups of the cell wall with acetyl groups. The product finally becomes hydrophobic.[143] A general reaction formula is shown below

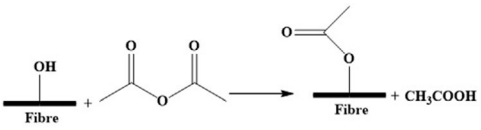

(4)

The acetylation treatment reduces the hygroscopic nature of natural fibers and increases the dimensional stability of composites. Also, in fiber-reinforced composites, acetylation can be used as a surface treatment. Stiffness, strength, and fracture behavior of fiber-reinforced composites are decided by the properties of the fiber/matrix interface, but the affinity between the hydrophilic fibers and the hydrophobic thermoplastic matrix is still limited in cellulosic composites, and the reinforcing capability of the fibers has potential for improvement.[151] Therefore, Joffrea et al.[154] indicated that acetylation clearly improved wood fibers' hydrophobicity and increased the strength of a wood–polylactic acid (PLA) composite. While the samples were fully soaked in water, the strength was increased up to over 30%. The fibers were much more dimensionally stable and maintained this adhesion with the PLA matrix under wet conditions for better stress transfer after acetylation.[155]

Another cellulose nanofiber reinforced PLA demonstrated that the storage modulus could reach up to 28 times higher than the pure PLA at 70 °C.[156] Partially acetylated CNF could be strengthened to high toughness (33 MJ m^{-3}) and stiffness (6 GPa) with high elasticity (30% strain) via wet spinning.[157] Therefore, acetylation pretreatment can also reduce energy consumption with improved CNF properties and shorter blending times. Apart from higher hydrophobicity, acetylated CNF had higher thermal stability and higher crystallinity.[158,159] The bast fibers extracted from Grewia Serrulata trees could provide reinforcement to unsaturated polyester resin.[160] The tensile strength and tensile modulus of composites was higher than untreated samples by 53% and 8%, respectively, after acetylation treatment on fibers. The fractography of the samples indicated that the bonding between the fibers and the matrix was obviously improved after treatment. The surface of fiber could be changed to hydrophobic or hydrophilic through acetylation such as simple reactive ball-milling technique,[161–164] and the change of this property could be applied to nanopapers,[165] oil sorbents,[166] and direct ink writing for 3D printing.[167]

In **Figure 19**, development of a new heterogeneous sensor for metal ions and antibacterial textile is shown.[168] Under different polarities of organic solvents, the spectroscopic characteristics of 4-(2-*N*,*N*-dimethylamino)ethylamino-*N*-(2-hydroxyethyl)-1,8-naphthalimide were investigated during the research. Acetylation treatment was completed by using chloroacetyl chloride as a bridge between dye and cellulose macromolecules to induce new functional groups on the surface of cotton fabric. The induction process included two removal steps of −H and −Cl groups. During the antibacterial test, the growth of *Bacillus cereus*, *Acinetobacter Johnsonii*, and *Pseudomonas aeruginosa* were decreased, which proved that the samples were successful smart textiles for antibacterial applications.

3.4. Benzoylation Treatment

For benzoylation, benzoyl chloride is commonly used in fiber treatment. The benzoyl group ($C_6H_5C{=}O$) is related to the decreased hydrophilic nature of the treated fiber, which improves the interaction with the hydrophobic polystyrene matrix as well.[142] The general reaction formulas are shown in Equations (5) and (6)

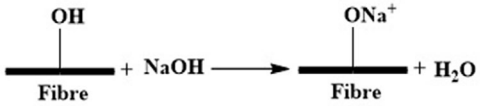

(5)

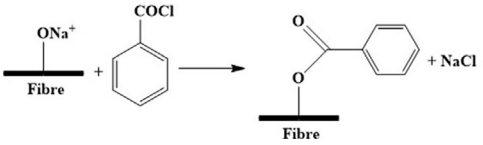

(6)

In nature, the areca nut palm is the source of the common masticatory nut, which is known as areca nut. Like other source of natural fiber, it is abundant and easy to obtain. To improve its uses as a commercial plant, the effect of surface modifications of areca sheath fibers through chemical treatments was explored.[169] The experimental results showed that the tensile and flexural strength of samples are significantly influenced by surface modifications: the tensile strength was increased as the bending strength was reduced after benzoylation treatment. The modified areca sheath fibers have the potential to be used for automobiles, in the packaging industry, as parcel, or panel boards, and many other applications. Another natural fiber, sugar palm fiber (SPF), was invented by benzoylation treatment.[170] The SPF was used to hybridize with glass fibers to reinforce epoxy composites. The experimental data indicated an increase of 9.86% and 9.92% of flexural maximum load and flexural strength for 3:7:90 v/v% ratio of SPF/GF/epoxy resin samples. In addition to benzoyl chloride, different functional groups can be applied to a benzene ring so that they are able to further promote benzoylation under suitable conditions; one example of which is benzylamine.[171] The periodate oxidation of cellulose led to the coupling with benzylamine and produced hemiacetal groups, which could act as a platform for

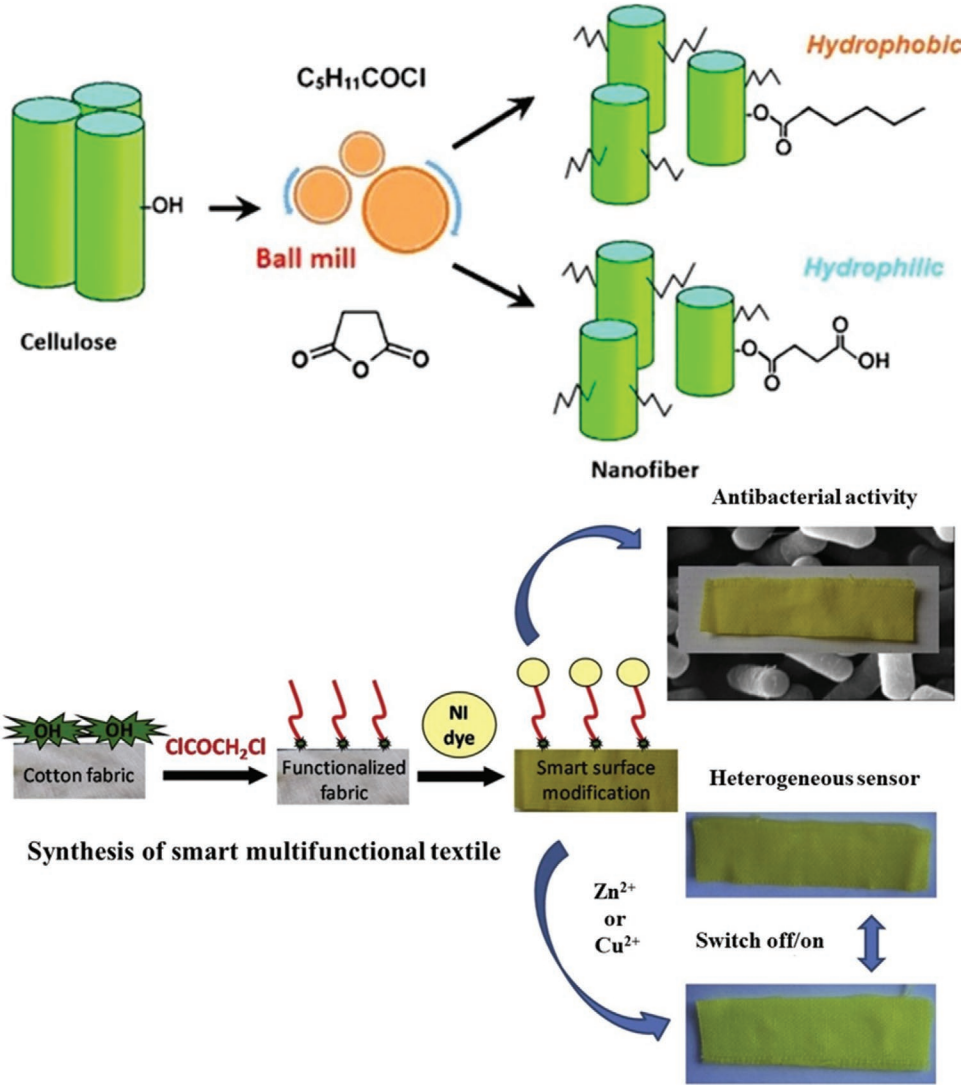

Figure 19. Milling with hexanoyl chloride/DMF(hydrophobic) or succinic Anhydride/DMSO (hydrophilic). Reproduced with permission.[161] Copyright 2012, Wiley-VCH (top). The manufacture process of sensor and NI dye chemical formula, the cotton fabric was treated with chloroacetyl chloride and formed linking with NI dyes. Reproduced with permission.[168] Copyright 2019, Elsevier (bottom).

subsequent coupling with other surface reactions. Up to five different bonding models were found in the research as shown in **Figure 20**a–e.

3.5. Maleated Coupling Agents

Maleated coupling agents are used worldwide to strengthen composites. They have two functions at the same time: to modify the fiber surface and achieve better interfacial bonding and mechanical properties by connecting with the PP matrix. The PP chain enhances the formation of maleic anhydride grafted polypropylene (MAPP), and then the covalent bonds are generated across the interface through the treatment of cellulose fibers with hot MAPP copolymers. The final product shows better wettability and higher interfacial adhesion of the fiber because the increased surface energy of cellulose fibers is closer to the surface energy of the matrix after treatment shown in Equations (7) and (8)[143,172]

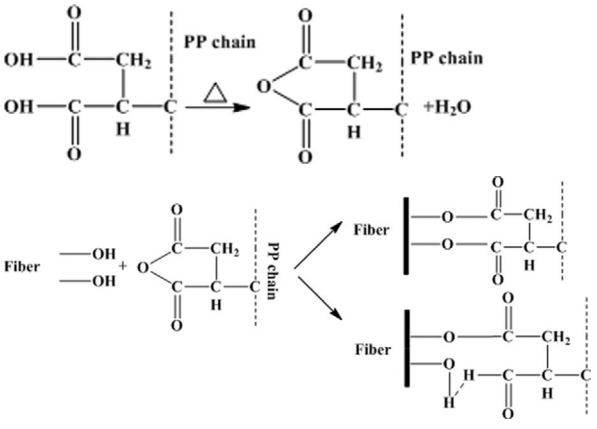

(7)

(8)

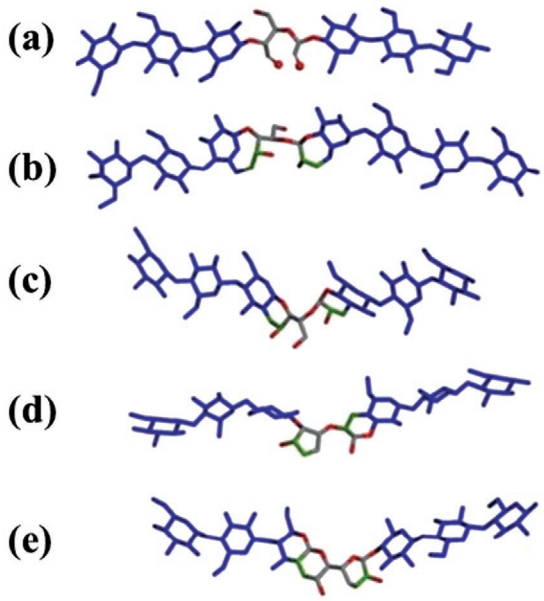

Figure 20. Model of carbonyl opening and intra-chain hemiacetal reorganizations: a) opening at C2 and C3 of a given AGU unit; b) hemiacetal cyclization bond at C2–O–C60 (7-member fused ring) and C3–O–C600 (8-member fused ring). c) C2–O–C30 (6-member fused ring) and C3–O–C200 (6-membered fused ring). d) C3–O–C6 (5-membered ring) for the carbonyl at C2. e) C2–O–C6 (6-membered ring). The newly formed hemiacetal moieties are colored in green. Reproduced with permission.[171] Copyright 2014, Springer.

In this case, banana fibers were again used. A PP/banana fiber (PP/BF) composite was developed by adding maleated coupling agent, MAPP as shown in **Figure 21**.[173] The bonding between the polymer matrix and the natural fiber was improved through the addition of MAPP. The results of yarn form samples showed that tensile strength and flexural strength were increased up to 294% and 72%, a highly notable result, and one which proves the great potential for natural fiber and the good adhesion ability of MAPP.

CNFs are important fiber materials for various applications and have attracted a great deal of interest because of their abundance, biodegradability,[174] robust mechanical properties,[175] and chemical tunability.[176] The chemical surface modification of CNFs is thought to be the better choice[177] to improve their hydrophilic surface limits[178] than the introduction of a surfactant, which results in a decrease of mechanical properties,[179] and the modification of matrix for less hydrophobic, which sacrifices some characteristics of the polymer.[180] Huang et al.'s[181] work further reduced the drawbacks of chemical modification, which often involves complicated procedures and hazardous chemicals like chlorides.[161] Instead, the milder and safer acyl anhydrides were used for esterification. The ball milling process in organic solvents had a dramatic effect on nanoscale dispersion and surface derivatization of CNFs, such as the succinylated NFs ($\zeta = -38.7$ mV at pH = 5.5) and the dispersity in *o*-xylene of *n*-dodecyl succinylated nanofibers for nanocomposites preparation. The Young's modulus and tensile strength of nanocomposites could reach up to 7.93 GPa (83% higher than pristine polyethylene) and of 44.7 MPa (28% higher than pristine polyethylene). This ball milling method will likely have further applications on the chemical surface treatment of different fiber materials.

3.6. Permanganate Treatment

Permanganate treatment is a method that uses the generation of MnO^{3-} ion for the formation of cellulose radical. The initiating graft copolymerization is performed by highly active Mn^{3+} ions as shown below[160]

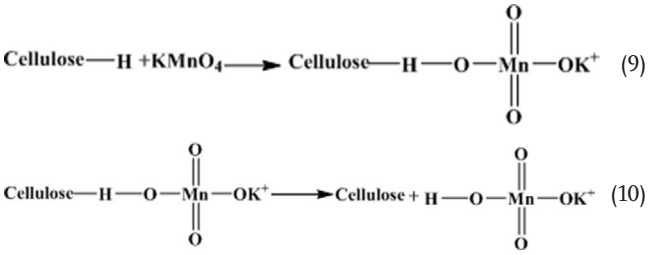

This example of permanganate treatment is taken from a separate part of Mahesha et al.'s[160] work, which treated bast fibers extracted from Grewia Serrulata trees with permanganate. The

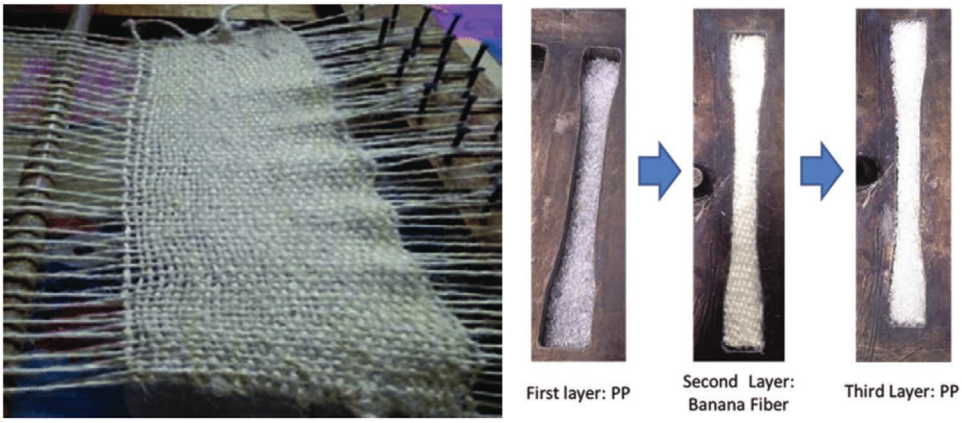

Figure 21. Knitting of banana fiber mat (left) /the compression molding process of 'dog-bone shape' PP/Banana mat composite sample using compression molding. Reproduced with permission.[173] Copyright 2017, Elsevier.

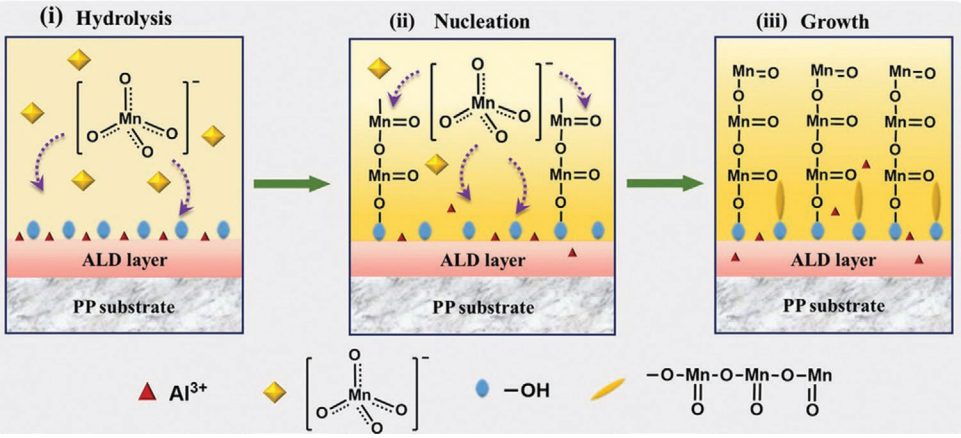

Figure 22. Detail mechanism of MnO_2 growth on MO@PP swatch. Reproduced with permission.[120] Copyright 2020, Wiley-VCH.

results clearly showed that the tensile strength, Young's modulus, flexural strength, and flexural modulus of permanganate treated fiber were increased by 15.1%, 132.1%, 24%, and 40%, respectively. Li et al. explored the effect of surface treatment of ultrahigh molecular weight PE fiber with $KMnO_4$,[182] and showed that the surface roughness, tear strength, and the hardness of the composites were increased. The interfacial adhesion strength was also greatly improved through permanganate treatment. In addition, $KMnO_4$ could be used to grow MnO_2 on metal oxide/fiber surface via hydrothermal process as established in **Figure 22**.[120] The resulting three layers of fiber composite performed as metal oxide filters, which provided excellent $PM_{2.5}$ removal efficiencies up to 90% and PM_{10} up to 98%, respectively. The permanganate treatment promoted this application to a new outstanding high-level performance.

3.7. Peroxide Treatment

Peroxide is the chemical with the form of R–OO–R, which contains the divalent ion $[O–O]^{2-}$. The free radicals of RO· are easily generated through self-decomposition of the peroxide: the hydrogen groups of the matrix and cellulose fibers are then reacted with RO· as in **Figure 23**.[142] In this case, the examples of reaction are shown by the following schemes

$$RO—OR \longrightarrow 2RO\cdot \quad RO\cdot + PE—H \longrightarrow ROH + PE \tag{11}$$

$$RO\cdot + Cellulose—H \longrightarrow ROH + Cellulose \quad PE + Cellulose \longrightarrow PE—Cellulose \tag{12}$$

Among reagents which contain the divalent ion O–O, hydrogen peroxide H_2O_2 is the most prevalent: it can even be seen in the chemistry lessons of middle school. Here, it has also been used to treat PAN-based fibers.[184] Due to the excellent wettability with hydrogen peroxide of PAN fibers, the surface modification was improved, and the oxidation stabilization time was reduced along with increased bulk density of the final product, forming a more conjugated structure. The Raman spectroscopy results indicated that the fibers contained the fewest fiber defects after modification while RI value was 1.06. The interfacial properties between carbon fibers and epoxy matrix were improved by supercritical water/hydrogen peroxide treatment.[185] The interfacial bonding was strengthened through these connections, with the maximal interlaminar shear strength and interface shear strength of CF/epoxy increasing up to 70.46 and 106.66 MPa, a 13.4% and 29.6% increase compared with untreated CF.

3.8. Other Chemical Treatments

Chemical treatments have a wide variety of different methods based on specific compounds and reaction environment: only some main methods are described in this article. Two final unique methods are introduced here.

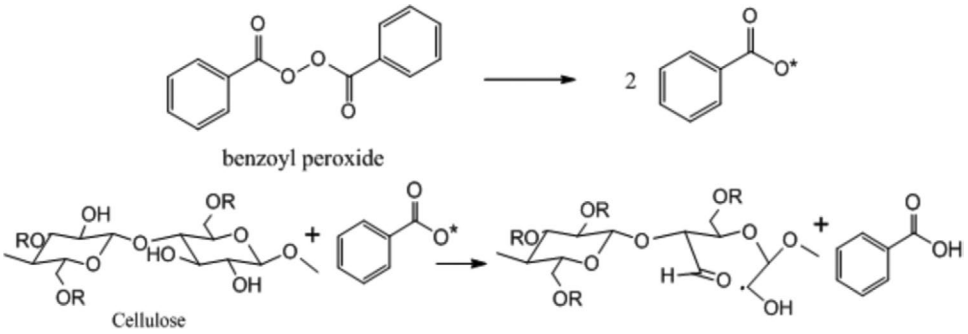

Figure 23. The Mechanism of Peroxide treatment of natural fibers. Reproduced with permission.[183] Copyright 2012, Hilaris.

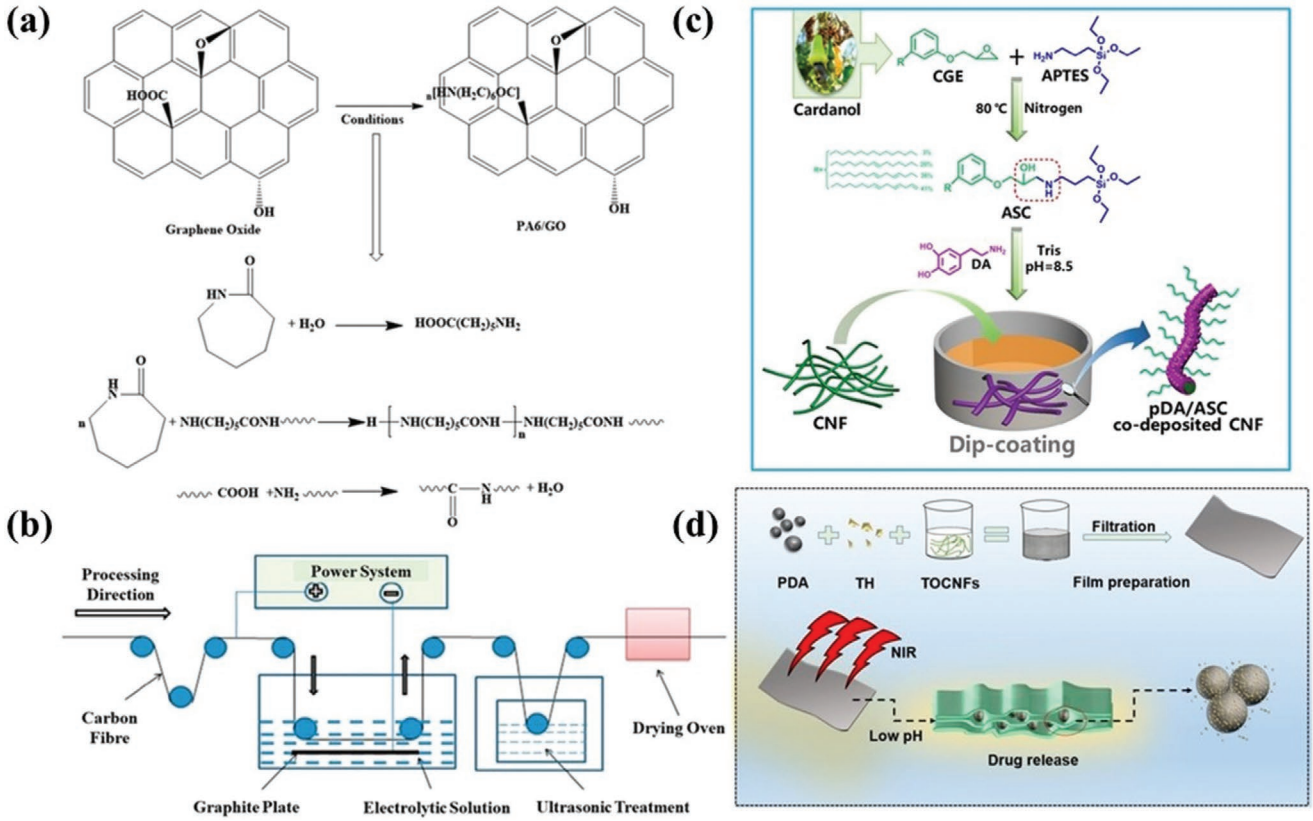

Figure 24. a) The Mechanism of PA6/GO Fiber to form -CONH- bonding. Reproduced with permission.[186] Copyright 2017, Wiley-VCH. b) The Process of electro polymerization treatment. Reproduced with permission.[187] Copyright 2019, Elsevier. c) The synthetic method of ASC and ASC/PDA-modified CNFs. Reproduced with permission.[196] Copyright 2019, Elsevier. d) The fabrication of the PDA/TOCNFs composite films for drug delivery. Reproduced with permission.[200] Copyright 2018, American Chemical Society.

First, GO was prepared to reinforce PA6 fiber by situ polymerization with caprolactam, adipic acid, water, and GO as shown in **Figure 24**a.[186] The COOH groups on the surface of GO were replaced by covalent bonds to the fiber, increasing its strength. The highest strength of the final product was 5.3 cN per dtex with an elongation of 38.8%, a good improvement. Wen et al.[187] explored an electrochemical deposition method to combine PAN-based CFs and GO with three different kinds of comonomers, including diacetone acrylamide (DAAM), acrylic acid (AA), and phenol (Pheno). The strong covalent bonds generated by electrografting led to the increase of tensile strength of GO-DAAM, GO-AA, and GO-Pheno electrografted CFs by 5%, 22.6%, and 17%, respectively. The whole process of electropolymerization treatment is shown in Figure 24b. For the native cellulose in water phase, 2,2,6,6-tetramethylpiperidine-1-oxyl radical (TEMPO)-mediated oxidation led to a high density (0.54 C m^{-2}) of the carboxylate groups formed on cellulose nanofiber surface to provide stable dispersions.[188] The TEMPO method was also used to connect PEG and CNF for high stiffness and tensile strength.[189] Another reinforcement of PVA was performed by using a cellulose derivate via allylation and epoxidation.[190] The fibers were allylated using allyl glycidyl ether and epoxidized to yield epoxy-NFC for surface coating. A conductive Ag-cell/RGO-cell paper was achieved by a scalable conventional papermaking process to mix the Ag-modified pulp fiber and GO-modified pulp fiber, and then the reduction of vitamin C followed.[192] The specific capacitance of this paper-based supercapacitor reached 222.5 F g^{-1} at current density of 1 A g^{-1}, and the product could be easily stored and reactivated by drying at 80 °C and wetting by 5 min.

Second, PDA is a versatile coating material on the surface of various materials via self-polymerization in aqueous conditions.[191] This property was exploited for the upscale production of next-generation green flexible electronics, in particular durable, transparent conductive cellulose-based nanopaper (TCCNP) with a high performance as seen in **Figure 25**a.[193] The versatile adhesion capability of PDA combined with AgNWs and NPCs and facilitated mechanical robustness and long-term durability of TCCNP, which had a high optoelectronic performance (14.2 Ω sq^{-1}, 90.93%@550 nm). In addition, PDA@NFC–AgNW TCCNP showed no obvious changes under large deformation (bending for 1000 cycles and peeling for 100 cycles) and had excellent air and corrosion stabilities in dry and wet environments. This is a promising TCCNP material made via an easy fabrication process for green transparent electrodes in the next-generation flexible and wearable optoelectronic devices. PDA also has the benefit of strengthening the material properties, such as tensile strength, Young's modulus, and elongation at break.

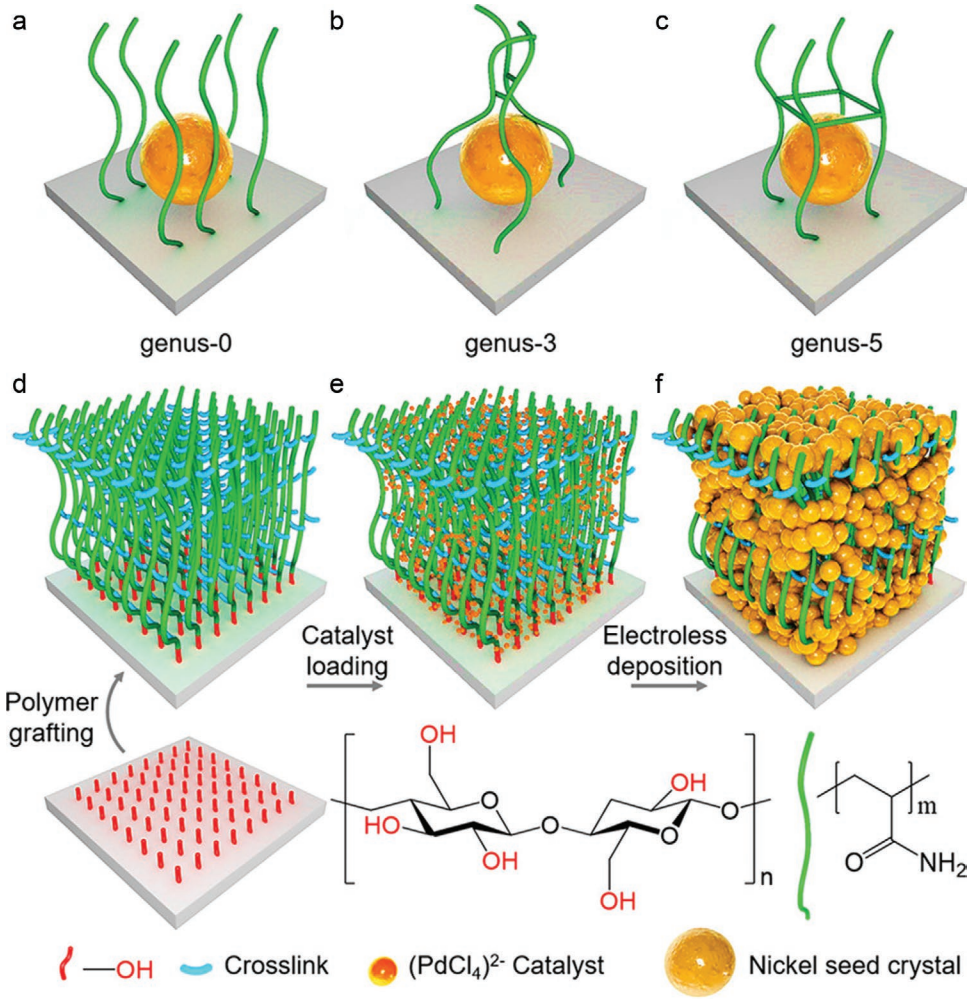

Figure 25. a) Genus-0, b) genus-3, and c) genus-5 surfaces to cage catalyst-based nickel seed crystal, and synthesis process of the PAMD fabrication through surface modification, including three steps d) to entangled graft of polymer networks across the gaps and surfaces of cotton fibers, e) immobilize catalysts in the polymer networks, and f) subsequent proceed ELD of nickel nanoparticles on the catalytic active sites to form a nickel nanoparticle film on the surface of cotton fibers. Reproduced with permission.[194] Copyright 2020, American Chemical Society.

Compared with the neat PVA film, PVA/PDA@CNC presented 75.8%, 69.2%, and 58.1% for these three properties, respectively.[195] Strong interfacial interactions significantly improved the thermal stability, antioxidant properties, and UV-resistance, which demonstrated a better ability for preventing food spoilage and nutrient substance loss caused by oxygen and water vapor. Poor interface strength and water resistance of natural fiber reinforced biopolymer composites were improved by the nanostructured layer of aminopropyltriethoxysilane (ASC)/PDA as indicated in Figure 24c.[196] This potential water-resistant biobased material achieved wet shear strength up to 1.27 MPa, which was 189% and 95% higher than the neat resin and pristine fiber. Nanocellulose fibers were also coated with PDA to combine them with Nafion, which increased the storage modulus of Nafion by 200% at 90 °C.[197] Due to the wide number of functional groups present in PDA, thermo-mechanical and chemical stability were enhanced significantly as well. Additionally, PDA is a safe chemical for human body since it is a main substance of natural melanin and can be degraded in vivo,[198,199] and could be applied on drug delivery in Figure 24d.[200] The TEMPO-mediated oxidized CNFs (TOCNFs) were combined with PDA to prepare pH/near-infrared-responsive film for the delivery of the drug tetracycline hydrochloride. This material exhibited good flexibility and mechanical strength, high biodegradability and biocompatibility, long period drug releasing (30 h, maximum $M_{drug}/M_{film} = 70\%$), and sensitive pH/NIR responses.

Besides the treatment methods described during previous sections, more studies have been undertaken using different chemical treatments. Chen et al.[194] have fabricated soft PDMS/cotton fabric, which formed a covalent and hydrogen-bonded entangled molecular topological cage to capture a catalyst-based nickel seed crystal through a thermally induced radical polymerization technique as shown in Figure 25b. Fiber surface modification succeeded in improving the adhesion and conductivity of metallic coating on the fiber surface via topological genus-3 and genus-5 structures. The nanoparticles aggregated into an extremely dense film (≈500 nm thickness) and the maximum resistance reached ≈3 Ω cm^{-1}, which achieved excellent electrical properties of the conductive fabric and which was

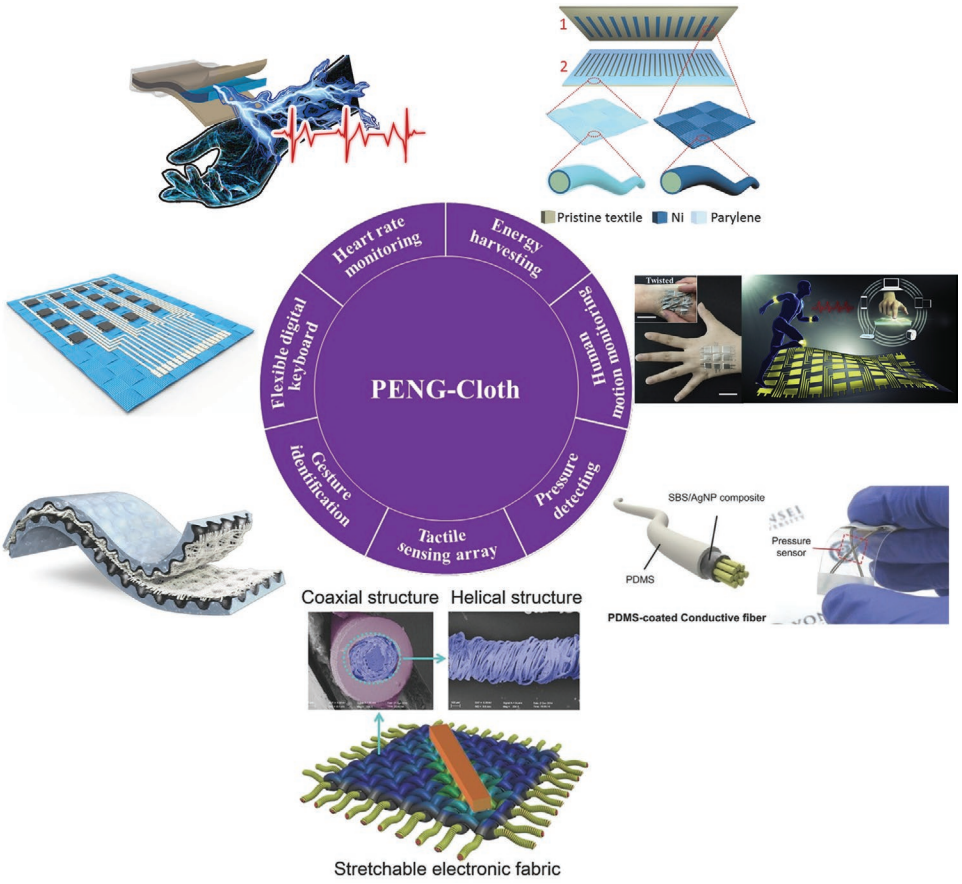

Figure 26. Different applications based on PENG-cloth, a) heart rate monitoring. Reproduced with permission.[205] Copyright 2018, Elsevier. b) flexible digital keyboard. Reproduced with permission.[206] Copyright 2017, Wiley-VCH. c) gesture identification. Reproduced with permission.[207] Copyright 2019, Wiley-VCH. d) tactile sensing array. Reproduced with permission.[208] Copyright 2016, Wiley-VCH. e) pressure detecting. Reproduced with permission.[209] Copyright 2015, Wiley-VCH. f) human motion monitoring. Reproduced with permission.[210] Copyright 2020, Elsevier. g) energy harvesting. Reproduced with permission.[211] Copyright 2016, Wiley-VCH.

then integrated into tights for human motion monitoring like breathing, speaking, blinking, head motions, and joint motions in rehabilitation training.

Since fiber-based materials are becoming more and more attractive in wearable electronics because of reliable flexibility and excellent electron transport property,[201] TE conversion is considered as a promising energy harvesting approach for wearable electronic devices. An all-organic TE fiber generator was made by poly(3,4-ethylenedioxythiophene) polystyrene sulfonate (PEDOT:PSS) and CNT fibers.[202] The p-type PEDOT:PSS-coated CNF (CNF/PP) and n-type CNT fibers were connected in regular order to form TE generator and provide a large power output of 375 μW. This promoted the further development of organic TE energy harvest in wearable electronics: textile-based NGs are one of the most popular research fields in wearable electronics. There are two typical forms, TENG-cloth and piezoelectric nanogenerator (PENG)-cloth.[202–204] Such relevant textile-based applications involved different functions like heart rate monitoring,[205] flexible digital keyboard, and[206] gesture identification;[207] details of which are shown in **Figures 26** and **27**

Excepting nanogenerators, other applications of textile-based wearable electronics for personal entertainment, health monitoring, virtual reality, human–machine interfaces, and even Internet of Things are rapidly being developed.[212–215] However, it is difficult to produce the ideal wearable electronic device due to the need to fulfil so many key requirements. The core desire is wearability, which means that the materials must be light-weight, soft, and flexible.[216] The user's movement ability cannot be reduced while wearing, and it should feel comfortable. The materials must withstand frequent deformation due to the motion of human activities. Considering skin contact, the materials must be nontoxic for long-term use on human body, in particular the skin-contacting layer.[217] The desire for reusability demands water resistance; the wearable electronics should be designed to work under sweat or wet conditions and have enough sensitivity, and normal washing of the textile should not damage the device.[218]

In this case, the conventional battery is unable to act as the wearable power supply, since it is unsafe and inconvenient due to the potential leak of electrode solution, large volume to carry, and the frequent exchange once the battery is dead.[219] Solutions to the problem of energy supply are technologies that can harvest mechanical energy from the surrounding environment or human motion to generate electricity.[220] For this purpose, nanogenerators are ideal. In addition, the energy harvesting

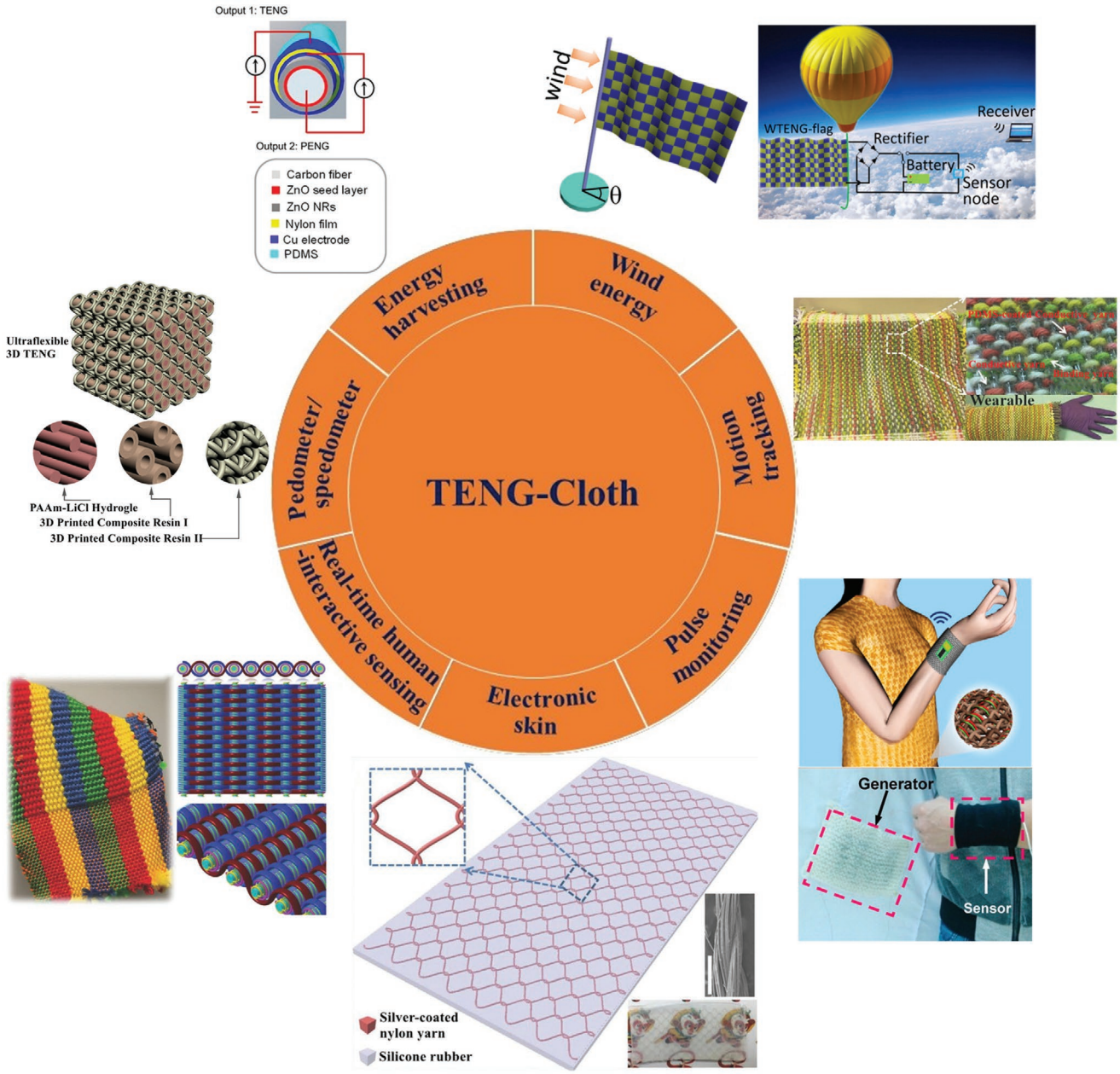

Figure 27. Different applications based on TENG-cloth. a) Energy harvesting. Reproduced with permission.[222] Copyright 2014, American Chemical Society. b) Pedometer/speedometer. Reproduced with permission.[223] Copyright 2018, Elsevier. c) Real-time human-interactive sensing. Reproduced with permission.[224] Copyright 2018, Wiley-VCH. d) Electronic skin. Reproduced with permission.[225] Copyright 2018, Wiley-VCH. e) Pulse monitoring. Reproduced with permission.[226] Copyright 2014, American Chemical Society. f) Motion tracking. Reproduced with permission.[227] Copyright 2017, Wiley-VCH. g) Wind energy. Reproduced with permission.[228] Copyright 2016, American Chemical Society.

materials should have a high electrical conductivity and must be relatively cheap to produce, otherwise common people are unable to afford the cost of final product, leading to a lack of general interest.[221]

Considering these requirements, fibers stand out as the best choice. Using fibers as one layer with coating and support provided by other suitable materials, based on unique requirements of different research goals (like metal nanowires, polymers etc.), and even combining them to be three or more layers of final composite is an ideal approach to develop new wearable electronics.

4. Self-Assembling via π–π Stacking

Regardless of physical or chemical treatments, fibers usually form strong covalent bonds or combine with each other by similar molecular interactions. The covalent attachments

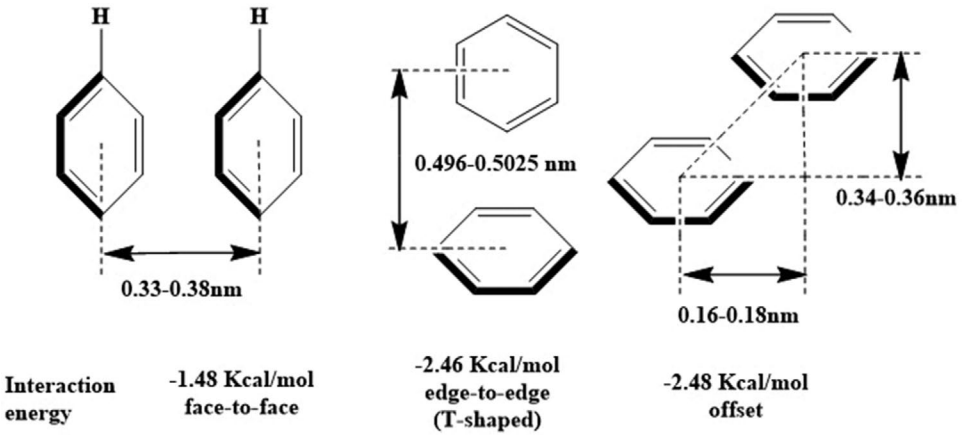

Figure 28. Three different forms of typical π–π stacking interaction structures. Reproduced with permission.[230] Copyright 2017, Springer.

often destroy some of the original conjugated structure, which can greatly compromise the properties of original materials. This situation is particularly serious in the treatment of graphene.[229] Its high conductivity relies on its unique 2D structure and carbon sp^2 hybridization, so the introduction of covalently bonded extra functional groups will seriously influence the regularity of its structure and decrease the unique properties of graphene.

In this case, a new method, π–π stacking interaction, was proposed and has been successfully used for fiber surface modification. However, the interactions from noncovalent modifications are typically weaker than from covalent interactions that may lead to some lower properties compared with covalent modifications. By contrast, noncovalent modifications are easy to be fabricated and reversible, so it can be predicted that more applications can be achieved by noncovalent modifications rather than by covalent modification. The common example of π–π stacking happens when two benzene rings interact, which is shown in **Figure 28**.

Besides hydrogen bonding, electrostatic interaction, and coordination, π–π stacking interactions have been applied as noncovalent approaches for surface modification. In exploration of noncovalent approaches for surface modification, Huang et al.[231] have done much work. In most aromatic systems, the cation–π interaction primarily contributes to the electrostatic interactions. By exploiting this mechanism, a graphene/polybenzimidazole (PBI) ink was successfully invented to coat on a PET substrate surface using a pulsed UV laser direct writing technique, which achieved the S- and N-doped graphene patterns on thin (0.3 mm thickness) PET and glass substrates from a specially formulated organic PBI ink. This method removes the requirements for substrate heating and metallic precursor, which protects the substrate from potential distortion and damages. In **Figure 29**a, the top left image is the PBI ink written on PET before laser irradiation, and the top right is the graphene pattern on PET after the irradiation on the ink track. Scanning electron microscope (SEM) images show the porous structure of the final product, and Raman spectroscopy revealed the presence of graphene and a reduction in the degree of disordered carbon atoms. Due to the electrostatic interactions, the connection between graphene and the PET is higher than through van der Waals forces. In addition, PDA is a π-bond conjugated polymer and has a good potential to be performed as a medium for improvement of the bonding between the graphene and PET. The π–π stacking interaction became a key factor of the formation of the ink.

Another successful example of π–π stacking using PDA is in Zeng et al.'s[232] research, which used PDA to coat aramid fibers and combine them with GO. The surface of aramid fibers was smooth and chemically inert, which led to a weak interface with the matrix. PDA formed a coating layer on the surface of fiber through pH-induced oxidative self-polymerization like in Figure 29b to enhance the interfacial adhesion strength of aramid fiber-reinforced composites. Hydrogen bonding and π–π stacking interactions between benzene rings on different layers further increased the mechanical properties of fibers, and the abundant functional groups on PDA surface strengthened the GO–PDA–aramid combination fibers.

Flexibility plays a key role in wearable electronics. However, repeated bending usually decreases the wearable device's conductivity due to the numerous microcracks formed in the metal coating layer. This is undesirable for flexible conductors. Thus, Zhu et al.[233] reported a novel, facile, and universal strategy (Figure 29c) for preparing conductive flexible substrates through tannic acid (TA) modification and electroless plating of metals with strong adhesion. Notably, TA was used as a bridge between the fiber surfaces and seeds of Pd^{2+} to capture Pd^{2+} ions and partially convert Pd^{2+} to Pd nanoparticles. Then, high-quality metal coatings for flexible electronics were acquired by site-selective electroless deposition (ELD) at room temperature. By varying the ELD time, highly stretchable conductors were produced through cracking control, and the high conductivity was maintained after repeated bending. From the analysis of XPS data, the Pd (0) and Pd (II) species in the Pd-PET sample are anchored by cation–π interaction between benzene groups in PET and Pd ions during the process. Zhu et al.[234] have done further research to link Pd^{2+} ions by PDA-modified substrates for catalyst application. Through immersing fibers into an alkaline aqueous solution, PDA was coated on fibers and then the catalyst was anchored via ion chelation. The polymer-bridged conductive composites were formed after the deposition of metal nanoparticles on the catalytic area. This in situ plating

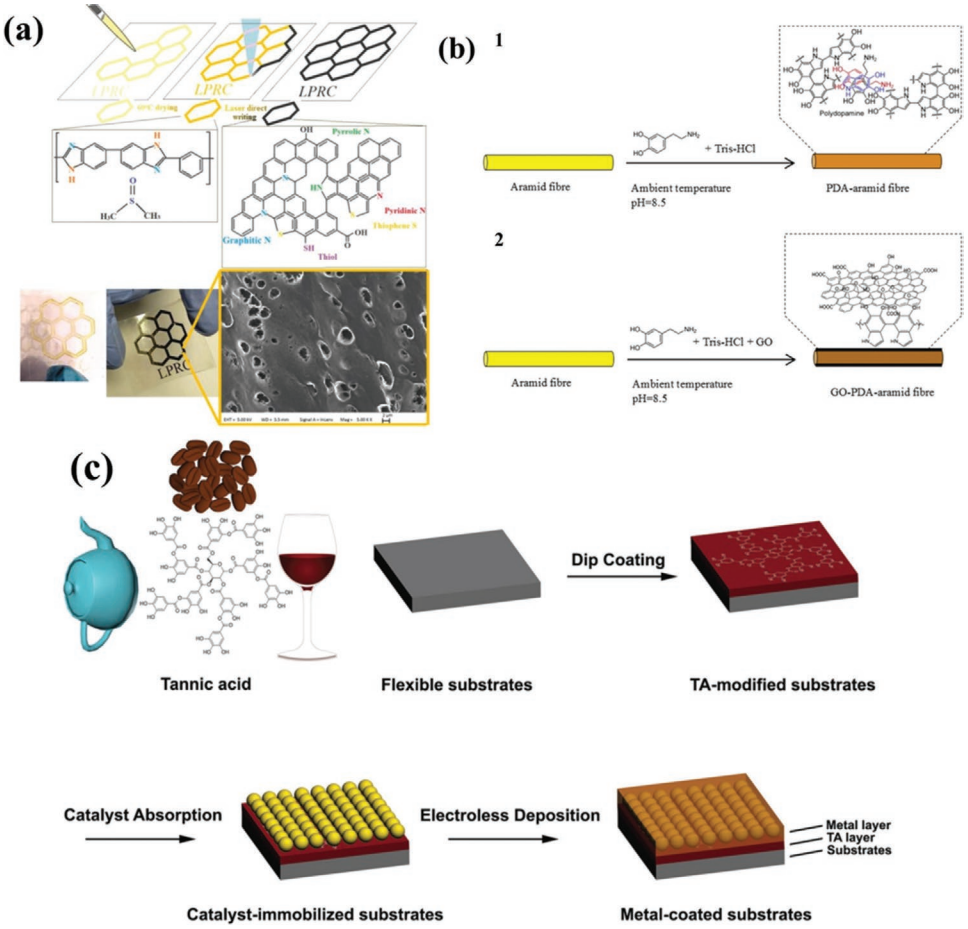

Figure 29. a) Optical and SEM images of graphene grown on PET after irradiation. Reproduced with permission.[231] Copyright 2018, Wiley-VCH. b) Schematic of PDA-treated aramid fiber in 1 and GO-PDA-treated aramid fiber preparation process in 2. Reproduced with permission.[232] Copyright 2018, Springer. c) The process of the fabrication of flexible conductors via TA modification and electroless deposition. Reproduced with permission.[233] Copyright 2019, Wiley-VCH.

method ensures that metallic nanoparticles are distributed on the surface of fibers continuously and uniformly. PDA/Pd catalyst was first employed in surface-catalyzed reactions and shows better performance than isolated Pd catalyst. This method of pH-induced polymerization of PDA could also be performed on Ni/Cu coated yarns(wool, cotton, nylon, and PET). The cotton yarn sample reached 0.05 Ω cm^{-1} at 60 min ELD, which was an incredible result. The adhesion and enhancement effect of PDA shows great potential for surface catalytic reaction.

Alongside these recent studies, previous work was also performed by Zhang et al.,[235] who proposed a π–π stacking method for graphene sheets. PEG macromolecules can be inserted into the interior of GO sheets' skeleton through hydrogen-bonding interactions between the GO nanosheet surface and PEG. However, the RGO and PEG have limited interaction because the C=O and O−H groups are removed during reduction of the GO. Therefore, pyrene, a π-orbital rich group, is introduced to increase interactions between PEG and RGO, as it has strong π–π stacking interactions with other polyaromatic materials. Although π–π stacking modification increases the doping density and the density of electron–hole puddles, it does not disrupt the sp^2 conjugation of the graphene sheets. The strong π–π interaction between graphene and functionalized PEG significantly improved the tensile strength of the composite film. The proposed model is shown in **Figure 30**a. In Chang et al.'s[236] work in Figure 30b, wool fibers were coated with ε-polylysine via electrostatic interactions to enhance their antimicrobial, hygroscopic, and finished properties. The results indicated promising antimicrobial performance of 96.98% and 97.93% against *Escherichia coli* and *Micrococcus luteus*, respectively.

A hybrid layer of polyethyleneimine/polydopamine (PEI/PDA) could also be used to coat carbon fibers, which improved the combination of CF and PU.[229] The interfacial adhesion was improved and connection of CF/PU layers was strengthened by π–π stacking interactions and hydrogen bonding. Besides fiber surface modification, hydrogen bonding, and π–π stacking, interactions can exist simultaneously in ionic liquids to achieve stable status as shown in Figure 30c.[237]

5. MOF Fiber for Wearable Electronics

MOFs are a series of compounds that consist of coordination of metal ions/clusters with organic ligands to form 1D/2D/3D structures, meaning that the porous crystalline framework is

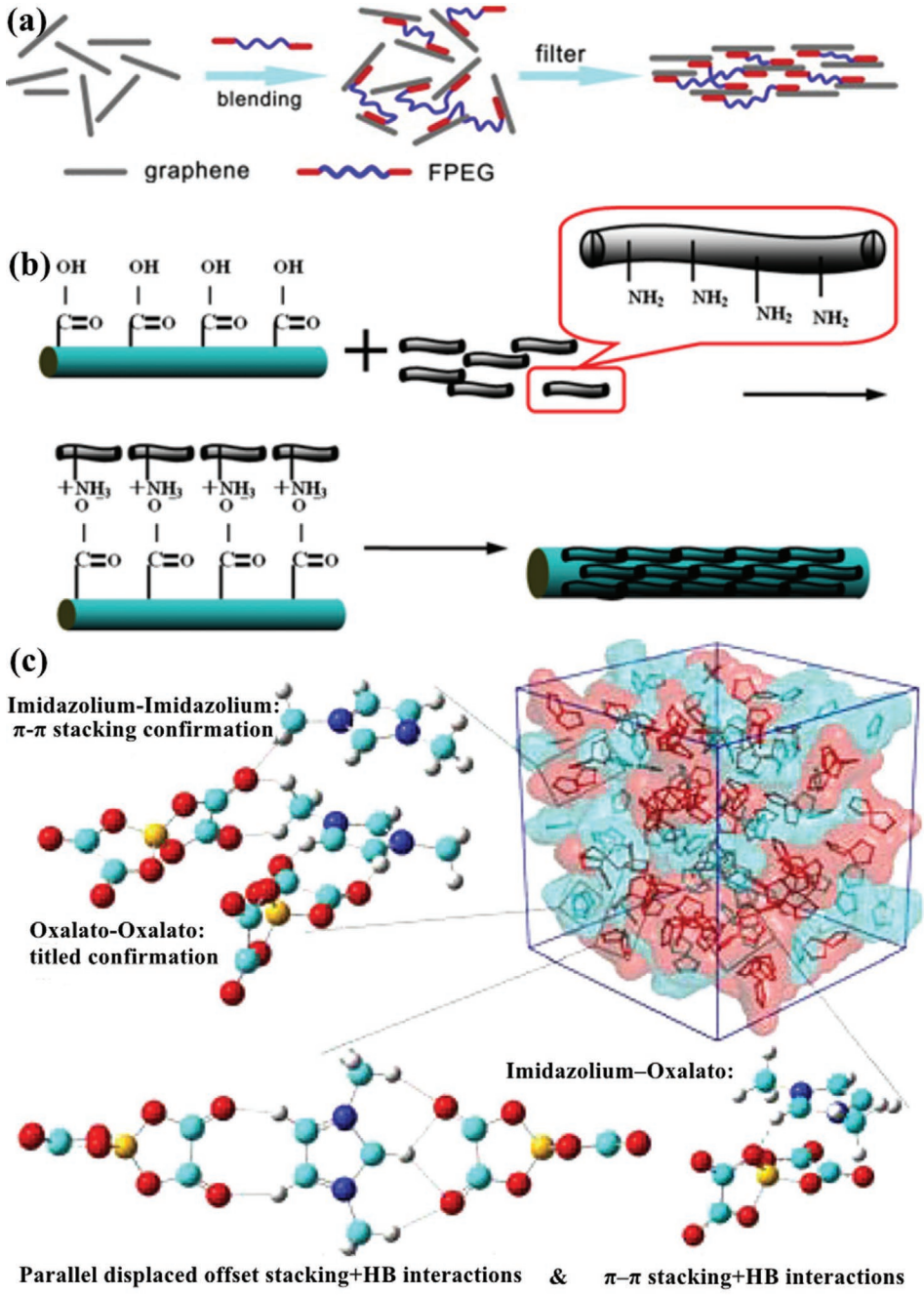

Figure 30. a) The cross-linking effect among the polymers and graphene sheets mediated by the π–π interactions. Reproduced with permission.[235] Copyright 2015, Elsevier. b) The model of a ε-PL layer adsorbed on wool fibers. Reproduced with permission.[236] Copyright 2012, Springer. c) The example of hydrogen bonding and π–π stacking interaction in imidazolium-oxalatoborate ionic liquid. Reproduced with permission.[237] Copyright 2017, American Chemical Society.

linked by strong bonds between inorganic and organic building blocks.[238–241](**Figure 31**) MOFs have become promising materials for applications in energy storage, gas adsorption/separation, photocatalysis, and drug delivery due to their large specific surface area, abundant and controllable porous structures, and diverse topological structure.[242,243] In particular, MOFs possess a large number of open active sites that can greatly support the access of different molecules, such as electrolytes, significantly promoting its applications for energy storage, such as supercapacitors.[244]

A flexible fabric electrode is constructed with a sphere–flake–sphere structure formed by a nickel–metal framework (Ni-MOF) and RGO as shown in **Figure 32**a.[245] The sphere–flake–sphere structure improved the conductivity and enhanced the electrochemical performance of flexible RGO/Ni-MOF/metallic fabric electrodes (RNMEs), reaching up to 260 mF cm^{-2}

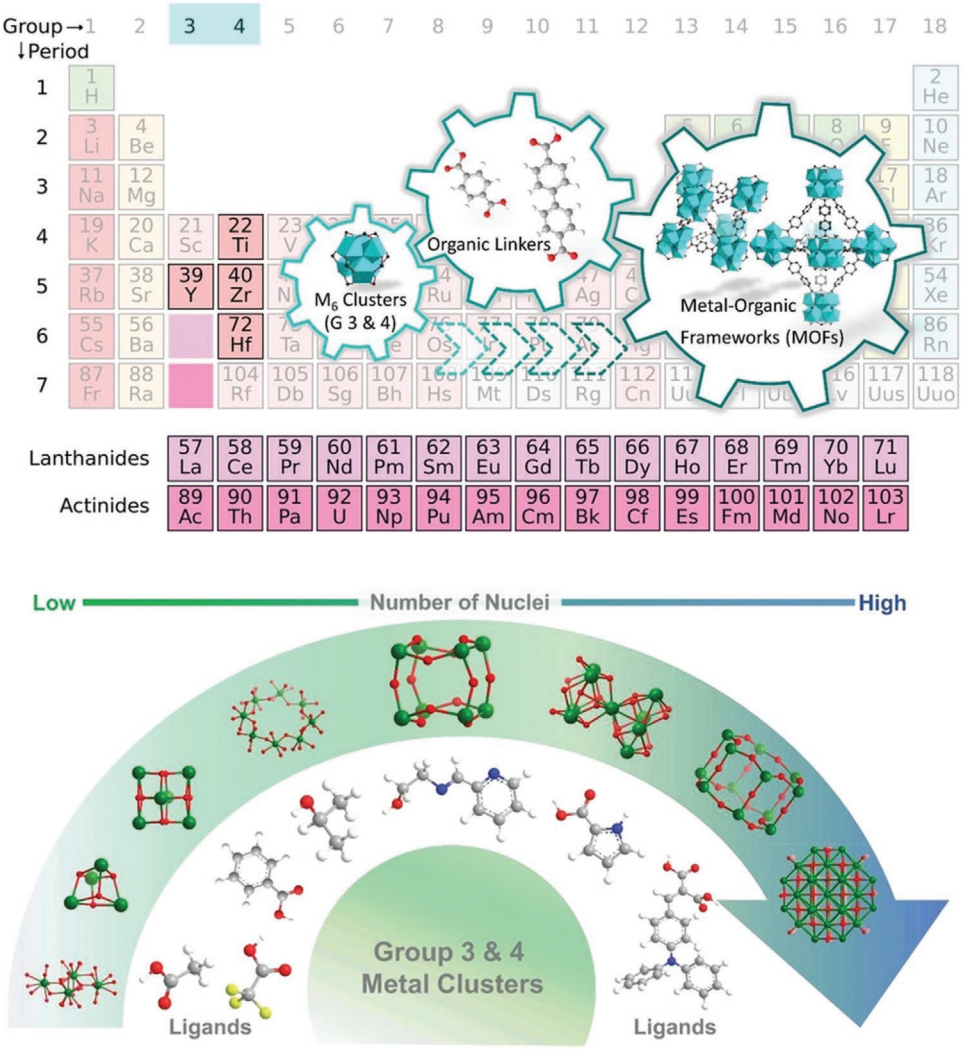

Figure 31. Potential metal ions for assembling with organic linkers into MOFs as shown in the groups of 3 and 4 periodic table. Reproduced with permission.[238] Copyright 2020, Wiley-VCH.

at a current density of 4 mA cm^{-2}. The areal capacitance of RNME samples showed a good cycle stability after undergoing 2000 charging/discharging cycles, maintaining over 70% of its original areal capacitance after 1500 charging/discharging cycles. This flexible all-solid-state asymmetric fabric supercapacitor shows a promising future for wearable smart textiles. Compared with another supercapacitor[244] made of CNT/Ni-MOF/GN, which was 898 and 230 mF cm^{-2} at 1 and 20 mA cm^{-2} and retained 93% after 4000 cycles, RGO/Ni-MOF demonstrated poorer stability due to higher conductivity of the CNT, but it demonstrated better electron transport effect due the graphene layer, changes of oxygen-containing groups, and the better porous structure of CNT/Ni-MOF/GN.

Alongside Ni-MOF materials, Zn-MOF series of materials also proved successful. Figure 32b showed the example of ZIF-8.[246] The polyaniline/ZnO/ZIF-8/graphene/polyester textile electrode exhibited great electrochemical performance (areal capacitance: 1.378 F cm^{-2} at 1 mA cm^{-2}) and high stability under different mechanical deformations. A flexible all-solid-state symmetric supercapacitor device was also fabricated, which showed a high energy density of 235 IWh cm^{-3} under the power density of 1542 IW cm^{-3}. The cobalt-based metal–organic framework-67(ZIF-67)[247] proved successful too. To release ZIF-67 from the restriction of poor conductivity and a limited cycling stability, a flexible and conductive textile carbon cloth was used as a support platform through a simple dripping method. The results indicated that the ZIF-67/CF achieved a very high areal capacitance (1756 mF cm^{-2} in 2.0 M KOH/H_2O at most) and a great specific capacitance (829 F g^{-1} for ZIF-67 at a mass loading of 1.9 mg cm^{-2}). The materials also displayed excellent reusability, with 103% capacitance retention after 15 000 cycles under current density of 40 mA cm^{-2}.

Along with supercapacitors, MOF derived $ZnCo_2O_4$/C coatings on CF showed good performance as structural lithium-ion batteries (SLIBs).[81] The MOF layer provided more active sites for electrochemical reactions and the thin carbon layers provided additional protection for higher durability, so the final product possessed high reversible capacity of 463 mA h g^{-1} at 50 mA g^{-1} even after 100 cycles: which is 201% higher than pristine CF. The sample was fabricated by simply mixing and

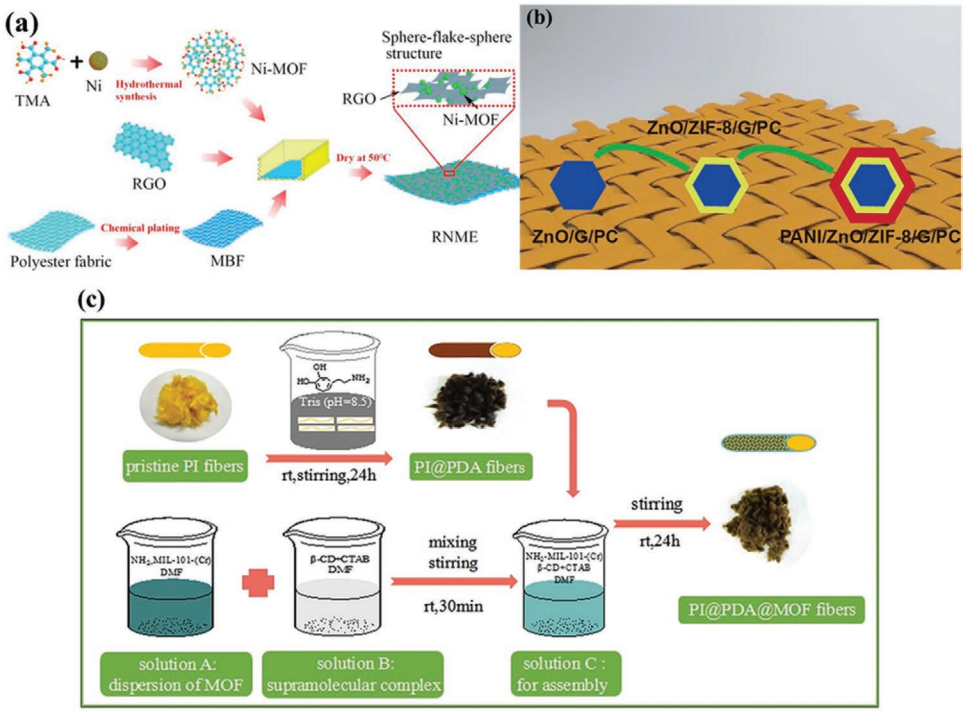

Figure 32. a) The fabrication process of RGO/Ni-MOF fiber. Reproduced with permission.[245] Copyright 2019, Elsevier. b) The example of 3D PANI/ZnO/ZIF-8/G/PC electrode material. Reproduced with permission.[246] Copyright 2018, Elsevier. c) The experimental process of PI/PDA/MOF fiber. Reproduced with permission.[248] Copyright 2019, Elsevier.

stirring, and finally annealing at 400 °C for 3 h under N_2 flow, which is a facile, low-cost method.

PDA has also been combined with MOFs. Xie et al. discovered a facile method to assemble the MOF [NH_2-MIL-101(Cr)] rapidly onto PDA dip-coated polyimide (PI) fibers at room temperature as described in Figure 32c.[248] PDA performed well in the role of a connecting layer, as expected. The hydrogen bonding interactions between PI fibers and MOF were confirmed by FTIR; this bonding strengthened the interlayer connection and further proved that PDA has great potential for noncovalent fiber surface modification. The MOF-cloth also had a high surface area (measured using Brunauer–Emmett–Teller surface area analysis) and high thermal stability due to the characteristics of the MOF crystals. The resultant fiber-based filter was able to capture the particulate matter at high temperature of 260 °C, with a working efficiency reaching ≈93% with a lower pressure drop of 57.5 Pa. This application may prove to be a new solution for pollution control at some industrial manufacturing processes.

6. Future Work

Despite the π–π stacking method and MOF coating having such great potential, there are still very few reports of these methods being used for fiber surface modification. The applications are limited, and few materials have ideal results, especially for long-term reusability. Surface modification relying on the formation of covalent bonds is still the most widely used method across the world. Other suitable materials alongside PDA ought to be found and combined with different fibers and polymers. More experiments can also be performed with PDA to produce more π–π stacking compounds, and to take advantage of the functional groups and self-polymerization characteristics of PDA. Discovery of other suitable materials will help to rapidly advance the emerging field of wearable electronics.

7. Conclusions

The concept of fiber surface modification and wearable electronics has been proposed for years, especially for cellulose nanofibers, and this research field is drawing increasing attention across the world with more and more new samples being manufactured. This review not only introduces the basic concepts of physical and chemical treatments of fiber surface modification and relevant fiber-based wearable electronics, but also explores the π–π stacking method, a novel noncovalent treatment method that due to the absence of covalent bonds produces less by-product and decreases waste handling costs. Its ability to minimize fiber surface damage and increase fiber/composite properties makes it promising as a next generation mainstream processing method.

Acknowledgements

This research was supported by the Henry Royce Institute for Advanced Materials, funded through EPSRC grants EP/R00661X/1, EP/P025021/1, and EP/P025498/1, and Short Research Visits UK Fluids Network, EP/N032861/1.

Conflict of Interest

The authors declare no conflict of interest.

Keywords

covalent interaction, fiber, surface modification, wearable electronics, π–π stacking

Received: May 18, 2021
Revised: June 29, 2021
Published online:

[1] S. J. Kadolph, *Textiles*, 11th ed., Pearson: Iowa State University, USA **2011**.
[2] A. Al-Lami, P. Hilmer, M. Sinapius, *Aerosp. Sci. Technol.* **2018**, *79*, 669.
[3] T. Coyle, J. Jones, C. Shaw, R. Friedrichs, *Sci. Justice* **2012**, *52*, 259.
[4] P. R. Kalyana Chakravarthy, T. Ilango a, S. Chezhiyan, *Mater. Today: Proc* **2020**, *21*, 684.
[5] Y. Wang, X. Liu, C. Zhu, A. Parsons, J. Liu, S. Huang, I. Ahmed, C. Rudd, N. Sharmin, *J. Mech. Behav. Biomed. Mater.* **2019**, *99*, 47.
[6] J. K. Pandey, A. K. Mohanty, M. Misra, *Biocomposites*, Elsevier, Amsterdam **2015**, pp.1–15.
[7] J. Yang, Q. Liu, Z. Deng, M. Gong, F. Lei, J. Zhang, X. Zhang, Q. Wang, Y. Liu, Z. Wu, C. F. Guo, *Mater. Today Phys.* **2019**, *8*, 78.
[8] J. Chen, H. Guo, X. Pu, X. Wang, Y. Xi, C. Hu, *Nano Energy* **2018**, *50*, 536.
[9] J. Hughes, F. Iida, *Sensors* **2018**, *18*, 3822.
[10] M. Stoppa, A. Chiolerio, *Sensors* **2014**, *14*, 11957.
[11] M.-C. Li, Q. Wu, R. J. Moon, M. A. Hubbe, M. J. Bortner, *Adv. Mater.* **2021**, *23*, 2006052.
[12] Man-made fiber, Available online, https://www.britannica.com/technology/man-made-fiber (accessed: March 2019).
[13] J. Cruz, R. Fangueiro, *Proc. Eng.* **2016**, *155*, 285.
[14] V. Koncar, *Smart Textiles and their Applications*, 1st ed., Elsevier Science, Amsterdam **2016**.
[15] G. Wu, M. Panahi-Sarmad, X. Xiao, K. Dong, X. Mei, S. Li, R. Li, X. Hou, *Adv. Mater. Technol.* **2021**, *6*, 2001275.
[16] A. M. Manich, M. J. Lis, S. Perez-Rentero, I. Algaba, M. Marti, D. Cayuela, *J. Appl. Polym. Sci.* **2021**, *138*, e50990.
[17] S. Pyo, J. Lee, K. Bae, S. Sim, J. Kim, *Adv. Mater.* **2021**, 2005902.
[18] J. H. Kim, K. H. Kim, G. H. Lee, J.-W. Kim, S. H. Han, C. S. Lee, S.-H. Kim, *Small Sci.* **2021**, *1*, 2000058.
[19] C. Shi, F. Hu, R. Wu, Z. Xu, G. Shao, R. Yu, X. Y. Liu, *Adv. Mater.* **2021**, 2005910.
[20] O. Ojuroye, R. Torah, S. Beeby, A. Wilde, *Sensors for Everyday Life*, Vol. *22*, Springer, Berlin **2016**, pp. 159–183.
[21] X. Aeby, A. Poulin, G. Siqueira, M. K. Hausmann, G. Nyström, *Adv. Mater.* **2021**, *33*, 2101328.
[22] D. Gong, C. Wei, Z. Liang, Y. Tang, *Small Sci.* **2021**, *1*, 2100014.
[23] C. Chen, J. Guan, N. W. Li, Y. Lu, D. Luan, C. Hong Zhang, G. Cheng, L. Yu, X. W. (David) Lou, *Adv. Mater.* **2021**, *33*, 2100608.
[24] S. Li, W. Zhang, R. Xing, C. Yuan, H. Xue, X. Yan, *Adv. Mater.* **2021**, *33*, 2100595.
[25] G. Yun, S.-Y. Tang, H. Lu, S. Zhang, M. D. Dickey, W. Li, *Small Sci.* **2021**, *1*, 2000080.
[26] S. Yang, P. Qiu, L. Chen, X. Shi, *Small Sci.* **2021**, 2100005.
[27] Q. Yang, Z. Xu, C. Gao, *J. Energy Chem.* **2018**, *27*, 6.
[28] J. Li, J. Zhang, H. Sun, D. Hong, L. Li, Y. Yang, X. Yong, C. Zhang, J. Cui, *Optik* **2019**, *195*, 163172.
[29] P. Li, H. Yan, Z. Xie, X. Zhao, D. Han, *Opt. Fiber Technol.* **2019**, *53*, 101998.
[30] X. Wang, H. Sun, X. Yue, Y. Yu, G. Zheng, K. Dai, C. Liu, C. Shen, *Compos. Sci. Technol.* **2018**, *168*, 126.
[31] X. Lin, B.-C. Seet, F. Joseph, *Electron. Lett.* **2016**, *52*, 6.
[32] Q. Li, Z. Ran, X. Ding, X. Wang, *Sensors* **2019**, *19*, 3745.
[33] R. Kennon, S. T. A. Hamdani, O. Atalay, S. Naqvi, M. D. Husain, *AATCC J. Res.* **2016**, *3*, 1.
[34] S. Çetiner, B. Göl, H. Köse, *J. Eng. Sci.* **2017**, *20*, 10.
[35] M. Liu, X. Pu, C. Jiang, T. Liu, X. Huang, L. Chen, C. Du, J. Sun, W. Hu, Z. L. Wang, *Adv. Mater.* **2017**, *29*, 1703700.
[36] Y. Cheng, X. Lu, K. H. Chan, R. Wang, Z. Cao, J. Sun, G. W. Ho, *Nano Energy* **2017**, *41*, 511.
[37] J. Ren, C. Wang, X. Zhang, C. Tian, K. Chen, Y. Yin, F. Torrisi, *Carbon* **2016**, *111*, 622.
[38] The high intensity of Openair-Plasma treatment makes it possible to significantly streamline the entire process, https://www.plasmatreat.co.uk/plasma-treatment/plasma-pretreatment/plasma-activation_surface-activation.html (accessed: July 2020).
[39] N. Savard, D. Potkinsc, *Radiat. Meas.* **2017**, *19*, 114.
[40] M. Wu, D. Zhang, X. Wen, *Optik* **2018**, *161*, 278.
[41] M. Vančoa, J. Krmelaa, F. Pešlováa, *Procedia Eng.* **2016**, *136*, 341.
[42] X. Lu, Y. Hu, J. Guo, C.-F. Wang, S. Chen, *Adv. Sci.* **2019**, *6*, 1901694.
[43] What is Plasma Treatment?, https://plasmatreatment.co.uk/henniker-plasma-technology/plasma-surface-technology/plasma-technology-what-is-plasma-treatment/plasma-treatment-explained/ (accessed: July 2019).
[44] F. F. Chen, *Introduction to Plasma Physics and Controlled Fusion*, Springer International Publishing, Berlin **1984**.
[45] J. P. Freidberg, *Plasma Physics and Fusion Energy*, Cambridge University Press, Cambridge **2008**.
[46] D. Schriver, M. Ashour-Abdalla, R. L. Richard, *J. Geophys. Res.* **1998**, *103*, 14879.
[47] S. Samal, *J. Cleaner Prod.* **2017**, *142*, 3131.
[48] A. J. Becker, T. N. Meyer, E. N. Smith, *Plasma Processing and Synthesis of Materials* (Eds: J. E. Edd, D. Apelian, J. Szekely), MRS-98, Pittsburgh, PA **1987**, pp. 335–346.
[49] R. Burkhard, W. Hoffelner, R. C Eschenbach, *Resour., Conserv. Recycl.* **1994**, *10*, 11.
[50] T. YoshidaZ. A. Munir, *Combustion and Plasma Synthesis of High Temperature Materials* (Eds: J. B. Holt) VCH Publishers, NY **1990**, pp. 328–339.
[51] A. I. Morozov, *Introduction to Plasma Dynamics*, 1st ed., CRC Press, Boca Raton, FL **2012**.
[52] S. Mukhopadhyay, R. Fangueiro, *J. Thermoplast. Compos. Mater.* **2009**, *22*, 135.
[53] S. Shahidi, J. Wiener, M. Ghoranneviss, *Eco-Friendly Textile Dyeing and Finishing*, IntechOpen Limited, London **2013**.
[54] M. J. Tsafack, J. Levalois-Grützmacher, *Surf. Coat. Technol.* **2007**, *201*, 5789.
[55] D. Chao, B. Ouyang, P. Liang, T. T. T. Huong, G. Jia, H. Huang, X. Xia, *Adv. Mater.* **2018**, *30*, 1804833.
[56] H. Qli, K. Sui, Z. Ma, D. Wang, X. Sun, J. Lu, *Text. Res. J.* **2002**, *72*, 93.
[57] M. Kajjouta, Y. Lemmouchic, C. Jamab, C. Rolandoa, F. Villasmuntae, F. Heinriche, A. Mazzaha, *React. Funct. Polym.* **2019**, *134*, 40.
[58] J. Zhang, Y. Cao, M. Qiao, L. Ai, K. Sun, Q. Mi, S. Zang, Y. Zuo, X. Yuan, Q. Wang, *Sens. Actuators* **2018**, *A 274*, 132.
[59] C. Wu, T. W. Kim, F. Li, T. Guo, *ACS Nano* **2016**, *10*, 6449.
[60] C. Wu, T. W. Kim, F. Li, T. Guo, *Nano Energy* **2017**, *32*, 367.
[61] *Ionizing Radiation, Health Effects and Protective Measures*, World Health Organization, IARC Press, France, **2016**.
[62] *Non Ionizing Radiation, Part 1: Static and Extremely Low Frequency (ELF) Electric and Magnetic Fields*, World Health Organization, IARC Press, France **2002**.

[63] B. Rauschenbach, *Encyclopedia of Materials: Science and Technology*, 2nd ed., Elsevier, NY **2001**, pp.7023–7027.
[64] Surface Modification of Polymeric Optical Fibers for Chemo- and Biosensor Technology, http://www.camd.unsw.edu.au/advanced-materials-3 (accessed: July 2019).
[65] N. N Andrianova1, A. M Borisov1, V. A Kazakov1, E. S Mashkova, M. A Ovchinnikov1, S. V Savushkina, N. M Chernenko, *J. Phys.: Conf. Ser.* **2017**, *941*, 012028.
[66] Y. Liang, F. Zhao, Z. Cheng, Q. Zhou, H. Shao, L. Jiang, L. Qu, *Nano Energy* **2017**, *32*, 329.
[67] H. Cheng, J. Liu, Y. Zhao, C. Hu, Z. Zhang, N. Chen, L. Jiang, L. Qu, *Angew. Chem., Int. Ed.* **2013**, *52*, 10482.
[68] Y. Liang, F. Zhao, Z. Cheng, Q. Zhou, H. Shao, L. Jiang, L. Qu, *J. Mater. Chem. A* **2015**, *3*, 2547.
[69] X. Yang, T.-H. Ku, S. K. Biswas, H. Yano, K. Abe, *Green Chem.* **2019**, *21*, 4619.
[70] M. G. Stanford, C. Zhang, J. D. Fowlkes, A. Hoffman, I. N. Ivanov, P. D. Rack, J. M. Tour, *ACS Appl. Mater. Interfaces* **2020**, *12*, 10902.
[71] D. Jiang, J. Zhang, C. Li, W. Yang, J. Liu, *New J.Chem.* **2017**, *41*, 11792.
[72] Annealing (metallurgy), https://en.wikipedia.org/wiki/Annealing_(metallurgy) (accessed: March 2019).
[73] I. Tharazi, A. B. Sulong, N. Muhamad, C. H. C. Haron, D. Tholibon, N. F. Ismail, M. K. F. M. Radzi, Z. Razak, *Proc. Eng.* **2017**, *184*, 478.
[74] C. Xia, S. Q. Shi, L. Cai, *Composites, Part B* **2015**, *78*, 138.
[75] A. Pospori, C. A. F. Marques, G. Sagias, H. Lamela-Rivera, D. J. Webb, *Opt. Express.* **2018**, *26*, 2013.
[76] B. M Prasad, M. M. Sain, *Mater. Res. Innovations* **2003**, *7*, 231.
[77] C. Brett, K. Waldron, *Physiology and Biochemistry of Plant Cell Walls*, 1st ed., Unwin Hyman, London, **1990**.
[78] J. M. Felix, P. Gatenholm, *J. Appl. Polym. Sci.* **1991**, *42*, 609.
[79] B. Xu, Y. Q. Fu, W. M. Huang, Y. T. Pei, Z. G. Chen, J. T. M. De Hosson, A. Kraft, R. L. Reuben, *Polymers* **2010**, *2*, 31.
[80] S. J. Kim, J. H. We, B. J. Cho, *RSC Energy Environ. Sci.* **2014**, *7*, 1959.
[81] H. Li, S. Wang, M. Feng, J. Yang, B. Zhang, *Chin. Chem. Lett.* **2019**, *30*, 529.
[82] N. Forsman, A. Lozhechnikova, A. Khakalo, L.-S. Johansson, J. Vartiainen, M. Österberg, *Carbohydr. Polym.* **2017**, *173*, 392.
[83] X. Hong, Y. Xu, R. Wang, P. Du, Z. Zhao, K. Huang, H. Tang, Y. Liu, M. Lei, H. Wu, *Adv. Mater. Interfaces* **2020**, *7*, 2000740.
[84] M. Xu, T. Li, L. Fei, H. Li, X. Guo, P. Hou, Y. Ying, W. Zhu, Y. Zhou, Y. Lin, Z. Zhang, Y. Lai, Y. Zhu, H. Zhang, H. Huang, *Adv. Funct. Mater.* **2020**, *30*, 2002626.
[85] G. Cappelletti, P. Fermo, *Smart Composite Coatings and Membranes*, Elsevier, Amsterdam **2016**, 421–452.
[86] D. L. Chandler, *Explained: Chemical Vapor Deposition*, MIT News Office, MA **2015**.
[87] A. Baptista, F. Silva, J. Porteiro, J. Míguez, G. Pinto, *Coatings* **2018**, *8*, 402.
[88] N. Suna, C. Wanga, L. Jiaob, J. Zhanga, D. Zhanga, *Ceram. Int.* **2016**, *43*, 1509.
[89] C. Maurer, U. Schulz, *Wear* **2014**, *317*, 246.
[90] G.-P. Li, F. Cao, K. Zhang, L. Hou, R. Cheng, W.-Y. Zhang, Y. Y. Wang, *Adv. Mater. Interfaces* **2019**, *7*, 1901525.
[91] M. Liu, S. Zhang, S. Liu, S. Cao, S. Wang, L. Bai, M. Sang, S. Xuan, W. Jiang, X. Gong, *Composites, Part A* **2019**, *126*, 105612.
[92] H. Fang, L. Yuan, G. Liang, A. Gu, *Electrochim. Acta* **2018**, *284*, 149.
[93] A. G. Cunha, M. Lundahl, M. Farhan Ansari, L.-S. Johansson, J. M. Campbell, O. J. Rojas, *ACS Appl. Nano Mater.* **2018**, *1*, 5279.
[94] D. Klemm, F. Kramer, S. Moritz, T. Lindström, M. Ankerfors, D. Gray, A. Dorris, *Angew. Chem., Int. Ed.* **2011**, *50*, 5438.
[95] R. Moon, A. Martini, J. Nairn, J. Simonsen, J. Youngblood, *Chem. Soc. Rev.* **2011**, *40*, 3941.
[96] A. Benitez, J. Torres-Rendon, M. Poutanen, A. Walther, *Biomacromolecules* **2013**, *14*, 4497.
[97] S. Iwamoto, A. Isogai, T. Iwata, *Biomacromolecules* **2011**, *12*, 831.
[98] A. Walther, J. V. I Timonen, I. Díez, A. Laukkanen, O. Ikkala, *Adv. Mater.* **2011**, *23*, 2924.
[99] K. M. O. Håkansson, A. B. Fall, F. Lundell, S. Yu, C. Krywka, S. V. Roth, G. Santoro, M. Kvick, L. Prahl Wittberg, L. Wågberg, D. Söderberg, *Nat. Commun.* **2014**, *5*, 4018.
[100] J. G. Torres-Rendon, F. H. Schacher, S. Ifuku, A. Walther, *Biomacromolecules* **2014**, *15*, 2709.
[101] S. Hooshmand, Y. Aitomäki, N. Norberg, A. P. Mathew, K Oksman, *ACS Appl. Mater. Interfaces* **2015**, *7*, 13022.
[102] H. Mertaniemi, C. Escobedo-Lucea, A. Sanz-Garcia, C. Gandía, A. Mäkitie, J. Partanen, O. Ikkala, M Yliperttula, H. S. C. D. N. T. . B. Applications, *Biomaterials* **2016**, *82*, 208.
[103] M. J. Lundahl, A. G. Cunha, E. Rojo, A. C. Papageorgiou, L. Rautkari, J. C. Arboleda, O. J. Rojas, *Sci. Rep.* **2016**, *6*, 30695.
[104] Y. Shen, H. Orelma, A. Sneck, K. Kataja, J. Salmela, P. Qvintus, A. Suurnäkki, A. Harlin, *Cellulose* **2016**, *23*, 3393.
[105] P. Mohammadi, M. S. Toivonen, O. Ikkala, W. Wagermaier, M. B. Linder, *Sci. Rep.* **2017**, *7*, 11860.
[106] M. Vuoriluoto, H. Orelma, M. Lundahl, M. Borghei, O. J. Rojas, *Biomacromolecules* **2017**, *18*, 1803.
[107] S. Ghasemi, M. Tajvidi, D. W. Bousfield, D. J. Gardner, W. M. Gramlich, *Polymers* **2017**, *9*, 392.
[108] J. Wang, S. Huang, X. Lu, Z. Xu, Y. Zhao, J. Li, X. Wang, *J. Mater. Chem. C* **2017**, *5*, 9673.
[109] C. Clemons, *J. Renewable Mater.* **2016**, *4*, 327.
[110] M. J. Lundahl, V. Klar, L. Wang, M. Ago, O. J. Rojas, *Ind. Eng. Chem. Res.* **2017**, *56*, 8.
[111] J. Zimmermann, F. A. Reifler, G. Fortunato, L.-C. Gerhardt, S. Seeger, A Simple, *Adv. Funct. Mater.* **2008**, *18*, 3662.
[112] C. Liu, W. Zhang, J. Sun, J. Wen, Q. Yang, H. Cuo, X. Ma, M. Zhang, *Appl. Surf. Sci.* **2014**, *322*, 95.
[113] Y. Lin, G. Ehlert, H. A. Sodano, *Adv. Funct. Mater.* **2009**, *19*, 2654.
[114] U. Galan, Y. Lin, G. Ehlert, H. A. Sodano, *Compos. Sci. Technol.* **2011**, *71*, 946.
[115] W. Seung, M. Kumar Gupta, K. Y. Lee, K.-S. Shin, J.-H. Lee, T. Y. Kim, S. Kim, J. Lin, J. H. Kim, S.-W. Kim, *ACS Nano* **2015**, *9*, 3501.
[116] A. R. Shirvan, N. H. Nejad, A. Bashari, *Fibers Polym.* **2014**, *15*, 1908.
[117] B. Xu, Z. Cai, *Appl. Surf. Sci.* **2008**, *254*, 5899.
[118] P. Fakhri, B. Amini, R. Bagherzadeh, M. Kashfi, M. Latifi, N. Yavari, S. A. Kani, L. Kong, *RSC Adv.* **2019**, *9*, 10117.
[119] W. Jingyu, W. Binbin, P. Larson, L. Yingtao, *Surf. Interfaces* **2019**, *16*, 188.
[120] Z. Dai, J. Zhu, J. Yan, J. Su, Y. Gao, X. Zhang, Q. Ke, G. N. Parsons, *Adv. Funct. Mater.* **2020**, *16*, 2001488.
[121] U. C. Paul, D. Fragouli, I. S. Bayer, A. Athanassiou, *Polymers* **2016**, *8*, 52.
[122] M. Zanini, A. Lavoratti, L. Kunz Lazzari, D. Galiotto, M. Pagnocelli, C. Baldasso, A. J. Zattera, *Cellulose* **2017**, *24*, 769.
[123] R. Sepe, F. Bollino, L. Boccarusso, F. Caputo, *Proc. Eng.* **2017**, *200*, 465.
[124] A. Jähn, M. W. Schröder, M. Füting, K. Schenzel, W. Diepenbrock, *Spectrochim. Acta, Part A* **2002**, *58*, 2271.
[125] M. K. B. Bakri, E. Jayamania, S. Hamdan, *Mater. Today: Proc.* **2017**, *4*, 2871.
[126] K. Abe, S. Iwamoto, H. Yano, *Biomacromolecules* **2007**, *8*, 3276.
[127] V. Fiore, G. Di Bella, A. Valenza, *S. Afr. J. Chem. Eng.* **2014**, *23*, 116.
[128] S. D. Gardner, G. He, C. U. Pittman Jr., *Carbon* **1996**, *34*, 1221.
[129] J. Lia, Y. F. Zhang, *Surf. Interface Anal.* **2009**, *41*, 610.
[130] X. Zhang, L. Liu, M. Li, Y. Chang, L. Shang, J. Dong, L. Xiao, Y. Ao, *RSC Adv.* **2016**, *6*, 29428.
[131] W. Jiao, W. Liu, F. Yang, L. Jiang, W. Jiao, R. Wang, *J. Mater. Sci.* **2017**, *52*, 13812.

[132] J. Melke, P. Jakes, J. Langner, L. Riekehr, U. Kunz, Z. Zhao-Karger, A. Nefedov, H. Sezen, C. W. Ll, H. Ehrenberg, C. Roth, *Carbon* **2014**, *78*, 220.
[133] M. Feng, S. Wang, Y. Yu, Q. Feng, J. Yang, B. Zhang, *J. Electrochem. Soc.* **2016**, *163*, A2225.
[134] G. Zhang, S. Sun, D. Yang, J.-P. Dodelet, E. Sacher, *Carbon* **2008**, *46*, 196.
[135] J. Han, S. Wang, S. Zhu, C. Huang, Y. Yue, C. Mei, X. Xu, C. Xia, *ACS Appl. Mater. Interfaces* **2019**, *11*, 44624.
[136] J. Han, Q. Ding, C. Mei, Q. Wu, Y. Yue, X. Xu, *Electrochim. Acta* **2019**, *318*, 660.
[137] D. A. Gopakumar, A. R. Pai, Y. B. Pottathara, D. Pasquini, L. C. . Morais, M. Luke, N. Kalarikkal, Y. Grohens, S. Thomas, *ACS Appl. Mater. Interfaces* **2018**, *10*, 20032.
[138] J. Q. Han, K. Y. Lu, Y. Y. Yue, C. T. Mei, C. B. Huang, Q. L. Wu, X. W. Xu, *Ind. Crops Prod.* **2019**, *128*, 94.
[139] F. Lossada, D. Jiao, J. Guo, D. Hoenders, A. Eckert, A. Walther, *ACS Appl. Polym. Mater.* **2019**, *1*, 3334.
[140] Y. Qin, X. Qiu, J. Y. Zhu, *Sci. Rep.* **2016**, *6*, 35602.
[141] W. Ouarhim, H. Essabir, M.-O. Bensalah, N. Zari, R. Bouhfid, *Composites, Part B* **2018**, *154*, 128.
[142] X. Li, G. Lope, *J. Polym. Environ.* **2007**, *15*, 25.
[143] R. Sepe, F. Bollino, L. Boccarusso, F. Caputo, *Composites, Part B* **2017**, *133*, 210.
[144] B. D. Ratner, A. S. Hoffman, *Biomater. Science: An Introduction to Materials in Medicine*, Academic Press, Oxford, UK **2013**, pp. 259–276.
[145] Y. Liu, J. Xie, N. Wu, L. Wang, Y. Ma, J. Tong, *Tribol. Int.* **2018**, *131*, 398.
[146] Q. Gao, Q. Zhu, Y. Guo, C. Q. Yang, *Ind. Eng. Chem. Res.* **2009**, *48*, 9797.
[147] B. Xu, Z. Cai, W. Wang, F. Ge, *Surf. Coat. Technol.* **2010**, *204*, 1556.
[148] C.-H. Xue, S.-T. Jia, J. Zhang, L.-Q. Tian, *Thin Solid Films* **2009**, *517*, 4593.
[149] J. Vartiainen, T. Malm, *J. Coat. Technol. Res.* **2016**, *13*, 1145,.
[150] Y. Guo, Y. Li, S. Wang, Z.-X. Liu, B. Cai, P.-C. Wang, *Int. J. Adhes. Adhes.* **2019**, *91*, 102.
[151] H. Lu, X. Wang, Y. Yao, J. Gou, D. Hui, B. Xu, Y. Q. Fu, *Composites, Part B* **2015**, *80*, 1.
[152] C. Goussé, H. Chanzy, M. L. Cerrada, E. Fleury, *Polymer* **2004**, *45*, 1569.
[153] C. Goussé, H. Chanzy, G. Excoffier, L. Soubeyrand, E. Fleury, *Polymer* **2002**, *43*, 2645.
[154] T. Joffrea, K. Segerholm, C. Persson, S. L. Bardage, C. L. L. Hendriks, P. Isaksson, *Ind. Crops Prod.* **2016**, *95*, 43.
[155] A. H. Tullo, *Chem. Eng. News* **2012**, *90*, 22.
[156] M. Jonoobi, A. P. Mathew, M. M. Abdi, M. D. Makinejad, K. Oksman, *J. Polym. Environ.* **2012**, *20*, 991.
[157] A. Tripathi, M. Ago, S. A. Khan, O. J. Rojas, *ACS Appl. Mater. Interfaces* **2018**, *10*, 44776.
[158] M. R. K. Sofla, W. Batchelor, J. Kosinkova, R. Pepper, R. Brown, T. Rainey, *Cellulose* **2019**, *26*, 4799.
[159] M. V. G. Zimmermann, M. P. Silva, A. J. Zattera, R. M. C. Santana, *J. Appl. Polym. Sci.* **2017**, *134*, 44760.
[160] G. T. Mahesha, B. Satish Shenoy, M. Vijaya Kini, N. H. Padmaraja, *Mater. Today: Proc.* **2018**, *5*, 138.
[161] P. Huang, M. Wu, S. Kuga, D. Wang, D. Wu, Y. Huang, *ChemSusChem* **2012**, *5*, 2319.
[162] X. Rao, S. Kuga, M. Wu, Y. Huang, *Cellulose* **2015**, *22*, 2341.
[163] S. Deng, R. Huang, M. Zhou, F. Chen, Q. Fu, *Carbohydr. Polym.* **2016**, *154*, 129.
[164] M. Zhou, M. Fan, Y. Zhao, T. Jin, Q. Fu, *Carbohydr. Polym.* **2016**, *140*, 383.
[165] A. G. Cunha, Q. Zhou, P. T. Larsson, L. A. Berglund, *Cellulose* **2014**, *21*, 2773.
[166] M. Vinícius, G. Zimmermann, A. J. Zattera, R. M. C. Santana, *Matéria (Rio J.)* **2019**, *24*, e12377.
[167] R. Ajdary, S. Huan, N. Z. Ezazi, W. Xiang, R. Grande, Hé. A. Santos, O. J. Rojas, *Biomacromolecules* **2019**, *20*, 2770.
[168] D. Staneva, E. Vasileva-Tonkova, I. Grabchev, *J. Photochem. Photobiol., A* **2019**, *382*, 111924.
[169] A. R. Banagar, S. C. Venkateshappa, S. S. Kamath, B. Bennehalli, *Mater. Today: Proc.* **2018**, *5*, 28080.
[170] S. N. A. Safri, M. T. H. Sultan, N. Saba, M. Jawaid, *Polym. Test.* **2018**, *71*, 362.
[171] N. Guigo, K. Mazeau, J.-L. Putaux, L. Heux, *Cellulose* **2014**, *21*, 4119.
[172] P. Mutjé, M. E. Vallejos, J. Gironès, F. Vilaseca, A. López, J. P. López, J. A. Méndez, *J. Appl. Polym. Sci.* **2006**,*102*, 833.
[173] N. Amir, K. A. Z. Abidin, F. B. M. Shiri, *Proc. Eng.* **2018**, *184*, 573.
[174] C. H. Park, Y. K. Kang, S. S. Im, *J. Appl. Polym. Sci.* **2004**,*94*, 248.
[175] S. Eichhorn, A. Dufresne, M. Aranguren, N. Marcovich, J. Capadona, S. Rowan, C. Weder, W. Thielemans, M. Roman, S. Renneckar, *J. Mater. Sci.* **2010**, *45*, 1.
[176] P. Tingaut, T. Zimmermann, F. Lopez-Suevos, *Biomacromolecules* **2009**, *11*, 454.
[177] S. Ifuku, M. Nogi, K. Abe, K. Handa, F. Nakatsubo, H. Yano, *Biomacromolecules* **2007**, *8*, 1973.
[178] J.-Y. Cavaille, H. Chanzy, E. Fleury, J.-F. Sassi, US *6117545*, **2000**.
[179] M. Mondragón, K. Arroyo, J. Romero-García, *Carbohydr. Polym.* **2008**, *74*, 201.
[180] N. Ljungberg, J. Y. Cavaillé, L. Heux, *Polymer* **2006**, *47*, 6285.
[181] P. Huang, Y. Zhao, S. Kuga, M. Wu, Y. Huang, *Nanoscale* **2016**, *8*, 3753.
[182] W. Li, L. Meng, R. Ma, *Polym. Test.* **2016**, *55*, 10.
[183] V. K. Kaushik, A. Kumar, S. Kalia, *Text. Sci.* **2012**, *1*, 101.
[184] C. Zhang, R. Li, J. Liu, S. Guo, L. Xu, S. Xiao, Z. Shen, *Ceram. Int.* **2019**, *45*, 13385.
[185] L. Meng, D. Fan, C. Zhang, Z. Jiang, Y. Huang, *Appl. Surf. Sci.* **2019**, *273*, 167.
[186] L. Tang, Y. Li, Y. Chen, P. Ji, C. Wang, H. Wang, Q. Huang, *J. Appl. Polym. Sci.* **2018**, *135*, 45834.
[187] Z. Wen, X. Qian, Y. Zhang, X. Wang, W. Wang, S. Song, *Composites, Part A* **2019**, *119*, 21.
[188] T. Saito, S. Kimura, Y. Nishiyama, A. Isogai, *Biomacromolecules* **2007**, *8*, 2485.
[189] H. Tang, N. Butchosa, Q. Zhou, *Adv. Mater.* **2015**, *27*, 2070.
[190] S. Virtanen, S. Vuoti, H. Heikkinen, P. Lahtinen, *Cellulose* **2014**, *21*, 3561.
[191] H. Lee, S. M. Dellatore, W. M. Miller, P. B. Messersmith, *Science* **2007**, *318*, 426.
[192] Q. Huang, Y. Yang, R. Chen, X. Wang, *EcoMat* **2021**, *3*, e12076.
[193] Y. Su, Y. Zhao, H. Zhang, X. Feng, L. Shib, J. Fang, *J. Mater. Chem. C* **2017**, *5*, 573.
[194] L. Chen, M. Lu, H. Yang, J. R. S. Avila, B. Shi, L. Ren, G. Wei, X. Liu, W. Yin, *ACS Nano* **2020**, *14*, 8191.
[195] S. Liu, Y. Chen, C. Liu, L. Gan, X. Ma, J. Huang, *Cellulose* **2019**, *26*, 9599.
[196] Z. Wang, S. Zhao, W. Zhang, C. Qi, S. Zhang, J. Li, *Appl. Surf. Sci.* **2019**, *478*, 441.
[197] F. Ram, P. Velayutham, A. Kumar Sahu, A. K. Lele, K. Shanmuganathan, *ACS Appl. Energy Mater.* **2020**, *3*, 1988.
[198] Y. Liu, K. Ai, L. Lu, *Chem. Rev.* **2014**, *114*, 5057.
[199] C. J. Bettinger, J. P. Bruggeman, A. Misra, J. T. Borenstein, R. Langer, *Biomaterials* **2009**, *30*, 3050.
[200] Y. Liu, Q. Wang, Q. Shen, M. Wu, C. Liu, Y. Zhang, G. Yu, B. Li, Y. Li, *ChemistrySelect* **2018**, *3*, 6852.
[201] L. Kong, C. Tang, H.-J. Peng, J.-Q. Huang, Q. Zhang, *SmartMat* **2020**, *1*, e1007.
[202] X. Lan, T. Wang, C. Liu, P. Liu, J. Xu, X. Liu, Y. Du, F. Jiang, *Compos. Sci. Technol.* **2019**, *182*, 107767.

[203] K. Dong, X. Peng, Z. L. Wang, *Adv. Mater.* **2019**, *32*, 1902549.
[204] L. Xue, W. Fan, Y. Yu, K. Dong, C. Liu, Y. Sun, C. Zhang, W. Chen, R. Lei, K. Rong, Q. Wang, *Adv. Fiber Mater.* **2021**.
[205] S. K. Ghosh, D. Mandal, *Nano Energy* **2018**, *53*, 245.
[206] M. Liu, X. Pu, C. Jiang, T. Liu, X. Huang, L. Chen, C. Du, J. Sun, W. Hu, Z. L. Wang, *Adv. Mater.* **2017**, *29*, 1703700.
[207] X. Hu, Y. Dou, J. Li, Z. Liu, *Small* **2019**, *15*, 1804805.
[208] J. Ge, L. Sun, F.-R. Zhang, Y. Zhang, L.-A. Shi, H.-Y. Zhao, H.-W. Zhu, H.-L. Jiang, S.-H. Yu, *Adv. Mater.* **2016**, *28*, 722.
[209] J. Lee, H. Kwon, J. Seo, S. Shin, J. H. Koo, C. Pang, S. Son, J. H. Kim, Y. H. Jang, D. E. Kim, T. Lee, *Adv. Mater.* **2015**, *27*, 2433.
[210] M. Zhu, M. Lou, I. Abdalla, J. Yu, Z. Li, B. Ding, *Nano Energy* **2020**, *69*, 104429.
[211] X. Pu, W. Song, M. Liu, C. Sun, C. Du, C. Jiang, X. Huang, D. Zou, W. Hu, Z. L. Wang, *Adv. Energy Mater.* **2016**, *6*, 1601048.
[212] J. Song, L. Gao, X. Tao, L. Li, *Materials* **2018**, *11*, 2120.
[213] J. Wang, X. Li, Y. Zi, S. Wang, Z. Li, L. Zheng, F. Yi, S. Li, Z. L. Wang, *Adv. Mater.* **2015**, *27*, 4830.
[214] M.-H. Yeh, H. Guo, L. Lin, Z. Wen, Z. Li, C. Hu, Z. L. Wang, *Adv. Funct. Mater.* **2016**, *26*, 1054.
[215] J. Chena, H. Guob, X. Pua, X. Wanga, Y. Xia, C. Hua, *Nano Energy* **2018**, *50*, 536.
[216] Q. Qiu, M. Zhu, Z. Li, K. Qiu, X. Liu, J. Yu, B. Ding, *Nano Energy* **2019**, *58*, 750.
[217] J. R. Windmiller, J. Wang, *Electroanalysis* **2013**, *25*, 29.
[218] A. Yu, X. Pu, R. Wen, M. Liu, T. Zhou, K. Zhang, Y. Zhang, J. Zhai, W. . Hu, Z. L. Wang, *ACS Nano* **2017**, *11*, 12764.
[219] Y. Wu, Y. Luo, J. Qu, W. A. Daoud, T. Qi, *Nano Energy* **2019**, *64*, 103948.
[220] Z. Lin, Y. Wu, Q. He, C. C. Sun, E. Fan, Z. Zhou, M. Liu, W. Wei, J. Yang, *RSC Nanoscale* **2019**, *11*, 6802.
[221] J. Yang, J. Che, Y. Su, Q. Jing, Z. Li, F. Yi, X. Wen, Z. Wang, W. Zhong Lin, *Adv. Mater.* **2015**, *27*, 1316.
[222] X. Li, Z.-H. Lin, G. Cheng, X. Wen, Y. Liu, S. Niu, Z. L. Wang, *ACS Nano* **2014**, *8*, 10674.
[223] B. Chen, W. Tang, T. Jiang, L. Zhu, X. Chen, C. He, L. Xu, H. Guo, P. Lin, D. Li, J. Shao, Z. L. Wang, *Nano Energy* **2018**, *45*, 380.
[224] K. Dong, J. Deng, W. Ding, A. C. Wang, P. Wang, C. Cheng, Y.-C. Wang, L. Jin, B. Gu, B. Sun, Z. L. Wang, *Adv. Energy Mater.* **2018**, *8*, 1801114.
[225] K. Dong, Z. Wu, J. Deng, A. C. Wang, H. Zou, C. Chen, D. Hu, B. Gu, B. Sun, Z. L. Wang, *Adv. Mater.* **2018**, *30*, 1804944.
[226] J. Zhong, Y. Zhang, Q. Zhong, Q. Hu, B. Hu, Z. L. Wang, J. Zhou, *ACS Nano* **2014**, *8*, 6273.
[227] K. Dong, J. Deng, Y. Zi, Y.-C. Wang, C. Xu, H. Zou, W. Ding, Y. Dai, B. Gu, B. Sun, Z. L. Wang, *Adv. Mater.* **2017**, *29*, 1702648.
[228] Z. Zhao, X. Pu, C. Du, L. Li, C. Jiang, W. Hu, L. W. Zhong, *ACS Nano* **2016**, *10*, 1780.
[229] Y. Liu, Y. Fang, X. Liu, X. Wang, B. Yang, *Compos. Sci. Technol.* **2017**, *151*, 164.
[230] Y. Zhao, J. Li, H. Gu, D. Wei, Y. . Xu, W. Fu, Z. Yu, *Interdiscip. Sci.: Comput. Life Sci.* **2017**, *7*, 211.
[231] Y. Huang, L. Zeng, C. Liu, D. Zeng, Z. Liu, X. Liu, X. Zhong, W. Guo, L. Li, *Small* **2018**, *14*, 1803143.
[232] L. Zeng, X. Liu, X. Chen, *Appl. Compos. Mater.* **2018**, *25*, 843.
[233] C. Zhu, E. Chalmers, L. Chen, Y. Wang, B. B. Xu, Y. Li, X. Liu, *Small* **2019**, 1902440.
[234] C. Zhu, X. Guan, X. Wang, Y. Li, E. Chalmers, X. Liu, *Adv. Mater. Interfaces* **2019**, *6*, 1801547.
[235] J. Zhang, Y. Xu, L. Cui, A. Fu, W. Yang, C. Barrow, J. Liu, *Composites, Part A* **2015**, *71*, 1.
[236] J. Chang, Z. Zhong, H. Xu, *Korean J. Chem. Eng.* **2012**, *29*, 507.
[237] Y.-L. Wang, A. Laaksonenb, M. D. Fayer, *J. Phys. Chem.* **2017**, *121*, 7173.
[238] L. Feng, J. Pang, P. She, J.-L. Li, J.-S. Qin, D.-Y. Du, H.-C. Zhou, *Adv. Mater.* **2020**, *32*, 2004414.
[239] H. Li, M. Eddaoudi, M. O'Keeffe, O. M. Yaghi, *Nature* **1999**, *402*, 276.
[240] H. Furukawa, K. E. Cordova, M. O'Keeffe, O. M. Yaghi, *Science* **2013**, *341*, 1230444.
[241] H. C. Zhou, J. R. Long, O. M. Yaghi, *Chem. Rev.* **2012**, *112*, 673.
[242] S. R. Batten, N. R. Champness, X. M. Chen, G.-J. Martinez, S. Kitagawa, L. Öhrström, M. O'Keeffe, M. P. Suh, J. Reedijk, *Pure Appl. Chem.* **2013**, *85*, 1715.
[243] D. Farrusseng, *Metal-Organic Frameworks: Applications from Catalysis to Gas Storage*, Wiley-VCH, Weinheim, Germany **2011**.
[244] J. Yang, P. Li, L. Wang, X. Guo, J. Guo, S. Liu, *J. Electroanal. Chem.* **2019**, *848*, 113301.
[245] C. Cheng, J. Xu, W. Gao, S. Jiang, R. Guo, *Electrochim. Acta* **2019**, *318*, 23.
[246] Y.-N. Liu, L.-N. Jin, H.-T. Wang, X.-H. Kang, S.-W. Bian, *J. Colloid Interface Sci.* **2018**, *530*, 29.
[247] J. Ma, J. Li, R. Guo, H. Xu, F. Shi, L. Dang, Z. Liu, J. Sun, Z. Lei, *J. Power Sources* **2019**, *428*, 124.
[248] F. Xie, N. Zhang, L. Zhuo, P. Qin, S. Chen, Y. Wang, Z. Lu, *Composites, Part B* **2019**, *168*, 406.

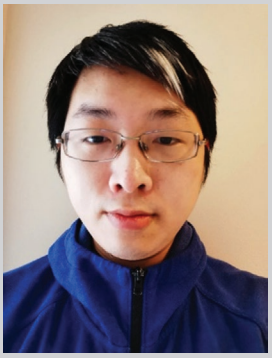

Ruimin Xiao received his B.Sc. degree from University of Reading and M.Sc. degree from University of Manchester. He is a Year 3 Ph.D. student in University of Manchester in Dr. Xuqing Liu's group. His research interests include fiber surface/interfacial engineering science and fiber surface functionalization.

Ben Bin Xu is a professor of Materials and Mechanics in the Department of Mechanical and Construction Engineering (MCE) and leads the research group of Smart Materials and Surfaces Lab at Northumbria University, United Kingdom. He obtained his Ph.D. in Mechanical Engineering (2011) at Heriot-Watt University in Edinburgh, and then he moved to the University of Massachusetts, Amherst (US) to work with Prof. Ryan C. Hayward as a postdoc research fellow in the Department of Polymer Science and Engineering. His research interests include responsive materials, soft matter, applied mechanics, microengineering, energy materials, and sustainable technologies.

Xuqing Liu is a tenured research fellow, in the Department of Materials at the University of Manchester. He leads the Research group of Fiber Surface Molecular Engineering, and is the academic lead for Fiber Chemistry. His group utilizes the basic principles in chemistry, material science, and textiles, and fashion to enable novel applications and development of flexible stretchable electronics in energy devices and functional and sustainable fashion. He is the fellow of the Royal Society of Arts and the chairman of Chinese Textile and Apparel Society (CTAS-UK).